

**Spectral and Structural Studies of Transition Metal
Complexes of Thiosemicarbazones Containing Ring
Incorporated at N(4)-position**

**Thesis Submitted to the
Cochin University of Science and Technology**

**In partial fulfillment of the
requirements for the degree of**

DOCTOR OF PHILOSOPHY

Under the Faculty of Science

By

Leji Latheef



**Department of Applied Chemistry
Cochin University of Science and Technology
Kochi-682 022**

September 2007



Phone Off. 0484-3922423
0484-2575804
Phone Res. 0484-2576904
Fax: 0484-2577595
Email: mrp@cusat.ac.in
mrp_k@yahoo.com

**DEPARTMENT OF APPLIED CHEMISTRY
COCHIN UNIVERSITY OF SCIENCE AND TECHNOLOGY
KOCHI - 682 022, INDIA**

**Prof. M.R. Prathapachandra Kurup
Professor**

13th September 2007

CERTIFICATE

This is to certify that the thesis entitled **“Spectral and structural studies of transition metal complexes of thiosemicarbazones containing ring incorporated at N(4)-position”** submitted by Ms. Leji Latheef, in partial fulfillment of the requirements for the degree of Doctor of Philosophy, to the Cochin University of Science and Technology, Kochi-22, is an authentic record of the original research work carried out by her under my guidance and supervision. The results embodied in this thesis, in full or in part, have not been submitted for the award of any other degree.


M. R. Prathapachandra Kurup
(Supervisor)

DECLARATION

I hereby declare that the work presented in this thesis entitled “**Spectral and structural studies of transition metal complexes of thiosemicarbazones containing ring incorporated at N(4)-position**” is entirely original and was carried out independently under the supervision of Professor M. R. Prathapachandra Kurup, Department of Applied Chemistry, Cochin University of Science and Technology and has not been included in any other thesis submitted previously for the award of any other degree.

13-09-07

Kochi-22



Leji Latheef

PREFACE

Coordination chemistry enjoys a prominent place in inorganic chemistry. Werner's coordination theory was the first attempt to explain the bonding in coordination complexes, and he concluded that in complexes the metal shows two different sorts of valencies *viz* primary and secondary valency. Primary valencies are non-directional and are the number of charges on the complex ion. In compounds, this charge is matched by the same number of charges from negative ions. Secondary valencies are directional. In modern terms the number of secondary valencies equals the number of ligand atoms coordinated to the metal. This is now called the coordination number.

In the quest of exploring the chelating behaviour of some ONS and NNS donor thiosemicarbazones in several metal complexes, we could get hold of more information about their nature of coordination and related structural, spectral and biological properties. The term "dinucleating ligands" was first introduced in 1970 by Robinson to portray the class of polydentate chelating ligands, and to bind simultaneously two metal ions. The possible applications of the complexes with this type of ligands vary from modeling the active sites of many metalloenzymes, to hosting and carrying small molecules or catalysis.

The work embodied in the thesis was carried out by the author in the Department of Applied Chemistry during 2004–2007. The thesis is only an introduction to our attempts to evaluate the coordination behaviour of a few compounds of our interest. The crucial aim of these investigations was to synthesize and characterize some transition metal complexes using the ligands benzaldehyde, 2-hydroxybenzaldehyde and 4-methoxybenzaldehyde N(4)-ring incorporated thiosemicarbazones.

The work is divided into seven chapters and the last section deals with summary and conclusion. Chapter 1 involves a brief foreword of the metal complexes of thiosemicarbazones including their bonding, stereochemistry and biological activities. The different analytical and spectroscopic techniques used for the analysis of the ligands and their complexes are discussed in this chapter. Chapter 2 deals with the synthesis and spectral characterization of the thiosemicarbazones and single crystal X-ray diffraction study of one of them. Chapter 3 describes the synthesis, spectral characterization, single crystal X-ray diffraction studies of copper(II) complexes with ONS/NS donor thiosemicarbazones. Chapter 4 deals with the synthesis, spectral characterization and single crystal X-ray diffraction studies of nickel(II) complexes. Chapter 5 contains the synthesis, structural and spectral characterization of the cobalt(III) complexes. Chapters 6 and 7 include the synthesis, structural and spectral characterization of zinc(II) and cadmium(II) complexes with ONS/NS donor thiosemicarbazones.

ACKNOWLEDGEMENT

The research described in this thesis was done at the Department of Applied Chemistry, CUSAT. The co-operation and support of many people during the course of this work has been very valuable to me. At least I owe those who helped me and I would like to express my sincere appreciation.

First and foremost, I wish to place on record my heartfelt gratefulness to my revered guide Prof. (Dr.) M.R. Prathapachandra Kurup, Department of Applied Chemistry for his intensive guidance and whole hearted support right through my research work,

I am greatly obliged to Dr. Girish Kumar (Head of the Department), Prof. (Dr.) K.K. Mohammed Yusuff and Dr. S. Prathapan for their kind consideration. I acknowledge all faculty members of the Department of Applied Chemistry for their support and advice. I also acknowledge all the non-teaching staff of the Department in taking care of all issues regarding the administration of my academic program.

I owe greatly to CSIR, New Delhi, for the award of Junior and Senior Research Fellowships.

I am indebted to Prof. (Dr.) P. Mathur, National Single Crystal X-ray Diffraction Facility, IIT-Bombay, Dr. E. Suresh, Analytical Sciences Division, CSMCRI, Bhavanagar, Gujarat, for single crystal X-ray diffraction studies. Acknowledgements are also due to the services provided by the Sophisticated Analytical Instrumentation Facility, IIT Bombay and Sophisticated Test and Instrumentation Centre, Kochi-22.

I am grateful to Dr. V. Suni, Dr. P.F. Raphel and Dr. Marthakutty Joseph for their help during the initial stages of my research possession. I am much obliged to Dr. Seena, Suja and Sheeja for their boundless support and timely help whenever I need it most. I am thankful to my lab mates Laly miss, Jessy miss, Annie miss, Jayakumar sir, Bessy, Mini, Manoj, Sreesh, Binu, Nancy, Reena, Neema, Dhanya and Sarika for their encouragement in my ways. I thank Dr. Luxmi Varma, Chemical Sciences and Technology Division and Ambili for their immense help in carrying out NMR studies at RRL, TVM.

I put into words my sincere gratitude to my parents Abdul Latheef and Pathumma and my dearest sister Lamna for their moral support, love and affection right through my life. I cannot leave out my husband Siraj, for his symbiotic support, for keeping me in a pleasant mood. He has given me a hand of support, love and care in all my activities. This work would not have been possible without their help and encouragement. My work is the result of their perseverance. For this reason I have dedicated this work to them.

Above all I stoop before God Almighty for having given me His strength and blessings to carry this work to conclusion.

Leji Latheef

Abbreviation

HL ¹	benzaldehyde 3-hexamethyleneiminylthiosemicarbazone
H ₂ L ²	2-hydroxybenzaldehyde 3-hexamethyleneiminylthiosemicarbazone
HL ³	4-methoxybenzaldehyde 3-hexamethyleneiminylthiosemicarbazone
H ₂ L ⁴	2-hydroxybenzaldehyde 3-tetramethyleneiminylthiosemicarbazone
DMF	N, N-dimethyl formamide
DMSO	dimethyl sulfoxide
CHCl ₃	chloroform
h	hours
L	ligand
B	base
ph	phenyl
TMS	tetramethyl silane
δ	isomer shift
py	pyridine
bipy	bipyridine
pic	picoline
phen	phenanthroline
TSC	thiosemicarbazone
SC	semicarbazone
BM	bohr magneton
α ²	in-plane σ bonding parameter
β ²	in-plane π bonding parameter
CT	charge transfer

CONTENTS

	Page No.
CHAPTER 1	
Thiosemicarbazones and their transition metal complexes: a brief prologue	
1.1. General introduction	1
1.2. Bonding and stereochemistry	3
1.3. Characterization techniques	8
1.3.1. Estimation of carbon, hydrogen and nitrogen	8
1.3.2. Magnetic susceptibility measurements	8
1.3.3. IR spectroscopy	10
1.3.4. Electronic spectroscopy	10
1.3.5. EPR spectroscopy	11
1.3.6. NMR spectroscopy	13
1.3.7. X-ray crystallography	13
1.4. Significance of thiosemicarbazones and their metal complexes	14
1.5. Objective and scope of the present work	17
References	18
CHAPTER 2	
Synthesis and characterization of thiosemicarbazone ligands	
2.1. Introduction	24
2.2. Experimental	26
2.2.1. Materials	26
2.2.2. Synthesis of ligand precursors	26
2.2.3. Synthesis of ligands	28
2.3. Characterization techniques	30
2.3.1. X-ray crystallography	30
2.4. Results and discussion	32
2.4.1. Crystal structure of H_2L^2	32
2.4.2. IR spectra	37
2.4.3. Electronic spectra	39
2.4.4. 1H NMR spectra	40
References	45
CHAPTER 3	
Synthesis, spectral and structural studies of Cu(II) complexes of N(4)-ring incorporated thiosemicarbazones of aromatic aldehydes	
3.1. Introduction	48
3.2. Experimental	49
3.2.1. Materials	49

3.2.2.	Synthesis of the complexes	49
3.2.3.	Physical measurements	51
3.2.4.	X-ray crystallography	52
3.3.	Results and discussion	53
3.3.1.	Crystal structure of [CuL ⁴ bipy]	54
3.3.2.	IR spectra	59
3.3.3.	Electronic spectra	64
3.3.4.	EPR spectra	67
	References	75

CHAPTER 4

Synthesis, spectral and structural studies of Ni(II) complexes of N(4)-ring incorporated thiosemicarbazones of aromatic aldehydes

4.1.	Introduction	78
4.2.	Experimental	79
4.2.1.	Materials	79
4.2.2.	Synthesis of the complexes	79
4.2.3.	Physical measurements	81
4.2.4.	X-ray crystallography	82
4.3.	Results and discussion	84
4.3.1.	Crystal structures of the compounds [NiL ² py], [NiL ² α-pic] and [NiL ² β-pic]	86
4.3.2.	Crystal structure of the compound [Ni ₂ L ₂ phen]	96
4.3.3.	IR spectra	102
4.3.4.	¹ H NMR Spectra	107
4.3.5.	Electronic spectra	110
	References	114

CHAPTER 5

Synthesis and spectral studies of Co(III) complexes of salicylaldehyde N(4)-ring incorporated thiosemicarbazones: crystal structure of a sulfenato complex

5.1.	Introduction	117
5.2.	Experimental	118
5.2.1.	Materials	118
5.2.2.	Synthesis of the complexes	118
5.2.3.	Physical measurements	120
5.2.4.	X-ray crystallography	120
5.3.	Results and discussion	121
5.3.1.	Crystal structure of the compound [Co(L ⁴ O)phenN ₃]	123
5.3.2.	IR spectra	129
5.3.3.	Electronic spectra	134
	References	137

CHAPTER 6

Synthesis, spectral and structural studies of Zn(II) complexes of salicylaldehyde N(4)-ring incorporated thiosemicarbazones

6.1.	Introduction	139
6.2.	Experimental	140
6.2.1.	Materials	140
6.2.2.	Synthesis of the complexes	140
6.2.3.	Physical measurements	142
6.2.4.	X-ray crystallography	142
6.3.	Results and discussion	144
6.3.1.	Crystal structure of the compound [Zn(HL ²) ₂]	145
6.3.2.	IR spectra	149
6.3.3.	Electronic spectra	153
6.3.4.	¹ H NMR spectra	156
	References	160

CHAPTER 7

Synthesis and spectral studies of Cd(II) complexes of N(4)-ring incorporated thiosemicarbazones

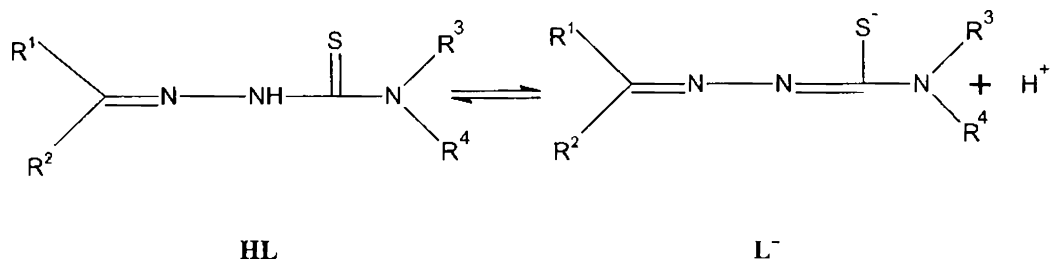
7.1.	Introduction	163
7.2.	Experimental	164
7.2.1.	Materials	164
7.2.2.	Synthesis of the complexes	164
7.2.3.	Physical measurements	165
7.3.	Results and discussion	165
7.3.1.	IR spectra	166
7.3.2.	Electronic spectra	170
7.3.3.	¹ H NMR spectra	172
	References	176
	Summary and conclusion	178

Thiosemicarbazones and their transition metal complexes: a brief prologue

1.1. General introduction

The coordination chemistry of thiosemicarbazones (TSCs) with transition metals [1-7], which began with Jensen's work [8], has been more intensively investigated as compared to that of main group elements [9-11]. Thiosemicarbazones are thiourea derivatives and the studies on their chemical and structural properties have received much attention due to the widespread application in the chemotherapeutic field [1, 4]. Thiosemicarbazones have been a subject of interest to researchers of different profiles. In view of the fact that these compounds form complexes with many metals are of diverse chemical, physical and structural characteristics, they are of special interest to coordination chemists [1, 2]. Thiosemicarbazones, with the general formula $R^1R^2C=N-NH-CS-NR^3R^4$ usually react as chelating ligands with transition metal ions by bonding through the sulfur and hydrazinic nitrogen atom. The group $N-C=S$ is of considerable chemotherapeutic interest and is responsible for the pharmacological activity. Thiosemicarbazones of α -(N)-heterocyclic aldehydes and ketones possess a broad spectrum of potentially useful chemotherapeutic activities such as antimalarial, antibacterial, antiviral activities [12, 13].

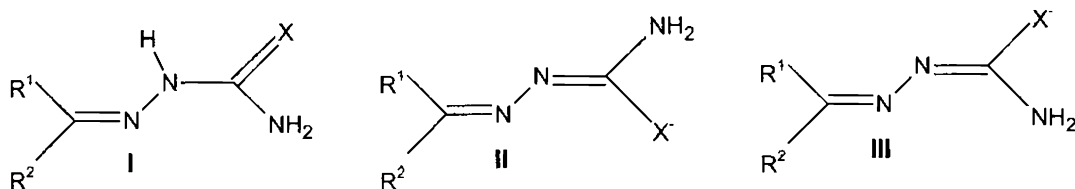
Heterocyclic thiones and thiosemicarbazones, which contain chemically active $N(H)C(S)$ or $=NN(H)C(S)$ chromophores, are useful model compounds for sulfur containing analogous of purine and pyrimidine bases, and thus have invited considerable interest in their coordination behavior [1-4, 14, 15]. Chemically



Scheme 1

The R¹ and R² groups may provide additional donor atoms and R³ and R⁴ are the N(4)-substituents.

Although the proton lost by the anions formally belongs to the hydrazinic –NH group, the anion is usually presented in the canonical form I, II and III and usually in the *Z*-configuration [17].



The IUPAC numbering scheme of the ligand is shown in Figure 1.1.

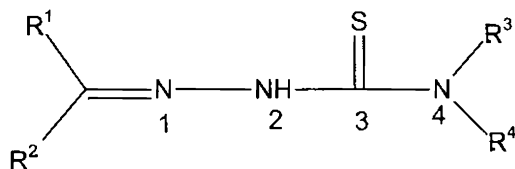


Figure 1.1. IUPAC numbering scheme of the ligand

1.2 Bonding and stereochemistry

The thiosemicarbazone moiety acts as a chelating agent for metal ions by bonding through the S atom and the hydrazine N atom. The thiosemicarbazones

exist in the thione form (IV) in the solid state and in solution, they are known to tautomerize to exist in a mixture of thione (IV) and thiol (V) forms.

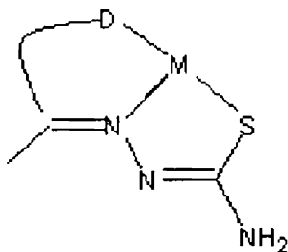


(Thione) (IV)

(Thiol) (V)

IV acts as a neutral bidentate ligand, while the loss of the thiol proton from V yields a singly charged bidentate ligand due to the loss of its proton. Therefore depending upon the preparative conditions (especially pH), the complex unit can be cationic, neutral or anionic. However, most investigations of metal thiosemicarbazone complexes have involved ligands in the uncharged (IV) or thiolate form, while definitive data on the complexes containing thiosemicarbazone in the thiol form (V) are generally lacking. Furthermore, it is possible to isolate complexes containing both tautomeric forms of the ligand. For *e.g.* Garg *et al.* [18] have prepared a copper(II) chelate of 2-acetylpyridine thiosemicarbazone containing neutral and anionic forms of the ligand.

When an additional donor site D is incorporated in such ligands, linked to the carbonylic carbon *via* one or two intervening atoms D, N, S tricoordination usually takes place.

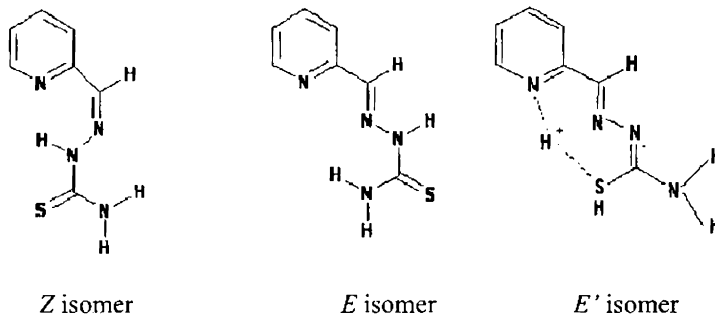


If the additional functionality can also lose a proton (*e.g.* phenolic group), anions of greater negative charge are formed. There are instances reported,

however, where the heterocyclic atom and the azomethine nitrogen are involved in bidentate coordination [19], and the sulfur atom is considered not to be coordinated, weakly coordinated to the same metal center, or coordinated to an adjacent metal center [20].

The thiosemicarbazone moiety (Figure 1.1) without substituents attached to the thione sulfur coordinates as either a neutral or anionic NS bidentate ligand, depending on the method of complex preparation [21], a third coordinating atom often gives ONS (e.g. 2-hydroxybenzaldehyde thiosemicarbazones) [22] or NNS (e.g. 2-acetylpyridine thiosemicarbazones) [20] donor tridentate ligands. A few examples of higher denticity involving one or more thiosemicarbazone moieties, as well as monodentate coordination have been reported [20].

Due to the presence of C=N bond, the thiosemicarbazones can exist in three isomeric forms *Z*, *E*, and *E'* [23]. The TSC may generally exist in the *E* form (*trans*) but in such situation the compound may act as a unidentate ligand, by bonding through sulfur only [24]. In case the sulfur center is substituted, the bonding may occur through the hydrazine nitrogen and the amide nitrogen [25]. *Z*, *E* and *E'* isomeric forms of 2-formylpyridine thiosemicarbazone are shown below. *E'* is the bifurcated E-hydrogen bonded ring isomer.



Thiosemicarbazones can coordinate to the metal either as a neutral ligand or as a deprotonated ligand through the NNS [20], ONS [22] or through the NNO atoms [17, 24, 26].

Thiosemicarbazones obtained by condensation of thiosemicarbazides with benzaldehyde, salicylaldehyde and substituted salicylaldehydes [4, 27, 28] form a class of versatile NS/NSO chelating ligands. They also stabilize uncommon oxidation states [29, 30], generate unfamiliar coordination numbers in the resultant transition metal complexes and participate in various types of redox reactions [31-34]. These ligands can act in a dianionic tridentate manner by deprotonation of both the phenol and the thioamide functions. They can also behave as monoanionic tridentate ligands coordinating to a metal centre through the deprotonated phenolic oxygen, thione sulfur and the azomethine nitrogen [29]. The importance of the coordination chemistry of such ONS donors increased markedly after the presence of ONS donor environment was detected at the active sites of some metalloenzymes [31-33]. West *et al.* [35] have shown that the nature of substituents attached at ^4N of 2-formyl- and 2-acetylpyridine thiosemicarbazones can influence the stereochemistry and stoichiometry of metal complexes. An important feature in the chemistry of thiosemicarbazones and their metal complexes is the acid character of the ^2NH ; this allows for either neutral or anionic ligands. When coordinated as anionic ligands, the conjugation is extended to include the thiosemicarbazone moiety (*i.e.* $\text{C}=\text{N}-\text{N}=\text{C}(\text{S}^-)-\text{N}$). If ^2N is alkylated, the thiosemicarbazone will function as the thione isomer without extended conjugation. Earlier reports suggest that stereochemistries adopted by 2-heterocyclic thiosemicarbazones of transition metal complexes often depend upon the anion of the metal salt used and the nature of the ^4N -substituents. Further, as indicated previously, the charge on the ligand is dictated by the thione-thiol equilibrium which in turn is influenced by the solvent and pH of the preparative medium.

Common stoichiometries encountered with 2-heterocyclic thiosemicarbazones are six coordinate having the general formula ML_2^{n+} , where $M=Cr(III)$, $Fe(III)$, $Co(III)$ and $Ni(II)$; $L=$ tridentate, anionic ligand and $n=0, 1$ and planar with the stoichiometry of MLX , where $M=Ni(II)$ or $Cu(II)$, $L=$ tridentate, anionic ligand and X is generally a halo or pseudohalo ligand.

The stereochemistries adopted by thiosemicarbazone ligands while interacting with transition metal ions depend essentially upon the presence of additional coordination centre in the ligand moiety and the charge on the ligand, which in turn is influenced by the thione \rightleftharpoons thiol equilibrium. For *e.g.* benzaldehyde thiosemicarbazone is generally found to act as neutral bidentate ligand, depending upon the pH of the synthetic medium yielding complexes of the type $[ML_2X_2]$ (where $M=Co(II)$, $Ni(II)$, $Cu(II)$, $Fe(II)$; $L=$ the ligand in the thione form and $X=$ the monoanionic ligand where as salicylaldehyde thiosemicarbazone is found to act as a tridentate uninegative ligand yielding compounds of type $[M(HL)_2]$, which may be spin - free or spin - paired. As a result of the above considerations, the most common stereochemistries encountered in thiosemicarbazone complexes are tetrahedral and square planar. On rare occasions five coordinated structures also obtained, as in the case of $Co(II)$, $Fe(II)$ and $Ni(II)$ complexes of acetone thiosemicarbazone [36-38] and the $Fe(II)$ complex of 2-acetylpyridine thiosemicarbazone [39].

HSAB considerations dictate that the degree of softness character of the metal depends upon the oxidation state of the metal, and it is found to be stronger for transition metals in low oxidation states. Thus the low spin d^8 ions $Pd(II)$, $Pt(II)$ and $Au(III)$ and d^{10} ions $Cu(I)$, $Ag(I)$, $Au(I)$ and $Hg(II)$ exhibit higher stability constants with this class of sulfur ligands because of the formation of strong σ bonds as well as $d_{\pi}-d_{\pi}$ bonds by donation of a pair of electrons to ligands [40].

Thiols but not thioethers cause spin-pairing of Co and Ni. Thiosemicarbazones are not capable of spin-pairing of Fe(III) ions, unlike other soft bases such as CN^- , diarsine and certain charged sulfur ligands [41]. Consequently, intermediate spin states are found to be stabilized [39]. This potential of the class of thiosemicarbazone ligands has not been recognized to the extent as for diethyldithiocarbamate ligands.

1.3. Characterization techniques

1.3.1. Estimation of carbon, hydrogen and nitrogen

Elemental analyses of C, H and N were done on a Vario EL III CHN elemental analyzer at the SAIF, Cochin University of Science and Technology, Kochi 22, India.

1.3.2. Magnetic susceptibility measurements

When a substance is placed in a magnetic field of strength H , the intensity of magnetic field in the substance is greater than H . If the field of the substance is greater than H , the substance is paramagnetic and if it is less than H , the substance is diamagnetic. Paramagnetism arises as a result of unpaired electron spins in the atom.

The mass magnetic susceptibility in $\text{cm}^3 \cdot \text{g}^{-1}$ (χ or χ_g) and the molar magnetic susceptibility (χ_m) in $\text{cm}^3 \cdot \text{mol}^{-1}$ are defined as follows where ρ is the density in $\text{g} \cdot \text{cm}^{-3}$ and M is molar mass in $\text{g} \cdot \text{mol}^{-1}$.

$$\chi_g = \chi_v / \rho$$

$$\chi_m = M\chi_g = M\chi_v / \rho$$

If χ is positive, then $(1+\chi) > 1$ and the material is called paramagnetic. In this case, the magnetic field is strengthened by the presence of the material.

Alternatively, if χ is negative, then $(1+\chi) < 1$, and the material is diamagnetic. As a result, the magnetic field is weakened in the presence of the material.

The magnetic susceptibility value calculated from magnetic measurements is the sum of paramagnetic and diamagnetic susceptibilities. To calculate the exact paramagnetic susceptibility (μ_{eff}), the value of diamagnetic susceptibility is subtracted from the susceptibility calculated from observed results [42]. When the structural formula of the complexes is correctly known, diamagnetic correction can be calculated from Pascal's constants.

$$\chi_M^{corr.} = \chi_M - (\text{Diamagnetic corrections})$$

From classical theory, the corrected paramagnetic molar susceptibility is related to the permanent paramagnetic moment of a molecule, μ_{eff} , by :

$$\chi_M^{corr.} = \frac{N^2 \cdot \mu_{eff}^2}{3RT}$$

where, N is Avogadro's number, R is the ideal gas constant, T is the absolute temperature and μ_{eff} is the effective magnetic moment and is expressed in Bohr magnetons (B.M). Solving the above expression, the effective magnetic moment is given by,

$$\mu_{eff} = \sqrt{\frac{3RT \cdot \chi_M^{corr.}}{N}} = 2.828 \sqrt{\chi_M^{corr.} \cdot T}$$

But, the field strength (H) used for the measurement is 5 k Oe. Then,

$$\mu_{eff} = 2.828 \sqrt{\frac{\chi_M^{corr.} \cdot T}{5 \times 10^3}}$$

1.3.3. IR spectroscopy

Infrared spectroscopy (IR spectroscopy) is the subset of spectroscopy that deals with the Infrared part of the electromagnetic spectrum. As with all spectroscopic techniques, it can be used to identify a compound and to investigate the composition of a sample.

Infrared spectroscopy works because chemical bonds have specific frequencies at which they vibrate corresponding to energy levels. The resonant frequencies or vibrational frequencies are determined by the shape of the molecular potential energy surfaces, the masses of the atoms and, eventually by the associated vibronic coupling. In order for a vibrational mode in a molecule to be IR active, it must be associated with changes in the permanent dipole [43].

Sample preparation method is to grind a quantity of the sample with a specially purified salt (usually potassium bromide) finely (to remove scattering effects from large crystals). This powder mixture is then crushed in a mechanical die press to form a translucent pellet through which the beam of the spectrometer can pass.

1.3.4. Electronic spectroscopy

Electronic spectroscopy is an analytical technique to study the electronic structure and its dynamics in atoms and molecules. In general an excitation source such as X-rays, electrons, or synchrotron radiation will eject an electron from an inner-shell orbital of an atom.

The Beer-Lambert law states that the absorbance of a solution is due to the solution's concentration. Thus UV/vis spectroscopy can be used to determine the concentration of a solution. It is necessary to know how quickly the absorbance changes with concentration.

The method is most often used in a quantitative way to determine concentrations of an absorbing species in solution, using the Beer-Lambert law:

$$A = -\log(I/I_0) = \epsilon \cdot c \cdot l$$

where A is the measured absorbance, I_0 is the intensity of the incident light at a given wavelength, I is the transmitted intensity, l is the path length through the sample, and c is the concentration of the absorbing species.

Samples for UV/vis spectrophotometry are most often liquids, although the absorbance of gases and even of solids can also be measured. Samples are typically placed in a transparent cell, known as a cuvette. Cuvettes are typically rectangular in shape, commonly with an internal width of 1 cm. (This width becomes the path length, l , in the Beer-Lambert law). Test tubes can also be used as cuvettes in some instruments. The best cuvettes are made of high quality quartz, although glass or plastic cuvettes are common. (Glass and most plastics absorb in the UV, which limits their usefulness to visible wavelengths.)

An ultraviolet-visible spectrum is essentially a graph of light absorbance versus wavelength in a range of ultraviolet or visible regions. Such a spectrum can often be produced by a more sophisticated spectrophotometer. Wavelength is often represented by the symbol λ . For the given substance, the wavelength at which maximum absorption in the spectrum occurs is called λ_{\max} , pronounced "Lambda-max".

1.3.5. EPR spectroscopy

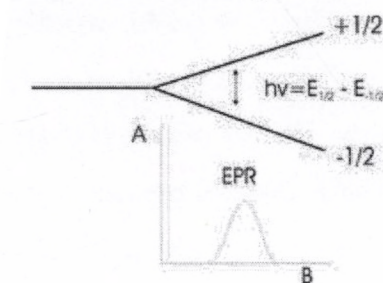
Electron Paramagnetic Resonance (EPR) is a spectroscopic technique which detects species that have unpaired electrons, generally meaning that the molecule in question is a free radical, if it is an organic molecule, or that it has transition metal ions if it is an inorganic complex. The basic physical concepts of the technique are

analogous to those of NMR, but instead of the spins of the atom's nuclei, electron spins are excited. Because of the difference in mass between nuclei and electrons, weaker magnetic fields and higher frequencies are used.

An electron has a magnetic moment. When placed in an external magnetic field of strength B_0 , this magnetic moment can align itself parallel or antiparallel to the external field. The former is at lower energy state than the latter (this is the Zeeman effect), and the energy separation between the two is $\Delta E = g_e \mu_B B_0$, where g_e is the gyromagnetic ratio of the electron, the ratio of its magnetic dipole moment to its angular momentum, and μ_B is the Bohr magneton. To move between the two energy levels, the electron can absorb electromagnetic radiation of the correct energy:

$$\Delta E = h\nu = g_e \mu_B B_0$$

where $h\nu$ is the microwave energy, and this is the fundamental equation of EPR spectroscopy. The paramagnetic centre is placed in a magnetic field and the electron caused to resonate between the two states; the energy absorbed as it does so is monitored, and converted into the EPR spectrum.



EPR signals can be generated by resonant energy absorption measurements made at different electromagnetic radiation frequencies ν in a constant external magnetic field. Measurements can be provided by changing the magnetic field B and using a constant frequency radiation. This means that an EPR spectrum is normally plotted with the magnetic field along the X-axis, with peaks at the field

that cause resonance.

1.3.6. NMR spectroscopy

Nuclear Magnetic Resonance is a physical phenomenon based upon the magnetic properties of an atom's nucleus. All nuclei that contain odd numbers of nucleons and some that contain even numbers of nucleons have an intrinsic magnetic moment. The most commonly used nuclei are hydrogen-1 and carbon-13, although certain isotopes of many other elements nuclei can also be observed.

1.3.7. X-ray crystallography

Crystallography is the experimental science of determining the arrangement of atoms in solids. In order for an object to be seen, its size needs to be at least half the wavelength of the light being used to see it. Since visible light has a wavelength much longer than the distance between atoms, it is useless to see molecules. In order to see molecules it is necessary to use a form of electromagnetic radiation with a wavelength on the order of bond lengths, such as X-rays. When X-rays are beamed at the crystal, electrons diffract the X-rays, which cause a diffraction pattern. Using the mathematical Fourier transform, these patterns can convert into electron density maps. These maps show contour lines of electron density. Since electrons more or less surround atoms uniformly, it is possible to determine where atoms are located. Unfortunately since hydrogen has only one electron, it is difficult to map hydrogens. To get a three dimensional picture, the crystal is rotated while a computerized detector produces two dimensional electron density maps for each angle of rotation. The third dimension comes from comparing the rotation of the crystal with the series of images. Computer programs use this method to come up with three dimensional spatial coordinates.

Single crystal X-ray crystallographic analyses of the compounds were carried out using Siemens SMART CCD area-detector diffractometer at the Analytical Science Division, Bhavanagar, Gujarat, India and the Argus (Nonius, MACH3 software) at Single Crystal X-Ray Diffraction Facility, IIT, Bombay. The structures were solved by direct methods and refined by least-square on F_0^2 using the SHELXL software package [44].

1.4. Significance of thiosemicarbazones and their metal complexes

Thiosemicarbazones are an important group of multidentate ligands with potential binding sites available for a wide variety of metal ions. These thiourea derivatives find substantial applications in different facets of different contemporary scientific research. Their biological activity depends on the parent aldehyde or ketone [45], and their potential use as antimalarial agents was first recognized with N(4)-substituted 2-acetylpyridine thiosemicarbazones [46]. The versatile antimicrobial nature of thiosemicarbazones and their metal complexes has been the focus of our research for the past decade [47, 48]. The metal complexes show more activities as compared to the free thiosemicarbazones and semicarbazones. It may have numerous applications *e.g.* anticancer [49], fungicides, antibacterial [50, 51], antiviral [52], antifungal [53], anti HIV [54, 55], antitumor activity [56, 57] and other biological activities [58-60]. Particularly first row of transition metal complexes with such ligands have a wide range of biological activities [61-63].

Base adducts of Cu(II) complexes have been prepared with N(4)-phenyl salicylaldehyde thiosemicarbazones. The thiosemicarbazones and its complexes showed growth inhibitory activity against the human pathogenic bacteria, *Salmonella typhi*, *Shigella dysenteriae*, *Staphylococcus*, *Photobacterium sp.* and *S. aureus* and the complexes against plant pathogenic fungi. An increase in the

coordination number from 4 to 5 in the complexes led to higher activity, probably due to increase in lipophilicity [64].

As early as 1946, Demagle reported that some thiosemicarbazones of cyclic aldehydes or ketones possessed antitubercular activity *in vitro* [65]. Screening revealed that only certain substituted benzaldehyde and heterocyclic thiosemicarbazones possess antitubercular activity [66, 67]. In some instances activity *in vivo* was also shown in animals and some compounds have been used in the treatment of lupus and pulmonary tuberculosis with encouraging results [68]. The antitubercular activity of a series of semi and thiosemicarbazones has been tested by Hoggarth *et al.* [66] namely a) thiosemicarbazones of variously substituted benzaldehydes b) thiosemicarbazones of heterocyclic aldehydes and c) ketone thiosemicarbazones.

The literature reports many studies on the antifungal activity of thiosemicarbazones and their metal complexes. Early in 1960, forty thiosemicarbazones derived from aliphatic and aromatic aldehydes and ketones together with many of their metal complexes were examined for toxicity against *chaetomium globosum*. Some of the ligands showed activity while the complexes were inactive [69]. Also metal complexes of p-anisaldehyde thiosemicarbazones have been screened for antifungal activity on *Allernarai sp.*, *Paecilomyces sp.* and *Pestalotia sp.* In some cases the complexes were more active than the free ligand [70].

The antiviral activity of thiosemicarbazones was first demonstrated by Hamre *et al.* [71, 72], who showed that p-acetamidobenzaldehyde-3-thiosemicarbazone and several of its derivatives were active against vaccine virus in mice. These studies were extended to include thiosemicarbazones of isatin, benzene, thiophene, pyridine and quinoline derivatives, which also showed activity

against vaccine-induced encephalitis. The nature of the aldehyde/ketone moiety was not as significant as the presence of the thiosemicarbazide side chain; the later was deemed essential for antiviral activity. The thiosemicarbazones have also been tested against a variety of other viral infections including herpesvirus, adenovirus, poliovirus, rhinovirus and RNA tumor virus with mixed results [73]. For example, the isatin thiosemicarbazones were found to be less active against herpes simplex virus (HSV) [74-76]; the heterocyclic thiosemicarbazone derivatives were active against HSV-1 and HSV-2 types [77].

Thiosemicarbazones exhibit antimalarial activities. An extensive series of thiosemicarbazones obtained from 2-acetylpyridine was tested by Klayman *et al.* [46] for antimalarial activity against *Plasmodium berghei* in mice. The molecular features essential for activity were found to be a 2-pyridylethylidene moiety, the presence of the thiocarbonyl sulfur, and, certain, bulky or cyclic substituents at the terminal N(4)-atom. The most active 2-acetylpyridine thiosemicarbazones were N(4)-phenyl and those with azacyclic substituents.

Thiosemicarbazone's complexes of certain radionuclides have demonstrated their potential as radiopharmaceuticals for diagnosis purposes as well as for radiotherapy. ^{62}Cu -ATSM (ASTSM- diacetyl-bis(N(4)-methyl thiosemicarbazone) is a promising PET tracer for noninvasive hypoxic tumor imaging [78-80].

Thiosemicarbazones shows antitumor activity also. Bis(thiosemicarbazones) [81-84] and N-heterocyclic thiosemicarbazones comprise two interesting series of experimental chemotherapeutic agents. 2-formylpyridine thiosemicarbazone, the first of the latter series to be examined for biological activity, showed mild antileukemic activity against 1-1210 tumor in mice [84]. However, it was found to be toxic at the therapeutic dose levels which led to synthesis of other aromatic and heterocyclic thiosemicarbazones as potential agents

[84]. However, the only active anticancer compounds besides glyoxal bis(thiosemicarbazones) were the N-heterocyclic thiosemicarbazones [85], 2-formyl-3-hydroxypyridine thiosemicarbazone [86] and 2-formyl-5-hydroxypyridine thiosemicarbazone [87]. All of the active 2-heterocyclic thiosemicarbazones are potent inhibitors of the biosynthesis of DNA in mammalian cells [88].

1.5. Objective and scope of the present work

Thiosemicarbazones constitute an important class of nitrogen sulfur donor ligands, because of the highly interesting chemical, biological and medicinal properties [1, 89]. The coordination chemistry of ONS donor ligands has been of considerable interest due to their remarkable structural and biological properties [17, 47]. The biological activity of certain thiosemicarbazones is due to the ability to form terdentate chelates with transition metal ions bonding through oxygen, nitrogen and sulfur atoms O-N-S. In some cases, lowering of the thiosemicarbazone's denticity leads to a decrease of activity [89] but the literature reports examples of biologically significant bidentate thiosemicarbazones. Thiosemicarbazones of salicylaldehyde [90, 91] and its derivatives are a class of versatile tridentate ONS donors capable of stabilizing both higher and lower oxidation states of transition metal ions [29, 30, 92]. Although capable of deprotonation at both the phenol and thioamide functions to give a dianionic ligand, they can also act as monoanionic chelating ligands, coordinating to a metal center through the deprotonated phenolic oxygen, the thione sulfur and the azomethine nitrogen [29]. The dianionic form of the ligand is favored at higher pH, whereas the monoanionic form is promoted at low pH.

Transition metal ions like Cu(II), Ni(II), Co(III), Zn(II) and Cd(II) were used for the synthesis of complexes. We have undertaken the work along the following lines:

- To synthesize the following N(4)-ring incorporated NS/ONS donor ligands :
 - benzaldehyde 3-hexamethyleneiminylthiosemicarbazone (HL¹)
 - 2-hydroxybenzaldehyde 3-hexamethyleneiminylthiosemicarbazone (H₂L²)
 - 4-methoxybenzaldehyde 3-hexamethyleneiminylthiosemicarbazone (HL³)
 - 2-hydroxybenzaldehyde 3-tetramethyleneiminylthiosemicarbazone (H₂L⁴)
- To characterize these ligands using elemental analyses, IR, electronic and ¹H NMR spectral studies.
- To synthesize Cu(II), Ni(II), Co(III), Zn(II), and Cd(II) complexes and characterization of these complexes using elemental analyses, magnetic susceptibility measurements, IR, electronic, EPR and ¹H NMR spectral studies.
- To isolate single crystals of the ligand and metal complexes and determine their structures using X-ray diffraction studies.

References

1. M.J.M. Campbell, *Coord. Chem. Rev.* 15 (1975) 279.
2. S. Padhye, G.B. Kauffman, *Coord. Chem. Rev.* 63 (1985) 127.
3. D.X. West, S.B. Padhye, P.B. Sonawane, *Struct. Bonding (Berlin)* 76 (1991) 4.
4. D.X. West, A.E. Liberta, S.B. Padhye, R.C. Chikate, P.B. Sonawane, A.S. Kumbhar, R.G. Yerande, *Coord. Chem. Rev.* 123 (1993) 49.
5. M.B. Ferrari, G.G. Fava, P. Tarasconi, C. Pelizzi, *J. Chem. Soc., Dalton Trans.* (1989) 361.

6. M.B. Ferrari, G.G. Fava, M. Lanfranchi, C. Pelizzi, P. Trasconi, *J. Chem. Soc., Dalton Trans.* (1991) 1951.
7. M.B. Ferrari, G.G. Fava, M. Lanfranchi, C. Pelizzi, P. Trasconi, *Inorg. Chim. Acta* 181 (1992) 253.
8. K.A. Jensen, E. Rancke-Madsen, *Z. Anorg. Allg. Chem.* 219 (1934) 243.
9. C.E. Holloway, M. Melnik, *J. Organomet. Chem.* 495 (1995) 1.
10. C.E. Holloway, M. Melnik, *Main Group Met. Chem.* 17 (1994) 799.
11. A. Varshney, J.P. Tandon, *Indian J. Chem. A* 24 (1985) 70.
12. D.L. Klayman, J.M. Hoch, J.P. Scovill, C. Lambross, A.S. Dobeck, *J. Pharm. Sci.* 73 (1984) 1763.
13. R.H. Dodd, C. Quannes, M. Robert Gero, P. Potier, *J. Med. Chem.* 32 (1989) 1272.
14. E.S. Raper, *Coord. Chem. Rev.* 61 (1985) 115.
15. E.S. Raper, *Coord. Chem. Rev.* 153 (1996) 199.
16. I.H. Hall, K.G. Rajendran, D.X. West, A.E. Liberta, *Anticancer Drugs* 4 (1993) 241.
17. J.S. Casas, M.S. Garcia-Tasenda, J. Sordo, *Coord. Chem. Rev.* 209 (2000) 197.
18. B.S. Garg, M.R.P. Kurup, S.K. Jain, Y.K. Bhoon, *Trans. Met. Chem.* 16 (1991) 111.
19. D.X. West, J.P. Scovill, J. Silverton, A. Bavoso, *Trans. Met. Chem.* 11 (1986) 123.
20. D.X. West, R.M. Makeever, J.P. Scovill, D.L. Klayman, *Polyhedron* 3 (1984) 947.
21. N.V. Gerbeleu, M.D. Revenco, V.M. Leovac, *Russ. J. Inorg. Chem.* 22 (1977) 1009.

22. C.K. Bhaskare, P.P. Hankare, R.S. Ranpure, *J. Indian Chem. Soc.* 65 (1988) 121.
23. D.X. West, G.A. Bain, R.J. Butcher, J.P. Jasinski, Y. Li, R.Y. Pozdniakiv, J.Valdez-Martinez, R.A. Toscano, S.H. Ortega, *Polyhedron* 15 (1996) 665.
24. P. Domiano, G.G. Fava, M. Nardelli, P. Sagarabotto, *Acta Crystallogr. B*25 (1969) 343; G. D. Andreetti, G. Fava, M. Nardelli, P. Sagarabotto, *Acta Crystallogr. B*26 (1970) 1005.
25. N. V. Gebeleu, M. D. Revenko, V. M. Leovats, *Russ. J. Inorg. Chem.* 22 (1977) 1009.
26. M.B. Ferrari, G. Fava, C. Pelizzi, *J. Chem. Soc., Dalton Trans.* (1992) 2153.
27. M. Soriano-Garcia, R.A. Toscano, J. Valdes-Martinez, J.M. Fernandez, *Acta Crystallogr. C*41 (1985) 498.
28. L.H. Reddy, K.G. Reddy, D.V. Reddy, *Proc. Ind. Sci. Acad.* 55 (1989) 517.
29. S. Purohit, A.P. Koley, L.S. Prasad, P.T. Manoharan, S. Ghosh, *Inorg. Chem.* 28 (1989) 3735.
30. A.P. Koley, S. Purohit, S. Ghosh, L.S. Prasad, P.T. Manoharan, *J. Chem. Soc., Dalton Trans.* (1988) 2607.
31. H.J. Kruger, G. Peng, R.H. Holm, *Inorg. Chem.* 30 (1991) 734.
32. R.H. Holm, *Coord. Chem.Rev.* 100 (1990)183.
33. L.S. Meriwether, W.F. Marzluff, W.G. Hodgson, *Nature* 212 (1966) 465.
34. R.J. Greenwood, G.L. Wilson, J.R. Pilbrow, A.G. Wedd, *J. Am. Chem. Soc.* 117 (1993) 5385.
35. K.D. Karlin, J. Zubieta (Editors), *Copper Coordination Chemistry; Biochemical and Inorganic Perspectives.* Adenine Press, New York (1983); *Biological and Inorganic Copper Chemistry.* Adenine Press, New York (1986).

36. N.V. Gerbeleu, K.I. Turta, J.T. Kashkaval, F. Tui, *Russ. J. Inorg. Chem.* 26 (1981) 1154.
37. M. Mathew, G.J. Palenik, G.R. Clark, *Inorg. Chem.* 12 (1973) 446.
38. U.N. Pandey, *J. Ind. Chem. Soc.* 55 (1978) 645.
39. Y.K. Bhoon, S. Mitra, J.P. Scovill, D.L. Klayman, *Trans. Met. Chem.* 7 (1982) 264.
40. M.A. Ali, S.E. Livingstone, *Coord. Chem. Rev.* 13 (1974) 101.
41. R.K.Y. Ho, S.E. Livingstone, T.N. Lockyer, *Aust. J. Chem.* 19 (1966) 1179.
42. J.E. Huheey, E.A. Keiter, R.L. Keiter, *Inorganic Chemistry*, 4th ed., Addison-Wesley publishing company, India, 1993.
43. A. Bozkurt, A. Rosen, H. Rosen, B. Onaral, *Biomedical Engineering Online* 4 (2005) 29.
44. G.M. Sheldrick, *SHELXL-97 and SHELXS-97 Program for the solution of Crystal Structures*, University of Göttingen, Germany, 1997.
45. S. Padhye, G.B. Kauffman, *Coord. Chem.* 63 (1985) 127.
46. D.L. Klayman, J.F. Bartoserich, T.S. Griffin, C.J. Manson, J.P. Scovill, *J. Med. Chem.* 22 (1979) 885.
47. R.P. John, A. Sreekanth, M.R.P. Kurup, S.M. Mobin, *Polyhedron* 21 (2002) 2515.
48. A. Sreekanth, M.R.P. Kurup, *Polyhedron* 23 (2004) 969.
49. Min. Wang, Liu-Fang. Wang, Yi-Zhi Ligands, Qin-Xi-Li, *Trans. Met. Chem.* 26 (2001) 307.
50. S.D. Dhumwad, K.B. Gudasi, T.R. Goudar, *Ind. J. Chem.* 33A (1994) 320.
51. N.N. Gulerman, S. Rollas, H. Erdeniz, M. Kiraj, *J. Pharm. Sci.* 26 (2001) 1.
52. K.H. Reddy, P.S. Reddy, P.R. Babu, *Trans. Met. Chem.* 25 (2000) 154.
53. H. Singh, L.D.S. Yadav, S.B.S. Mishra, *J. Inorg. Nucl. Chem.* 43 (1981) 1701.

54. S. Chandra, Sangeetha, *Spectro. Chim. Acta* 60A (2004) 147.
55. L. Mishra, A.K. Singh, Y. Maeda, *J. Ind. Chem. Soc.* 9 (2005) 131.
56. S. Chandra, L.K. Gupta, K.K. Sharma, *J. Saudi. Chem. Soc.* 9 (2005) 131.
57. M.A. Akbar, H.A. Mirza, A. Monsur, M. Nazimuddin, *Polyhedron* 20 (2001) 1045.
58. N.K. Singh, S.B. Singh, *Ind. J. Chem.* 40A (2001) 1070.
59. V. Mishra, S.N. Pandeya, S. Ananthan, *Acta Pharm. Turc.* 42 (2000) 139.
60. D. Jamal, M.A. Quraishi, *J. Electrom. Soc. India* 49 (2000) 56.
61. E.M. Jouad, A. Riou, M. Allian, M.A. Khan, G.M. Bouet, *Polyhedron* 20 (2001) 67.
62. Z. Xinde, C. Wang, Z. Lu, Y. Dang, *Trans. Met. Chem.* 22 (1997) 13.
63. S. Chandra, K. Gupta, *Trans. Met. Chem.* 27 (2002) 196.
64. P. Bindu, M.R.P. Kurup, T.R. Satyakeerthy, *Polyhedron* 18 (1999) 321.
65. G. Domagk, R. Dimer, O. Lenz, B.K. Keppler, *J. Inorg. Biochem.* 59 (1995) 215.
66. E. Hoggarth, A. Martin, M. Storey, E. Young, *J. Pharmacol.* 4 (1949) 248.
67. R. Donovan, F. Pansy, G. Stryker, J. Bernestein, *J. Bacteriol.* 59 (1950) 675.
68. G. G. Domagk, *Nordisk Medicine* 39 (1948) 1322.
69. B.G. Benns, B.A. Gingras, C.H. Bayley, *Appl. Microbiology* 8 (1960) 353.
70. K.N. Thimmaiah, G.T. Chadrapa, Rangaswami, Jayarama, *Polyhedron* 3 (1984) 1237.
71. D. Hamre, K. Brownlee, R. Donovan, *J. Immunol.* 67 (1950) 305.
72. D. Hamre, J. Bernestein, R. Donovan, *Proc. Soc. Expt. Biol. Med.* 73 (1950) 229.
73. W. Levinson, W.A. Corter, In *Selective Inhibitors of Viral Functions*, CRS Press 213 (1972).
74. D. Hutfield, G. Csonka, *Lancet* 1 (1964) 329.

75. G. Underwood, F. Nichol, *Appl. Microbiol.* 22 (1971) 558.
76. T. Munro, L. Sabena, *J. Gen. Virol.* 7 (1970) 55.
77. C. Shipman, S.H. Smith, J.C. Drach, D.L. Klayman, *Antimicrob. Agents Chemother.* 19 (1981) 682.
78. P.J. Blower, J.R. Dilworth, R.I. Maurer, G.D. Mullen, C.A. Reynolds, Y. Zheng, J. *Inorg. Biochem.* 85(1) (2001) 15.
79. J.R. Ballinger, *Semic. Nucl. Med.* 31(4) (2001) 321.
80. K.S. Chao, W.R. Bosch, S. Mutic, J.S. Lewis, F. Dehdashti, M.A. Mintun, J.F. Dempsey, C.A. Perez, J.A. Purdy, M.J. Welch, *Int. J. Radiat. Oncol. Biol. Phys.* 5 (2001) 1171.
81. F.A. French, R. Freedlander, *Cancer Res.* 21 (1960) 505.
82. W. Regelson, J.F. Holland, R.W. Talley, *Cancer Chemother. Rep.* 51 (1967) 171.
83. W.K. Subczynski, W.E. Antholine, J.S. Hyde, D.H. Petering, *J. Am. Chem. Soc.* 109 (1987) 46.
84. R.W. Brockman, J.R. Thomson, M.J. Bell, H.E. Skipper, *Cancer Res.* 21 (1956) 349.
85. F.A. French, E.J. Blanz, *Cancer Res.* 21 (1961) 349.
86. F.A. French, E.J. Blanz, *Cancer Res.* 26 (1966) 1638.
87. F.A. French, E.J. Blanz, *Cancer Res.* 9 (1966) 585.
88. A.C. Sartorelli, *Biochem. Biophys. Res. Comm.* 27 (1967) 26.
89. D.X. West, S.B. Padhye, P.B. Sonawane, *Struct. Bonding, Springer, Heidelberg* 76 (1991) 1.
90. V.M. Leovac, A.F. Petrovic, *Trans. Met. Chem.* 8 (1983) 337.
91. A.F. Petrovic, M.L. Vukadin, B. Riber, *Trans. Met. Chem.* 11 (1986) 207.
92. A.P. Koley, R. Nirimala, L.S. Prasad, S. Ghosh, P.T. Manoharan, *Inorg. Chem.* 31(1992) 1764.

Synthesis and characterization of thiosemicarbazone ligands

2.1. Introduction

The coordinating ability of thiosemicarbazones to both transition and main group metallic cations is attributed to the extended delocalization of electron density over the thiosemicarbazone skeleton, which is enhanced by substitution at N(4)-position. Condensation of thiosemicarbazides with aldehydes or ketones extends the electron delocalization along azomethine bond. 2-hydroxybenzaldehyde N(4)-substituted thiosemicarbazones, as well as heterocyclic thiosemicarbazones, which derives from the presence of several potential donor atoms, their flexibility, and their ability to coordinate in either neutral or deprotonated forms, have been the subject of extensive investigations [1], because of their ability to strongly coordinate metal ions as tridentate ligands and their wide spectrum of biological applications [2]. Due to their good complexing properties, biological activity, and analytical application, semi-/thiosemi-/isothiosemicarbazides and their Schiff bases of different denticity, as well as their metal complexes, have been the subject of many studies. Apparently, the most numerous among them are the complexes with tridentate salicylaldehyde semi-/thiosemi-/isothiosemicarbazones [3].

Thiosemicarbazone of salicylaldehyde [4, 5] and its derivatives are a class of versatile tridentate ONS donors capable of stabilizing both higher and lower oxidation states of transition metal ions [6-8]. Although capable of deprotonation at

both the phenol and thioamide functions to give a dianionic ligand, they can also act as monoanionic chelating ligands, coordinating to a metal centre through the deprotonated phenolic oxygen, the thione sulfur and azomethine nitrogen [6]. The dianionic form of the ligand is favored at higher pH, whereas the monoanionic form is promoted at low pH. However, the coordination chemistry of substituted or unsubstituted thiosemicarbazones of salicylaldehyde is quite unexplored with a few previous reports [9-12]. This prompted our study into the synthesis and characterization of substituted thiosemicarbazones using aromatic aldehydes and its metal complexes. Here we have synthesized the following four new ligands using benzaldehyde, 2-hydroxybenzaldehyde, 4-methoxybenzaldehyde, 3-hexamethyleneiminyl thiosemicarbazide and 3-tetramethyleneiminyl thiosemicarbazide.

- Benzaldehyde 3-hexamethyleneiminylthiosemicarbazone [HL¹]
- 2-Hydroxybenzaldehyde 3-hexamethyleneiminylthiosemicarbazone [H₂L²]
- 4-Methoxybenzaldehyde 3-hexamethyleneiminylthiosemicarbazone [HL³]
- 2-Hydroxybenzaldehyde 3-tetramethyleneiminylthiosemicarbazone [H₂L⁴]

This chapter deals with the synthesis and spectral characterization of thiosemicarbazone ligands. It also deals with X-ray diffraction studies of H₂L². The IUPAC numbering scheme is not very appropriate for describing the structural data of thiosemicarbazones because the numbering of C and N atoms on the thiosemicarbazone chain does not run into the numbering of substituted groups. This is probably why a variety of different numbering schemes have been used in the literature. In this chapter, the following numbering scheme is used for the four ligands, except in X-ray diffraction studies. The structure and numbering schemes are given in Figure 2.1

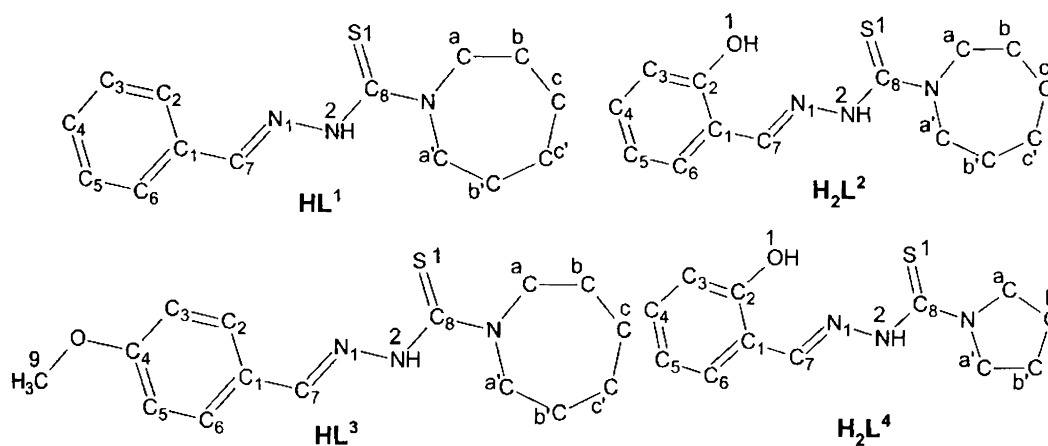


Figure 2.1. Structures and numbering schemes of the thiosemicarbazones

2.2. Experimental

2.2.1 Materials

The reagent grade benzaldehyde (Merck), 4-methoxybenzaldehyde (SRL chemicals), 2-hydroxybenzaldehyde (SRL chemicals), carbon disulfide (Merck), N-methylaniline (Merck), sodium chloroacetate (Merck) and hydrazine hydrate 98% (Glaxo–Fine Chemicals) were used as received. Hexamethyleneimine (Fluka) and tetramethyleneimine (Fluka) were used as received. The solvents were purified and dried by using standard methods and procedures.

2.2.2 Synthesis of ligand precursors

Step 1:-

Preparation of carboxy methyl-N-methyl-N-phenyl dithiocarbamate

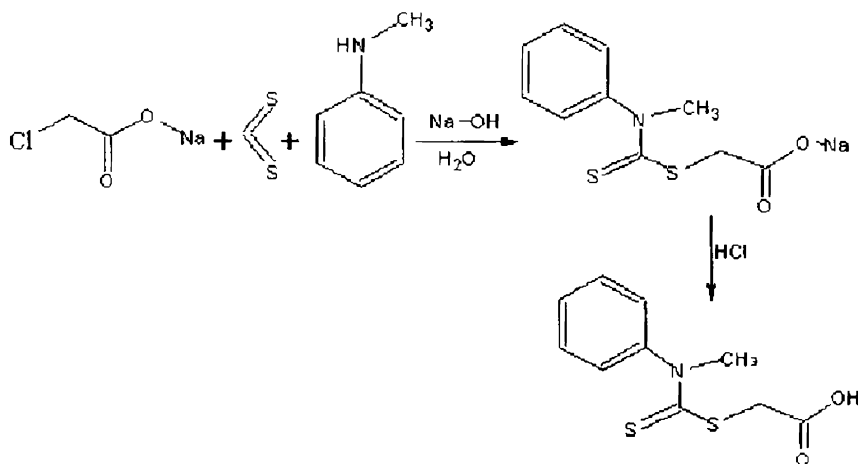
A mixture consisting of 12 ml CS₂ (15.2 g, 0.2 mol) and 21.6 ml (21.2 g, 0.2 mol) of N-methylaniline were stirred with a solution of 8.4 g (0.21 mol) of NaOH in 250 ml water for 4 h. When the organic layer had disappeared, the straw-colored solution was treated with 23.2 g of sodium chloroacetate and allowed to stand

overnight (17 h). The solution was acidified with conc. HCl (25 ml) and the solid that separated was washed with water, filtered and dried. This afforded 39.7 g (82%) of the pale buff colored carboxymethyl-N-methyl-N-phenyl dithiocarbamate (m.p 197-198 °C). (Scheme 2.1).

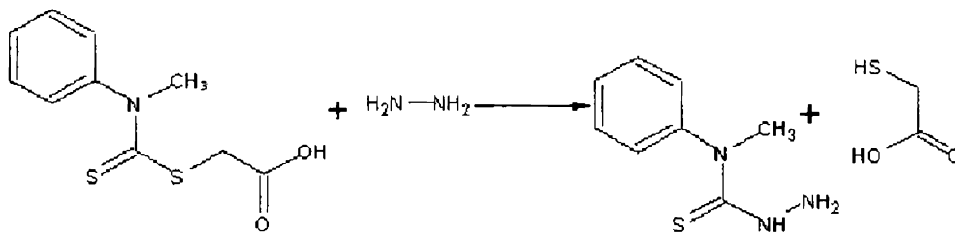
Step 2:-

Preparation of N-methyl-N-phenyl-3-thiosemicarbazide

A mixture of 17.8 g of carboxymethyl-N-methyl-N-phenyl dithiocarbamate, 20 ml of hydrazine hydrate and 10 ml of water was heated on the rings of the water bath for 22 minutes. The compound separated was filtered, washed with water, dried and recrystallized from 2:1 alcohol. Yield 78%. m.p. 124-125 °C (Scheme 2.2) [13].



Scheme 2.1

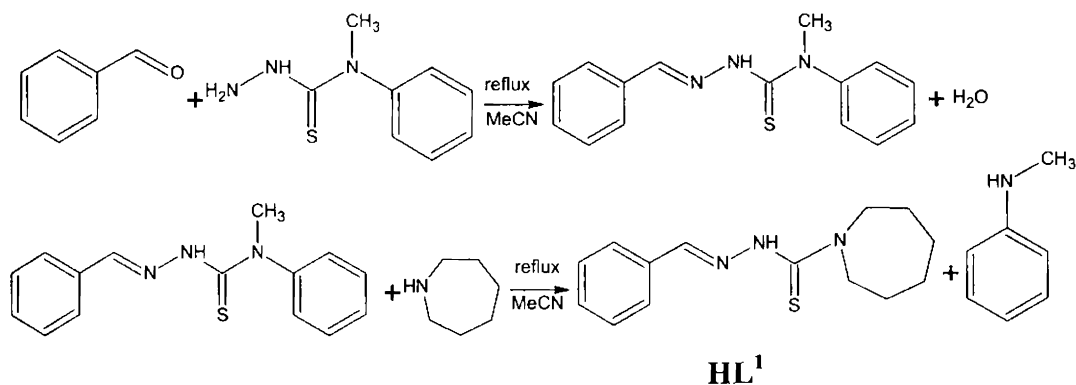


Scheme 2.2

2.2.3 Synthesis of ligands

i) Benzaldehyde 3-hexamethyleneiminyl thiosemicarbazone [HL¹]

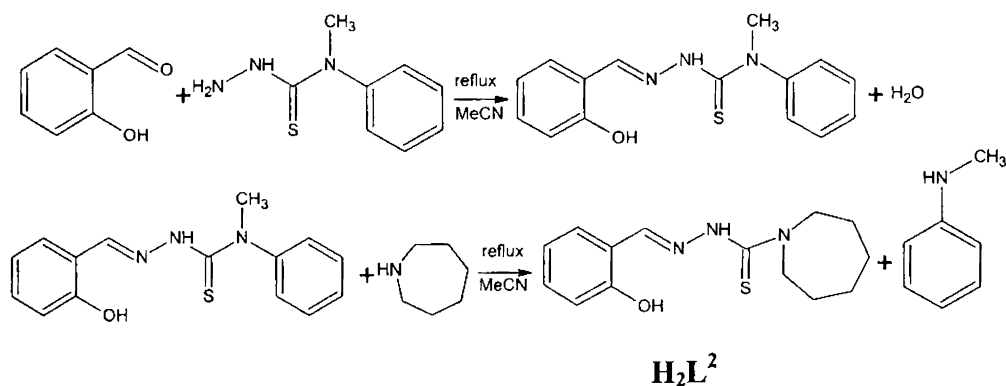
A solution of 1 g (5.52 mmol) of 4-methyl-4-phenyl-3-thiosemicarbazide in 5 ml acetonitrile was treated with 0.586 g (5.52 mmol) of benzaldehyde and 0.547 g (5.52 mmol) of hexamethyleneimine and refluxed for 40 minutes. The solution was chilled (overnight) and fine colorless needles of the compound separated out. The solution was filtered, washed well with cold acetonitrile. The compound was recrystallized from ethanol and dried *in vacuo* over P₄O₁₀ (Scheme 2.3) [14].



Scheme 2.3

ii) 2-Hydroxybenzaldehyde 3-hexamethyleneiminyl thiosemicarbazone [H₂L²]

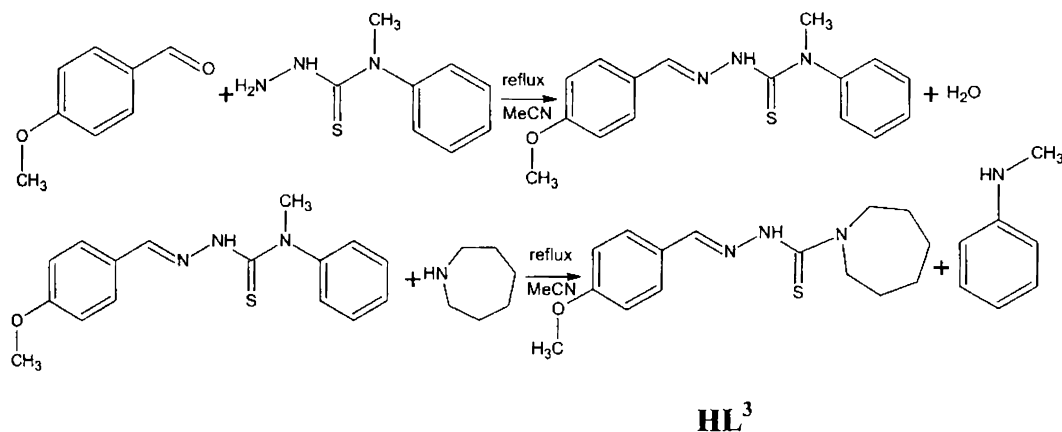
A solution of 1 g (5.52 mmol) of 4-methyl-4-phenyl-3-thiosemicarbazide in 5 ml acetonitrile was treated with 0.674 g (5.52 mmol) of 2-hydroxybenzaldehyde and 0.547 g (5.52 mmol) of hexamethyleneimine and refluxed for 40 minutes. The solution was chilled (overnight) and the crystals that separated were filtered and washed well with cold acetonitrile. The compound was recrystallized from ethanol and dried *in vacuo* over P₄O₁₀ (Scheme 2.4).



Scheme 2.4

iii) 4-Methoxybenzaldehyde 3-hexamethyleneiminyl thiosemicarbazone [HL³]

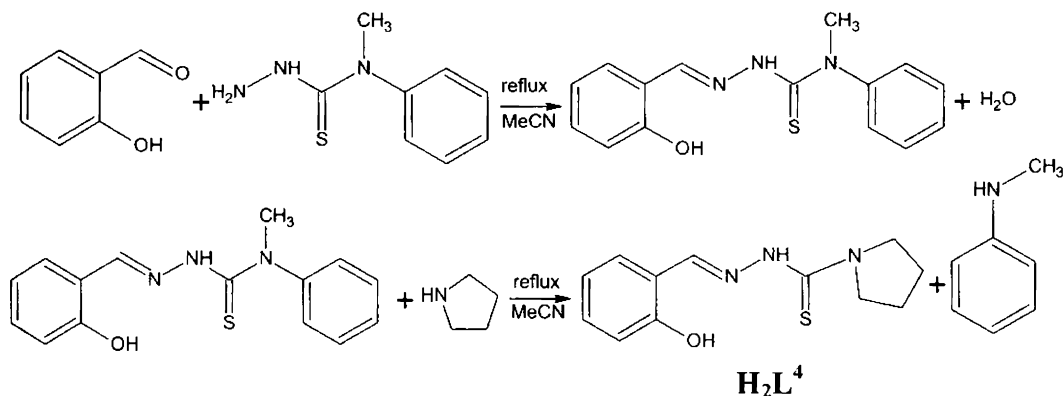
A solution of 1 g (5.52 mmol) of 4-methyl-4-phenyl-3-thiosemicarbazide in 5 ml acetonitrile was treated with 0.752 g (5.52 mmol) of 4-methoxybenzaldehyde and 0.547 g (5.52 mmol) of hexamethyleneimine and refluxed for 40 minutes. The solution was chilled (overnight) and colorless needles of the compound separated out. The solution was filtered, washed well with cold acetonitrile. The compound was recrystallized from ethanol and dried *in vacuo* over P₄O₁₀ (Scheme 2.5).



Scheme 2.5

iii) 2-Hydroxybenzaldehyde 3-tetramethyleneiminyl thiosemicarbazone [H_2L^4]

A solution of 1 g (5.52 mmol) of 4-methyl-4-phenyl-3-thiosemicarbazide in 5 ml acetonitrile was treated with 0.674 g (5.52 mmol) of 2-hydroxybenzaldehyde and 0.393 g (5.52 mmol) of pyrrolidine and refluxed for 40 minutes. The solution was chilled (overnight) and fine colorless needles of the compound separated out. The solution was filtered, washed well with cold acetonitrile. The compound was recrystallized from ethanol and dried *in vacuo* over P_4O_{10} (Scheme 2.6).



Scheme 2.6

2.3. Characterization techniques

The ligands were characterized by using partial elemental analyses, IR spectra, electronic spectra, 1H NMR spectra and single crystal X-ray diffraction. The details regarding these techniques are given in Chapter 1.

2.3.1. X-ray crystallography

The colorless block crystals of H_2L^2 , suitable for X-ray diffraction studies were obtained by slow evaporation of its solution in ethanol. A crystal having approximate dimensions $0.35 \times 0.30 \times 0.25 \text{ mm}^3$ was sealed in a glass capillary and intensity data was measured at room temperature (293 K). The crystal structure data and structure refinement parameters for the compound are given in Table 2.1.

The X-ray diffraction data was measured at room temperature and data acquisition and cell refinement was done using the Argus (Nonius, MACH3 software) [15]. The Maxus (Nonius software) were used for data reduction [16]. The structure was solved by direct methods with the program SHELXS-97 and refined by full matrix least squares on F^2 using SHELXL-97 [17]. The graphical tool used was DIAMOND version 3.1d [18] and PLATON [19]. All C-bound H atoms were positioned geometrically and treated riding on their parent C atoms, with C–H distances of 0.93 and 0.97 Å. All non-hydrogen atoms were refined anisotropically, atom H1O1 {on O1} atom H2N (on N2) were located from different maps and were refined with isotropic displacement parameters.

Table 2.1. Crystal data and structure refinement parameters for H₂L²

Empirical formula	C ₁₄ H ₁₉ N ₃ O ₃ S
Formula weight	277.38
Temperature	293(2) K
Wavelength	0.71073 Å
Crystal system	Monoclinic
Space group	<i>P</i> 2 ₁ / <i>n</i>
Unit cell dimensions	a = 6.448 (11) Å α = 90° b = 14.099(2) Å β = 94.617(12)° c = 15.924(2) Å γ = 90°
Volume	1443.0(4) Å ³
Z	4
Density (calculated)	1.277 g/cm ³
Absorption coefficient	0.221 mm ⁻¹
F(000)	592
Crystal size	0.35 x 0.30 x 0.25 mm ³
θ range for data collection	1.93 to 24.98 °
Index ranges	-7 ≤ h ≤ 0, -16 ≤ k ≤ 0, -18 ≤ l ≤ 18
Reflections collected	2764
Independent reflections	2524 [R(int) = 0.0203]
Refinement method	Full-matrix least-squares on F ²
Data / restraints / parameters	2524 / 0 / 180
Goodness-of-fit on F ²	0.981
Final R indices [I > 2σ(I)]	R ₁ = 0.0444, wR ₂ = 0.0892
R indices (all data)	R ₁ = 0.1402, wR ₂ = 0.1106
Largest diff. peak and hole	0.144 and -0.162 e.Å ⁻³

2.4. Results and discussion

The preparation of the thiosemicarbazones from 4-methyl-4-phenyl thiosemicarbazide in a single step involves a simultaneous occurrence of condensation between aromatic aldehyde and NH_2 of the thiosemicarbazide moiety and transamination in which the N-methylaniline from 4-methyl-4-phenyl thiosemicarbazide is replaced by the amine present in the solution. Since, the reaction depends on the strength of the bases, and hence N-methylaniline acts as a good leaving group in the reaction. The solvent also plays an important role in the reaction. Here, acetonitrile is used as solvent and mild refluxing condition is adopted. The ligand HL^1 , HL^3 and H_2L^4 are pale yellow in color and H_2L^2 is colorless. The analytical data of the ligands are presented in Table 2.2.

Table 2.2. Analytical data

Compound	Empirical formula	Found (Calcd.) %		
		C	H	N
HL^1	$\text{C}_{14}\text{H}_{19}\text{N}_3\text{S}$	64.14 (64.33)	7.69 (7.33)	16.01 (16.08)
H_2L^2	$\text{C}_{14}\text{H}_{19}\text{N}_3\text{OS}$	60.25 (60.62)	7.37 (6.90)	15.09 (15.15)
HL^3	$\text{C}_{15}\text{H}_{21}\text{N}_3\text{S}$	61.69 (61.82)	7.49 (7.26)	14.34 (14.42)
H_2L^4	$\text{C}_{12}\text{H}_{15}\text{N}_3\text{OS}$	57.69 (57.81)	6.29 (6.06)	16.89 (16.85)

2.4.1. Crystal structure of H_2L^2

The molecular structure of H_2L^2 along with the atom numbering scheme is given in Figure 2.2. Selected bond lengths and bond angles are listed in Table 2.3. H_2L^2 crystallizes with one molecule per asymmetric unit into triclinic crystal system with a space group of $P2_1/n$. It adopts an *E* configuration about the $\text{N}_2\text{--C}_8$ and $\text{C}_7\text{--N}_1$ bonds relative to the $\text{N}_1\text{--N}_2$ bond. The $\text{N}_1\text{--N}_2\text{--C}_8\text{--S}_1$ torsion angle of $-6.0(3)^\circ$ indicates that the thione S_1 and hydrazine N_1 atoms are in the *Z* configuration with respect to the $\text{C}_8\text{--N}_2$ bond, similar to 2-pyridineformamide 3-

hexamethyleneiminyl thiosemicarbazone [20] but in contrast to the parent salicylaldehyde thiosemicarbazone [21], where an *E* configuration exists. The *Z* configuration eliminates the possibility of any steric repulsion between the bulky rings. As a result, atom N1 lies trans to N3, with an N1–N2–C8–N3 torsion angle of 174.1 (2)°. The C8–S1 and C8–N2 bond distances are similar to the C=S double and C–N single bonds in thiosemicarbazones [21-23] and suggest the thione form for H₂L². It is implicit from the literature that the delocalization of electron density along the thiosemicarbazide moiety is a characteristic of thiosemicarbazones. For instance, the C–S distance is always an intermediate between a C–S single and a C=S double bond (1.82 and 1.56 Å, respectively) [24]. It was pointed out that apparently the parent aldehyde or ketone moiety has a strong influence on the C–S bond distance [24]. The C8–S1 bond length H₂L² is in agreement with values in salicylaldehyde thiosemicarbazone [21] and does not differ significantly from the corresponding lengths in the thiosemicarbazones of some different aldehydes and ketones [25-31]. The presence of electron density delocalization is again confirmed by the N1–N2, N2–C8 and C8–N3 bond lengths. Of the two C8–N bonds, C8–N3 is significantly shorter than C8–N2, suggesting greater double-bond character for the former bond and indicating increased electron localization at this substituted end. This is confirmed by the typical double-bond nature [1.269(3) Å] of the C7=N1 bond.

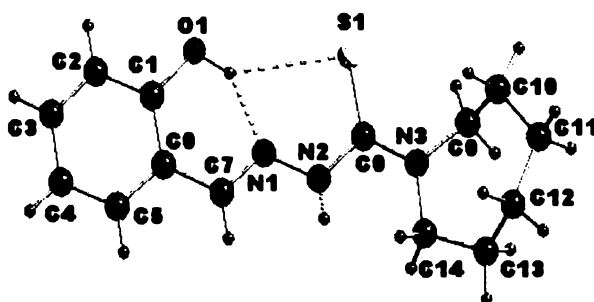


Figure 2.2. Molecular structure of H_2L^2 . Intramolecular hydrogen bonding interactions are shown as dashed lines

The salicylaldehyde thiosemicarbazone moiety, excluding atom N3, is almost planar, with a maximum deviation from the mean plane of 0.151(1) Å for atom S1. The hexamethylenimine ring adopts a chair conformation [the puckering parameters [32] are $Q_T=0.799(3)$ Å, $\theta_2=38.4(3)^\circ$, $\psi_2=45.6(3)^\circ$ and $\psi_3=73.95(3)^\circ$]. The Cg(1) plane [comprising atoms C1–C6, with a maximum deviation of 0.003(2) Å for atom C5] makes an angle of 40.59(13)° with a mean plane through the hexamethylenimine ring (atoms N3/C9–C14).

Table 2.3. Selected bond lengths (Å) and bond angles (°) for the ligand (H_2L^2)

Bond lengths (Å)		Bond angles (°)	
S1–C8	1.684(3)	C8–N2–N1	119.3(3)
N2–C8	1.362(3)	C8–N2–H2N	121.1(17)
N2–N1	1.356(3)	N1–N2–H2N	119.4(17)
N2–H2N	0.78(2)	C8–N3–C9	120.0(2)
N3–C8	1.336(3)	N1–C7–C6	119.4(2)
N3–C9	1.454(3)	C1–O1–H1O1	110(2)
C7–N1	1.269(3)	C7–N1–N2	120.0(2)
C7–C6	1.442(3)	N3–C8–N2	115.4(2)
O1–C1	1.344(3)		
O1–H1O1	0.92(3)		

There are two intramolecular and two intermolecular hydrogen bonds (Table 2.4 and Figure 2.3) in H_2L^2 . The packing of the molecules in the crystal lattice is given in Figure 2.4. The intramolecular N1⋯H1O1–O1 hydrogen bond is

very strong, as indicated by the bond length of 1.76(3) Å, which is shorter than the value of 1.96(3) Å seen in salicylaldehyde thiosemicarbazone [20] and similar to the values in some hydrazones [33, 34]. Simultaneously, atom H1O1 is involved in a weaker hydrogen bond with atom S1, forming a five-membered ring, N1/H1O1/S1/C8/N2. The intermolecular hydrogen bonds involving atoms H5 and H7 with atoms O1ⁱ and S1ⁱ [symmetry code: (i) x+1, y, z], respectively, form infinite one-dimensional chains of molecules along the *a* axis. The strengths of these four hydrogen bonds have a direct influence on the angles subtended at atoms C1 and C8 (Table 2.4). The weak C9–H9B⋯π interaction with Cg(1) reinforces the packing stability along *c* axis.

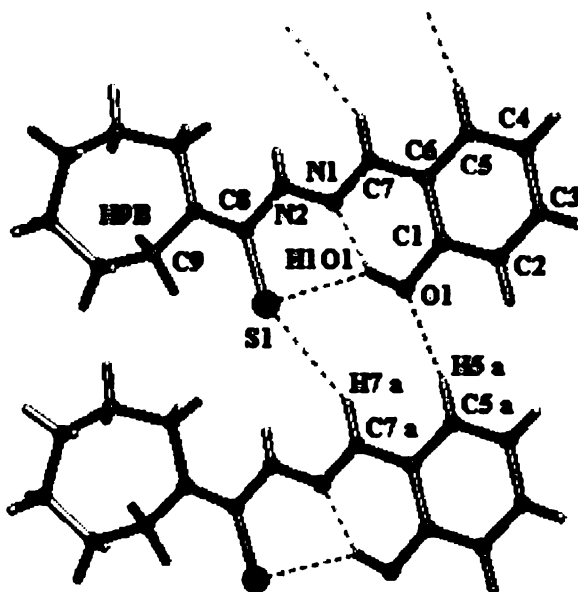


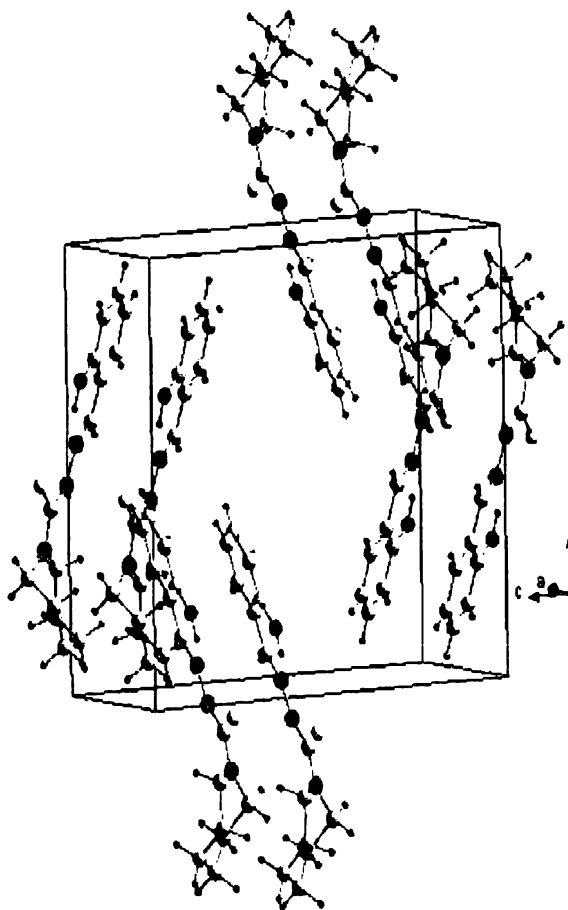
Figure 2.3. Intra and intermolecular hydrogen bonding interactions of H₂L²

Table 2.4. Hydrogen-bond geometry ($\text{\AA},^\circ$)

D—H \cdots A	D—H	H \cdots A	D \cdots A	D—H \cdots A
O1—H1O1 \cdots N1 ⁱ	0.92(3)	1.76(3)	2.562(3)	144(3)
O1—H1O1 \cdots S1 ⁱ	0.92(3)	2.82(3)	3.600(3)	143(3)
C5—H5 \cdots O1 ⁱⁱ	0.93	2.42	3.239(4)	147
C7—H7 \cdots S1 ⁱⁱ	0.93	2.87	3.706(6)	150
C9—H9B \cdots Cg(1) ⁱⁱⁱ	0.97	2.96	3.758(1)	141

Symmetry Codes: (i) x, y, z ; (ii) $x+1, y, z$; (iii) $-x+1, -y+1, -z$.

Cg(1) = C1, C2, C3, C4, C5, C6

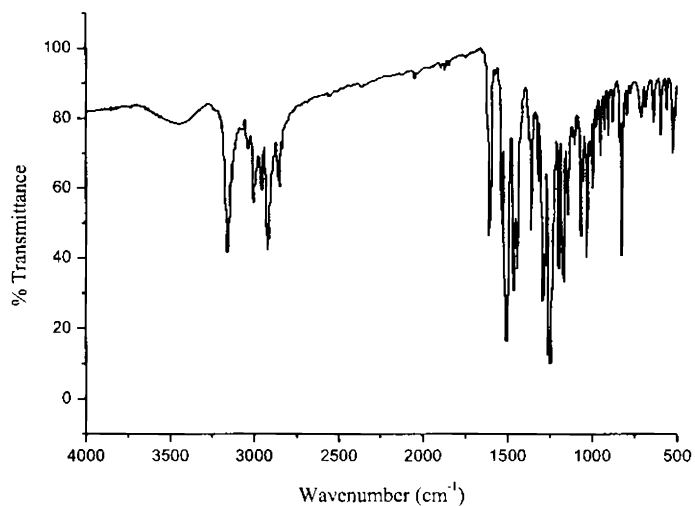
Figure 2.4. Unit cell packing diagram of H_2L^2

2.4.2. IR spectra

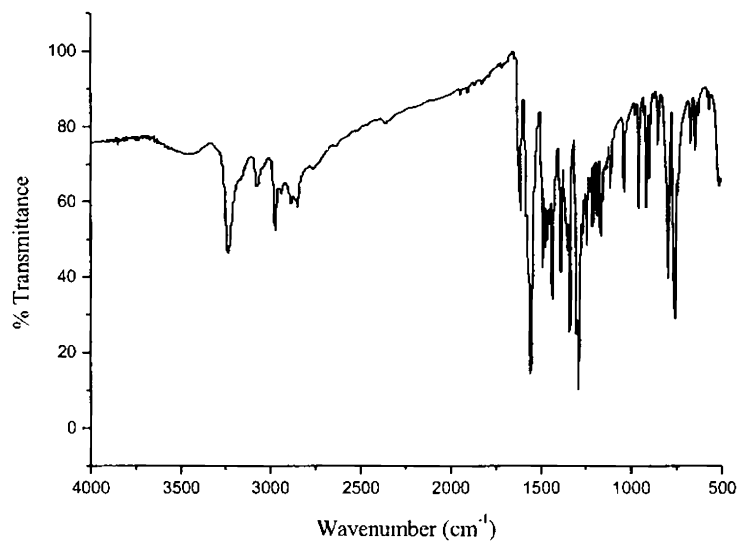
The characteristic IR bands for the ligands (HL¹, H₂L², HL³ and H₂L⁴) provide significant indications regarding the geometry are listed in Table 2.5. IR spectra of H₂L² and H₂L⁴ show bands at 3315 and 3232 cm⁻¹ region due to intermolecular hydrogen bonded phenolic -OH groups. All the ligands have bands in the range of 3050–3160 cm⁻¹ due to -NH groups present in the molecule. Absence of any bands in the range 2500–2800 cm⁻¹ points towards the lack of -SH stretching absorptions in the molecule. It reveals the presence of only the thione tautomer in the solid state. The azomethine stretching vibrations, C=N_{azo}, characteristics of a Schiff base, are observed at ~ 1615 cm⁻¹ [35-37]. The thiocarbonyl group shows stretching and bending vibrations at ~ 1320 and 840 cm⁻¹, while additional bands in the broad region of 1500–700 cm⁻¹ are due to vibrations involving interactions between C=S stretching and C-N stretching of the C=S group attached to a nitrogen atom [38]. Medium bands observed in the range 1030–1070 cm⁻¹ are assigned to hydrazinic N-N bonds [39]. The 1600-1400 cm⁻¹ region of the spectra is complicated by the presence of thioamide bands and ring breathing vibrations of the phenyl rings. IR spectra of the ligands HL³ and H₂L⁴ are presented in Figure 2.5.

Table 2.5. Selected IR bands (cm⁻¹) of the ligands (HL¹, H₂L², HL³ and H₂L⁴)

Ligands	$\nu(\text{O-H})$	$\nu(\text{N-H})$	$\nu(\text{C=N})$	$\nu(\text{N-N})$	$\nu/\delta(\text{C=S})$	$\nu(\text{C-O})$	$\nu(\text{C-C-O})$
HL ¹	...	3091	1624	1064	1334, 837
H ₂ L ²	3315	3050	1612	1037	1324, 861	1271	1100
HL ³		3154	1607	1064	1312, 821		
H ₂ L ⁴	3232	3072	1622	1034	1338, 839	1288	1108



HL³



H₂L⁴

Figure 2.5. IR spectra of the ligands HL³ and H₂L⁴

2.4.3. Electronic spectra

In contrast to the infrared spectrum, the electronic spectrum is not used primarily for the identification of individual functional groups, but rather to show the relationship between functional groups, chiefly conjugation [40]. The electronic spectral data of the ligands HL¹, H₂L², HL³ and H₂L⁴ in DMF solution are presented in Table 2.6. The $\pi \rightarrow \pi^*$ transitions of the phenyl ring are observed in the 35300-36500 cm⁻¹ region. The $n \rightarrow \pi^*$ transitions of the imine function of the thiosemicarbazone moiety are observed in the region of 28700-31200 cm⁻¹ [41, 42]. Electronic spectra of the ligands are presented in Figure 2.6.

Table 2.6. Electronic spectral assignments for the ligands

Ligands	$\pi - \pi^*$	$n - \pi^*$
HL ¹	32150	28730
H ₂ L ²	36110	29500
HL ³	35340	31150
H ₂ L ⁴	36490	30210

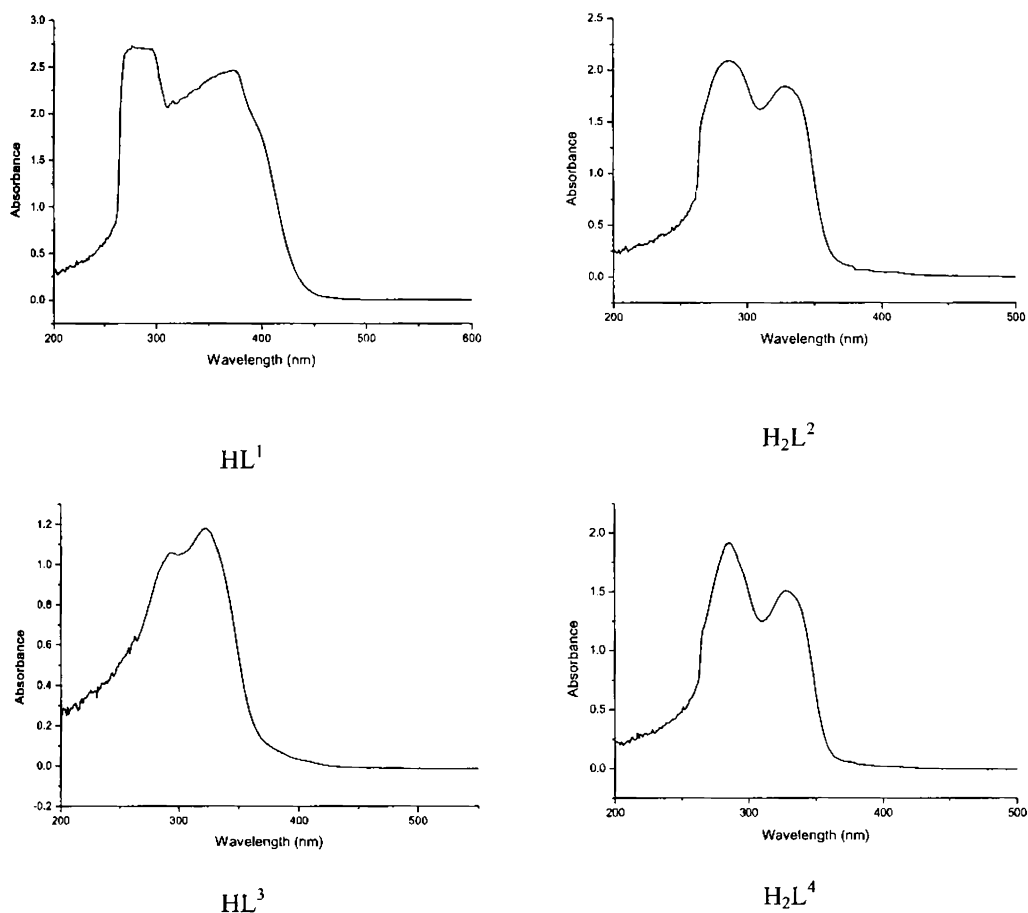


Figure 2.6. Electronic spectra of the ligands

2.4.4. 1H NMR spectra

Proton Magnetic Resonance spectroscopy is a helpful tool for the preparation of organic compounds in conjugation with other spectrometric informations. The 1H NMR spectra of the ligands recorded in $CDCl_3$ are given in Table 2.7. The ligands do not show any peak attributable to $-SH$ proton but they show peaks assignable to the secondary $N-H$ protons.

In the spectra of HL^1 and HL^3 , sharp singlets at $\delta = 7.96$ (HL^1) and 8.25 ppm (HL^3) corresponds to $^7CH=$ proton. Absence of any coupling interactions by

^2NH due to the unavailability of protons on neighboring atoms render singlet peak for the imine proton at $\delta=8.77$ (HL^1) and 8.66 ppm (HL^3) are assigned to the ^2NH protons. The $^a\text{CH}_2$ protons adjacent to the ring nitrogen produces a triplet at $\delta=4.02$ (HL^1) and 4.01 ppm (HL^3) due to coupling with nearby $^b\text{CH}_2$ protons. The $^b\text{CH}_2$ protons due to coupling with $^a\text{CH}_2$ and $^c\text{CH}_2$ protons resonate as the multiplet observed at $\delta=1.94$ (HL^1) and 1.93 ppm (HL^3). $^c\text{CH}_2$ protons also resonate as the multiplet at $\delta=1.64$ (HL^1) and 1.62 ppm (HL^3). In the case of HL^1 , the *ortho* protons of the phenyl ring *viz.* ^2CH and ^6CH are observed at $\delta=7.28$ ppm. The *meta* positioned protons of the aromatic ring ^3CH and ^5CH are observed at $\delta=7.57$ ppm. The *para* positioned proton ^4CH resonate as triplet at $\delta=7.65$ ppm. For HL^3 , the phenyl group is disubstituted and the *ortho* protons of the phenyl ring *viz.* ^2CH and ^6CH are observed at $\delta=7.53$ ppm and the *meta* positioned protons ^3CH and ^5CH resonate at 6.92 ppm. The $-\text{OCH}_3$ protons in HL^3 appear as a singlet at $\delta=3.83$ ppm.

The spectra of diprotic ligands (H_2L) show sharp singlets, which integrates as one hydrogen at $\delta \sim 10.08$ ppm is assigned to the proton attached to the oxygen atom. The downfield shift of this proton is assigned to its intra and intermolecular hydrogen-bonding interactions. The hydrogen bonding decreases the electron density around the proton, and thus moves the proton absorption to a lower field [36]. Absence of any coupling interactions by ^2NH due to the unavailability of protons on neighboring atoms render singlet peak for the imine proton at $\delta=8.89$ (H_2L^2) and 8.58 ppm (H_2L^4). The presence of electron withdrawing azomethine group near to the ^7CH proton leads to its resonance as a singlet at $\delta=7.99$ (H_2L^4) and 8.00 ppm (H_2L^4). Aromatic protons ^4CH , ^6CH , ^3CH , ^5CH appear as a multiplet in the range of 6.67-7.30 ppm [12]. Aliphatic protons of hexamethyleneiminyl and tetramethyleneiminyl rings were observed as three signals at $\delta \sim 3.60$, 1.70 and 1.52

ppm assigned to positions a, b and c respectively. NMR assignments are in agreement with values already reported [41, 43-45]. ^1H NMR spectra of the ligands are presented in Figures 2.7-2.10.

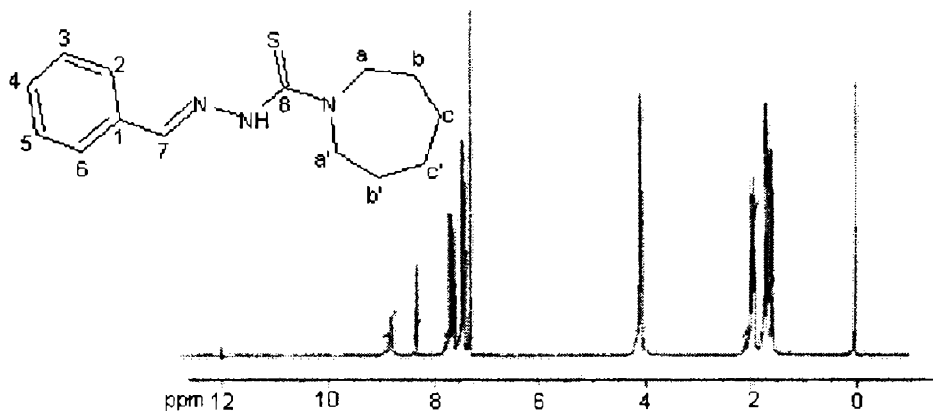


Figure 2.7. ^1H NMR spectrum of HL^1

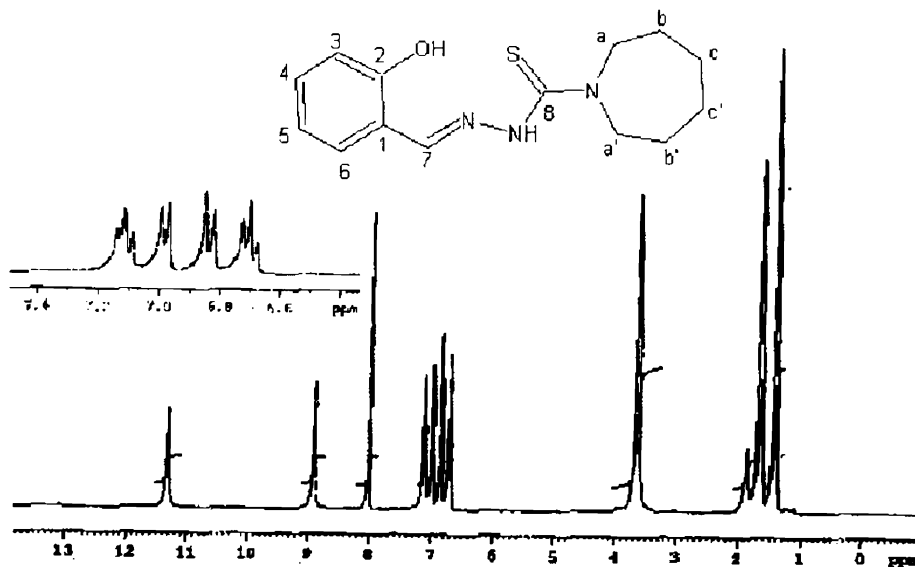


Figure 2.8. ^1H NMR spectrum of H_2L^2

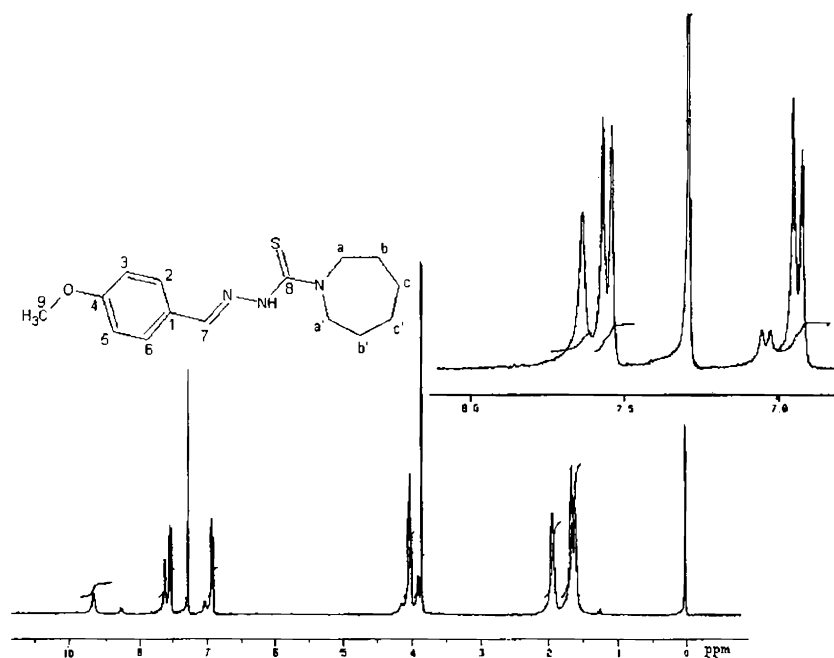
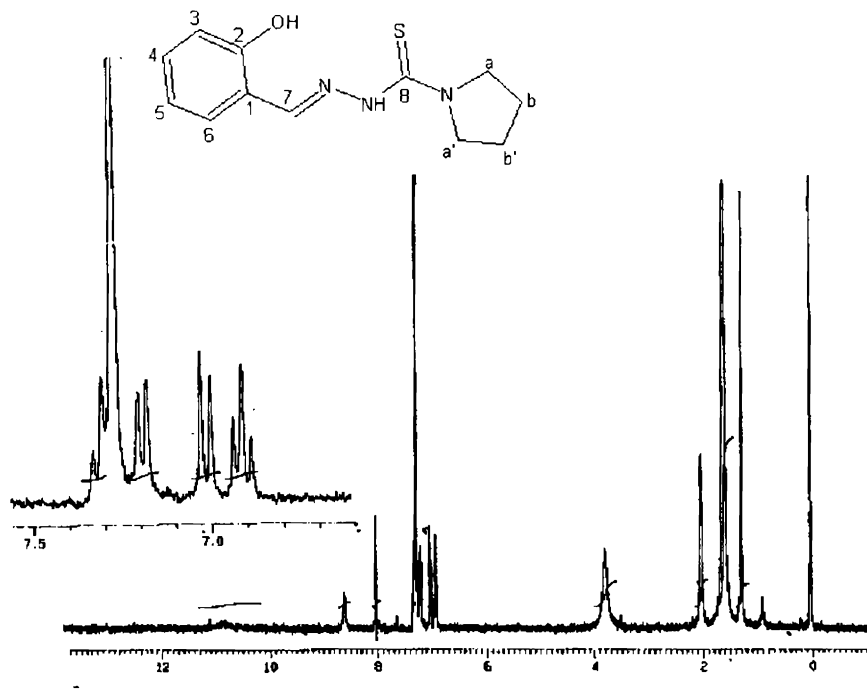
Figure 2.9. ¹H NMR spectrum of HL³Figure 2.10. ¹H NMR spectrum of H₂L⁴

Table 2.7. ^1H NMR (CDCl_3) assignments of the ligands (δ in ppm)

Compound	OH	Aromatic Protons							^2NH	$^7\text{CH}=\text{}$	$^a\text{CH}_2$	$^b\text{CH}_2$	$^c\text{CH}_2$
		$\text{H}^2\text{ Ph}$	$\text{H}^3\text{ Ph}$	$\text{H}^4\text{ Ph}$	$\text{H}^5\text{ Ph}$	$\text{H}^6\text{ Ph}$	$\text{H}^6\text{ Ph}$	$\text{H}^6\text{ Ph}$					
HL^1	----	7.63	7.57	7.28	7.57	7.63	7.63	8.77	7.96	4.02	1.94	1.64	
H_2L^2	11.3	----	6.80	6.97	6.67	7.09	7.09	8.89	7.99	3.63	1.66	1.42	
HL^3	----	7.53	6.92	----	6.92	7.53	7.53	8.66	8.25	4.01	1.93	1.62	
H_2L^4	10.3	----	6.99	7.21	6.90	7.29	7.29	8.58	8.00	3.59	1.73	----	

References

1. D.X. West, A.E. Liberta, S.B. Padhye, R.C. Chikate, P.B. Sonawane, A.S. Kumbhar, R.G. Yerande, *Coord. Chem. Rev.* 123 (1993) 49.
2. S.B. Padhye, G.B. Kauffman, *Coord. Chem. Rev.* 63 (1985) 127.
3. V.M. Leovac, L.S. Vojinovic, K.M. Szecsenyi, V.I. Cesljevic, *J. Serb. Chem. Soc.* 68 (2003) 919.
4. V.M. Leovac, A.F. Petrovic, *Trans. Met. Chem.* 8 (1983) 337.
5. A.F. Petrovic, M.L. Vukadin, B. Riber, *Trans. Met. Chem.* 11 (1986) 207.
6. S. Purohit, A.P. Koley, L.S. Prasad, P.T. Manoharan, S. Ghosh, *Inorg. Chem.* 28 (1989) 3735.
7. A.P. Koley, S. Purohit, L.S. Prasad, P.T. Manoharan, S. Ghosh, *J. Chem. Soc., Dalton Trans.* 2607 (1988).
8. A.P. Koley, S. Purohit, L.S. Prasad, P.T. Manoharan, S. Ghosh, *Inorg. Chem.* 31 (1992) 305.
9. M.A. Ali, M.H. Kabir, M.N. Nazimuddin, S.M.M.H. Majumder, M.T.H. Tarafder, M.A. Khair, *Indian J. Chem.* 27A (1988) 1064.
10. D.X. West, M.M. Salberg, G.A. Bain, A.E. Liberta, J.V. Martinez, S.H. Ortega, *Trans. Met. Chem.* 21 (1996) 206.
11. P. Bindu, M.R.P. Kurup, *Trans. Met. Chem.* 22 (1997) 578.
12. P. Bindu, M.R.P. Kurup, *Indian J. Chem.* 36A (1997) 1094.
13. J.P. Scovill, D.L. Klayman, C.F. Franchino, *J. Med. Chem.* 25 (1982) 1261.
14. L. Latheef, E. Manoj, M.R.P. Kurup, *Acta Crystallogr. C* 62 (2006) 16.
15. Nonius (1997) MACH3 software. B.V. Nonius, Delft, The Netherlands.
16. G.M. Sheldrick, *Acta Crystallogr. A* 46 (1990) 467.
17. G.M. Sheldrick, *SHELXL-97 and SHELXS-97 Program for the solution of Crystal Structures*, University of Göttingen, Germany, 1997.

18. K. Brandenburg, DIAMOND version 3.1d, Crystal Impact GbR, Bonn, Germany, 2006
19. A. L. Spek, *J. Appl. Cryst.* 36 (2003) 7.
20. E. Bermejo, A. Castineiras, I. Garcia-Santos, *Allg. Chem.* 630 (2004) 1096.
21. D. Chattopadhyay, S.K. Mazumdar, T. Banerjee, S. Ghosh, T.C.W. Mak, *Acta Crystallogr.* C44 (1988) 1025.
22. A. Usman, I.A. Razak, S. Chantrapromma, H.-K. Fun, V. Philip, A. Sreekanth, M.R.P. Kurup, *Acta Crystallogr.* C58 (2002) 0652.
23. V. Philip, V. Suni, M.R.P. Kurup, *Acta Crystallogr.* C60 (2004) o856.
24. I.E. Huheey, E.A. Keiter, R.L. Keiter (1993). *Inorganic Chemistry, Principles of Structure and Reactivity*, 4th ed. New York: Harper Collins College Publishers.
25. G.I. Palenik, D.E. Rendle, W.S. Carter, *Acta Crystallogr.* B30 (1974) 2390.
26. M. Mathew, G.I. Palenik, *Inorg. Chim. Acta* 5 (1971) 349.
27. M. Dinçer, N. Ozdemir, A. Cukurovali, I. Yilmaz, *Acta Crystallogr.* E61 (2005) o880.
28. G.A. Bain, D.X. West, I. Krejci, I. Valdes-Martinez, S. Hernandez-Ortega, R.A. Toscano, *Polyhedron* 16 (1997) 55.
29. A. Sreekanth, M.R.P. Kurup, *Polyhedron* 23 (2004) 969.
30. A. Sreekanth, M.R.P. Kurup, H.-K. Fun, *J. Mol. Struct.* 737 (2005) 61.
31. P.F. Rapheal, E. Manoj, M.R.P. Kurup, E. Suresh, *Acta Crystallogr.* E61 (2005) o2243.
32. D. Cremer, I.A. Pople, *J. Am. Chem. Soc.* 97 (1975) 1354.
33. W-Y. Liu, Y-Z. Li, *Acta Crystallogr.* E60 (2004) o694.
34. H.M. Ali, S. Puvaneswary, W.F. Basirun, S.W. Ng, *Acta Crystallogr.* E61 (2005) o1013.

35. S.K. Jain, B.S. Garg, Y.K. Bhoon, D.L. Klayman, J.P. Scovill, *Spectrochim. Acta* 41A (1985) 407.
36. R.M. Silverstein, G.C. Bassler, T.C. Morrill, *Spectrometric Identification of Organic Compounds*, 4th ed. Wiley, New York, 1981.
37. D.X. West, Y. Yang, T.L. Klein, K.I. Goldberg, A.E. Liberta, *Polyhedron* 14 (1995) 3051.
38. D.X. West, A.M. Stark, G.A. Bain, A.E. Liberta, *Trans. Met. Chem.* 21 (1996) 289.
39. M. Joseph, M. Kuriakose, M.R.P. Kurup, E. Suresh, A. Kishore, S.G. Bhat, *Polyhedron* 25 (2006) 61.
40. W. Kemp, *Organic Spectroscopy*, 3rd ed. Macmillan, Hamsphire, 1996.
41. R.P. John, A. Sreekanth, M.R.P. Kurup, A. Usman, A.R. Ibrahim, H.-K. Fun, *Spectrochim. Acta* 59A (2003) 1349.
42. D.X. West, I.S. Billeh, J.P. Jasinski, J.M. Jasinski, R.J. Butcher, *Trans. Met. Chem.* 23 (1998) 209.
43. P. Bindu, M.R.P. Kurup, T.R. Satyakeerthy, *Polyhedron* 18 (1999) 321.
44. S. Jayasree, K.K. Aravindakshan, *Trans. Met. Chem.* 18 (1993) 85.
45. M. Nazimuddin, M.A. Ali, F.E. Smith, *Polyhedron* 10 (1991) 327.

Synthesis, spectral and structural studies of Cu(II) complexes of N(4)-ring incorporated thiosemicarbazones of aromatic aldehydes

3.1. Introduction

Copper is one of the most abundant (25th in order of abundance) element in the earth's crust. It occurs to the extent of 68 ppm by weight. The metal is used in the electrical industry because of its high conductivity. It is also used for water pipes because of its inertness.

The coordination chemistry of heterocyclic thiones containing $-\text{N}(\text{H})-\text{C}=\text{S}- \leftrightarrow -\text{N}=\text{C}-(\text{SH})-$ functional group is of immense interest because such compounds (a) mimic cysteine sulfur coordination in metalloenzymes (b) show electronic and structural properties of the active sites in copper blue proteins involving S, N coordination. Similarly, thiosemicarbazones containing the $=\text{N}-\text{NH}-\text{C}=\text{S}- \leftrightarrow =\text{N}-\text{N}=\text{C}-(\text{SH})-$ group are important ligands due to coordination with a variety of donor atoms and their numerous biochemical properties [1-3].

Thiosemicarbazide and thiosemicarbazone complexes of copper have attracted particular attention over the past decade in the context of their wide spectrum of biological activity and applications as radiopharmaceuticals [4]. The Cu(II) complex of thiosemicarbazone of salicylaldehyde can exist both in a monomeric solvated 4-coordinate form and as a phenolic oxygen bridged dimer where each copper is 5-coordinate. The thiosemicarbazone ligand is SNO bound

via 5- and 6-membered chelate rings [5]. The common oxidation states of copper are I (d^{10}), II (d^9), and III (d^8). The most common oxidation state of Cu is (II), and Cu(II) complexes have been extensively studied. These complexes have tetrahedral, octahedral, square planar and trigonal bipyramidal geometries [6]. Due to the presence of unpaired electron, all the copper(II) complexes are paramagnetic.

This chapter deals with the synthesis and characterization of mononuclear and binuclear Cu(II) complexes with different N(4)-ring incorporated thiosemicarbazone ligands. The structure of one of the compounds has been solved by single crystal X-ray diffraction studies and was found to be distorted square pyramidal in geometry.

3.2. Experimental

3.2.1. Materials

The thiosemicarbazone ligands were synthesized as discussed in Chapter 2 and solvents were purified by distillation. Pyridine, γ -picoline, 1,10-phenanthroline (Ranbaxy fine chemicals), 2,2'-bipyridine (Central drug house chemicals) and $\text{Cu}(\text{OAc})_2 \cdot \text{H}_2\text{O}$ (Fluka) were used as received.

3.2.2. Synthesis of the complexes

[CuL¹]₂·H₂O (1): This complex was synthesized by refluxing an ethanolic solution of HL¹ (2 mmol, 0.522 g) with an aqueous solution of $\text{Cu}(\text{OAc})_2 \cdot \text{H}_2\text{O}$ (1 mmol, 0.199 g) for 4 h. The complex formed was filtered, washed with ethanol and finally with ether and dried over P_4O_{10} *in vacuo*.

[[CuL²]₂] (2): This complex was synthesized by refluxing an ethanolic solution of H₂L² (1 mmol, 0.277 g) with an aqueous solution of $\text{Cu}(\text{OAc})_2 \cdot \text{H}_2\text{O}$ (1 mmol, 0.199 g) for 4 h in an alkaline medium. The brown colored product formed was filtered, washed with ethanol and finally with ether and dried over P_4O_{10} *in vacuo*.

[Cu(HL²)₂] (3): Ethanolic solution of the ligand H₂L² (2 mmol, 0.554 g) and an aqueous solution of Cu(OAc)₂·H₂O (1 mmol, 0.199 g) in 2:1 ratio was refluxed for 2-3 h. The complex formed was filtered, washed with ethanol and finally with ether and dried over P₄O₁₀ *in vacuo*.

[CuL²bipy] (4): To a solution of H₂L² (1 mmol, 0.277 g) in hot ethanol was added heterocyclic base 2,2'-bipyridine (1 mmol, 0.156 g) with constant stirring. To this was added an aqueous solution of Cu(OAc)₂·H₂O (1 mmol, 0.199 g) and the resulting solution was then refluxed for 3 h. The product formed was filtered, washed with ethanol and finally with ether and dried over P₄O₁₀ *in vacuo*.

[CuL²phen] (5): Solutions of H₂L² (1 mmol, 0.277 g) and heterocyclic base 1,10-phenanthroline (1 mmol, 0.198 g) were mixed and to this was added an aqueous solution of Cu(OAc)₂·H₂O (1 mmol, 0.199 g) and refluxed for 2-3 h. The green colored product formed was filtered, washed with ethanol and finally with ether and dried over P₄O₁₀ *in vacuo*.

[CuL²γ-pic]·2H₂O (6): The H₂L² (1 mmol, 0.277 g) was dissolved in ethanol, to which was added a slight excess of heterocyclic base γ-picoline (3 mmol, 0.279 g) with constant stirring. This was followed by the addition of an aqueous solution of Cu(OAc)₂·H₂O (1 mmol, 0.199 g) and then refluxed for 4h. The resulting solution was then concentrated on a water bath and cooled at room temperature, filtered and kept overnight. The brown colored product formed was filtered, washed with ethanol and ether and dried *in vacuo* over P₄O₁₀.

[CuL³]₂·0.5H₂O (7): Ethanolic solutions of the ligand HL³ (2 mmol, 0.582 g) and Cu(OAc)₂·H₂O (1 mmol, 0.199 g) in 2:1 ratio was refluxed for 2 h. The complex formed was filtered, washed with ethanol and finally with ether and dried over P₄O₁₀ *in vacuo*.

[Cu(HL⁴)₂] (8): This complex was synthesized by refluxing an ethanolic solution

of H_2L^4 (2 mmol, 0.498 g) with an aqueous solution of $\text{Cu}(\text{OAc})_2 \cdot \text{H}_2\text{O}$ (1 mmol, 0.199 g) for 4 h. The complex formed was filtered, washed with ethanol and finally with ether and dried over P_4O_{10} *in vacuo*.

[CuL⁴py]·3H₂O (9): To a hot ethanolic solution of the ligand H_2L^4 (1 mmol, 0.249 g), added an aqueous solution of $\text{Cu}(\text{OAc})_2 \cdot \text{H}_2\text{O}$ (1 mmol, 0.199 g) with constant stirring. This was followed by the addition of slight excess of the base pyridine (3 mmol, 0.237 g). The above brown solution was then refluxed for about 3 h. The complex formed was filtered, washed with ethanol and ether and dried *in vacuo* over P_4O_{10} .

[CuL⁴bipy] (10): An ethanolic solution of H_2L^4 (1 mmol, 0.249 g) was mixed with an aqueous solution of $\text{Cu}(\text{OAc})_2 \cdot \text{H}_2\text{O}$ (1 mmol, 0.199 g) and this was followed by the addition of the base bipy (1 mmol, 0.156 g) in the solid form. The resulting solution was then refluxed for 2h, when green shining crystals began to separate. This was filtered, washed with ethanol and ether and dried *in vacuo* over P_4O_{10} .

3.2.3. Physical measurements

Elemental analyses were carried out using a Vario EL III CHN analyzer at SAIF, Kochi, India. Magnetic susceptibility measurements were carried out at IIT, Roorkee, at room temperature in the polycrystalline state on a PAR model 155 Vibrating Sample Magnetometer (VSM) at 5 k Oe. field strength using $\text{Hg}[\text{Co}(\text{SCN})_4]$ as a calibrant. Diamagnetic corrections were made using Pascal's constants. The FT-IR spectra were recorded on a Thermo Nicolet AVATAR 370 DTGS FTIR Spectrometer using KBr pellets in the range 500-4000 cm^{-1} at SAIF, Cochin University of Science and Technology, Kochi 22, India and Far-IR spectra were recorded in the range 50-500 cm^{-1} on a Nicolet Magna 550 FT-IR spectrophotometer using polyethylene pellets at SAIF, IIT, Bombay, India. Electronic spectra were recorded on a UVD-3500 UV-VIS-Double beam

Spectrophotometer from solutions in DMF. The EPR spectra were recorded on a Varian E-112 Spectrometer using TCNE as the standard at SAIF, IIT, Bombay, India.

3.2.4. X-ray crystallography

A dark green crystal of the compound **10** having approximate dimensions $0.35 \times 0.20 \times 0.15 \text{ mm}^3$ was sealed in a glass capillary and intensity data were measured at room temperature (293 K). The crystallographic data and structure refinement parameters for the compound are given in Table 3.1.

Table 3.1. Crystal data and experimental parameters for compound **10**

Empirical formula	$\text{C}_{22} \text{H}_{21} \text{Cu N}_5 \text{O S}$
Temperature	293(2) K
Formula weight	467.06
Wavelength	0.71073 Å
Crystal system	Monoclinic
Space group	$P 2_1/n$
Unit cell dimensions	$a = 9.0400(5) \text{ Å}$ $b = 19.773(2) \text{ Å}$ $c = 12.613(3) \text{ Å}$ $\alpha = 90^\circ$ $\beta = 108.590(12)^\circ$ $\gamma = 90^\circ$
Volume	$2136.9(6) \text{ Å}^3$
Z	4
Calculated density	1.452 g/cm^3
Absorption coefficient	1.143 mm^{-1}
F(000)	964
Crystal size	$0.35 \times 0.20 \times 0.15 \text{ mm}^3$
θ range for data collection	1.99 to 24.99°
Index ranges	$-10 \leq h \leq 10, -23 \leq k \leq 0, -14 \leq l \leq 0$
Reflections collected	3914
Independent reflections	3736 [R(int) = 0.0298]
Refinement method	Full-matrix least-squares on F^2
Data / restraints / parameters	3736 / 0 / 271
Goodness-of-fit on F^2	1.024
Final R indices [$I > 2\sigma(I)$]	$R1 = 0.0428, wR2 = 0.0914$
R indices (all data)	$R1 = 0.1028, wR2 = 0.1058$

The X-ray diffraction data were measured at room temperature and data acquisition and cell refinement were done using the Argus (Nonius, MACH3 software) [7]. The Maxus (Nonius software) were used for data reduction [8]. The structure was solved by direct methods with the program SHELXS-97 and refined by full matrix least squares on F^2 using SHELXL-97 [9]. The graphical tool used was DIAMOND version 3.1d [10]. All non-hydrogen atoms were refined anisotropically and all hydrogen atoms were geometrically fixed at calculated positions.

3.3. Results and discussion

The ligands gave complexes more readily under reflux in the aqueous-ethanol/methanol medium. Complexes **1**, **6**, **7** and **9** contain uncoordinated water molecules. The complexes **1**, **3**, **7** and **8** were readily formed by refluxing their respective ligands and $\text{Cu}(\text{OAc})_2 \cdot \text{H}_2\text{O}$ in 2:1 ratio and have the general formula $[\text{ML}_2]$ (for complexes **1** and **7**) and $[\text{M}(\text{HL})_2]$ (for complexes **3**, and **8**). The complex **2** was prepared using H_2L^2 ligand and $\text{Cu}(\text{OAc})_2 \cdot \text{H}_2\text{O}$ in 1:1 ratio in alkaline medium and has the general formula $[(\text{ML})_2]$. The complexes **4**, **5**, **6**, **9** and **10** were assigned the general formula MLB , where B are heterocyclic bases, pyridine, 2,2'-bipyridine, 1,10-phenanthroline or γ -picoline and were prepared by refluxing their respective ligands with $\text{Cu}(\text{OAc})_2 \cdot \text{H}_2\text{O}$ and heterocyclic bases in the 1:1:1 ratio. From the structural, elemental and spectral studies, the compounds **1-10** were assigned the empirical formula $[\text{CuL}^1_2]$ (**1**), $[(\text{CuL}^2)_2]$ (**2**), $[\text{Cu}(\text{HL}^2)_2]$ (**3**), $[\text{CuL}^2\text{bipy}]$ (**4**), $[\text{CuL}^2\text{phen}]$ (**5**), $[\text{CuL}^2\gamma\text{-pic}] \cdot 2\text{H}_2\text{O}$ (**6**), $[\text{CuL}^3_2] \cdot 0.5\text{H}_2\text{O}$ (**7**), $[\text{Cu}(\text{HL}^4)_2]$ (**8**), $[\text{CuL}^4\text{py}] \cdot 3\text{H}_2\text{O}$ (**9**), $[\text{CuL}^4\text{bipy}]$ (**10**) respectively and X-ray quality single crystals of the complex **10** were obtained from its solution in methanol by slow evaporation over a period of 8 days. The analytical data of the complexes are presented in Table 3.2.

Table 3.2. Analytical data

Compound	color	μ_{eff} (B.M)	Anal: Found (Calcd.) %		
			C	H	N
[CuL ¹] ₂ ·H ₂ O (1)	brown	2.02	56.00(55.83)	6.20(6.36)	13.97(13.95)
[(CuL ²) ₂] (2)	brown	1.25	50.08(49.60)	4.73(5.06)	12.25(12.40)
[Cu(HL ²) ₂] (3)	brown	2.04	54.35(54.57)	6.12(5.89)	13.63(13.64)
[CuL ³ bipy] (4)	green	1.64	57.99(58.22)	5.12(5.09)	14.10(14.15)
[CuL ³ phen] (5)	green	1.59	60.05(60.16)	4.90(4.85)	13.43(13.49)
[CuL ³ γ -pic]·2H ₂ O (6)	brown	1.54	51.74(51.32)	5.60(6.03)	12.34(11.97)
[CuL ³] ₂ ·0.5H ₂ O (7)	brown	1.62	55.38(55.15)	6.82(6.33)	12.91(12.86)
[Cu(HL ⁴) ₂] (8)	brown	1.92	51.44(51.46)	4.91(5.04)	14.89(15.00)
[CuL ⁴ py]·3H ₂ O (9)	brown	1.65	45.36(45.99)	4.62(5.15)	13.10(12.62)
[CuL ⁴ bipy] (10)	green	1.52	56.42(56.58)	4.45(4.53)	14.88(14.99)

Magnetic moments of the complexes were calculated from magnetic susceptibility measurements. Mononuclear Cu(II) complexes exhibit magnetic moments in the range 1.5-2.05 B.M, which are close to their spin-only value. Magnetic moment of binuclear Cu(II) complex **2** is 1.25 B.M which was in the range of 1.15-1.40 B.M, found for binuclear complexes. This low magnetic moment may be attributed to the presence of a strong antiferromagnetic spin-spin interaction involving an oxygen-bridged binuclear structure similar to those proposed for the Cu(II) complexes of analogous tridentate ligands [11].

3.3.1. Crystal structure of [CuL⁴bipy]

The molecular structure of the compound along with atom numbering scheme is given in Figure 3.1 and selected bond lengths and bond angles are summarized in Table 3.3.

The compound crystallized with one monomer per asymmetric unit into monoclinic crystal system with a space group *P21/n*. The copper in the

mononuclear complex is five coordinated and is having an approximate square pyramid (SPY) geometry around the copper(II) ion. The copper centre is coordinated by the phenolato oxygen, O1, azomethine nitrogen N1, and the thiolato sulphur S1, of the thiosemicarbazone and the pyridine nitrogens N5 and N4, of bipyridine. The donor atoms O1, N1, S1 of the thiosemicarbazone and N5 of the bipyridine occupy the equatorial position and the other bipyridine nitrogen N4 occupies the axial position at a larger distance. The large bond distance at the axial Cu1–N4 position supports the lack of out of plane π -bonding. This fact is in accordance with the absence of superhyperfine splitting due to N4 in the EPR spectrum of the compound. The Cu–N and Cu–O bond lengths vary in the range 1.951(4) to 2.016(4) Å. The C7–N1 and N2–C8 bond lengths are comparable to that for C=N bond length. Of these two, N2–C8 bond length is larger due to enolization of the ligand in complex formation. The O1–Cu1–N4 and S1–Cu1–N4 bond angles indicate a slight tilting of the axial Cu1–N4 bond in the direction of O1–Cu1 bond and away from the S1–Cu1 bond. The N4–Cu1–S1 bond angle is shorter compared to our previous reports [12, 13]. The Cu1–N1 bond length is shorter compared to the Cu–N bond lengths of bipyridine indicates that the thiosemicarbazone moiety dominates equatorial bonding. The rather small bite angle [N1–Cu1–S1= 85.27(9)° and O1–Cu1–S1= 164.44(9)°] defines largest distortion of the geometry. One of the reasons for the deviation from an ideal stereochemistry is the restricted bite angle imposed by both the L²⁻ and bipy ligands. The bite angle around the metal *via* N4–Cu1–N5 of 76.95(12)° may be considered normal, when compared with an average value of 77° cited in the literature [12, 14-16]. In a five-coordinated system, the angular structural parameter (τ) is used to propose an index of trigonality. The τ is defined by $\tau = (\alpha - \beta) / 60$, (Where $\tau = 0$ for a square pyramidal geometry and 1 for trigonal bipyramidal geometry), and α and β are the trans angles [17]. The τ value for the complex is

0.15, indicates that the coordination around Cu(II) is best described as distorted square pyramid with copper displaced by 0.1921(5) Å from the plane containing the four donor atoms N5, S1, N1 and O1 towards the pyridyl nitrogen N4, which is evident from the bond angles of N1–Cu1–N5= 173.28(13)°, and O1–Cu1–S1= 164.44(9)°.

Table 3.3. Selected bond lengths (Å) and bond angles (°) for [CuL⁴bipy]

Bond lengths (Å)		Bond angles (°)	
Cu1–O1	1.954(3)	O1–Cu1–N1	92.89(12)
Cu1–N1	1.952(3)	O1–Cu1–N5	89.66(11)
Cu1–N5	2.050(3)	N1–Cu1–N5	173.28(13)
Cu1–N4	2.227(3)	O1–Cu1–N4	95.43(11)
Cu1–S1	2.273(11)	N1–Cu1–N4	108.96(12)
S1–C8	1.743(4)	N4–Cu1–N5	76.95(12)
O1–C1	1.314(5)	O1–Cu1–S1	164.44(9)
N1–C7	1.296(5)	N1–Cu1–S1	85.27(9)
N1–N2	1.396(4)	N5–Cu1–S1	90.60(9)
N2–C8	1.317(5)	N4–Cu1–S1	99.79(8)
N3–C8	1.348(5)		

The dihedral angle formed by the least square plane Cg(1) and Cg(4) is 11.12° [Cg(1)= Cu1, N1, N2, C8, S1 and Cg(4)= Cu1, O1, C1, C6, C7, N1]. This small deviation from coplanarity would certainly not hinder the delocalization of electrons in the coordination sphere, and the stability of the complex is sustained.

Ring puckering analysis indicates that Cg(3) ring comprising of N3, C9, C10, C11 and C12 adopts an envelop conformation on C11. [$\theta(2)$ = 0.1955 Å and $\phi(2)$ = 103.5615°]

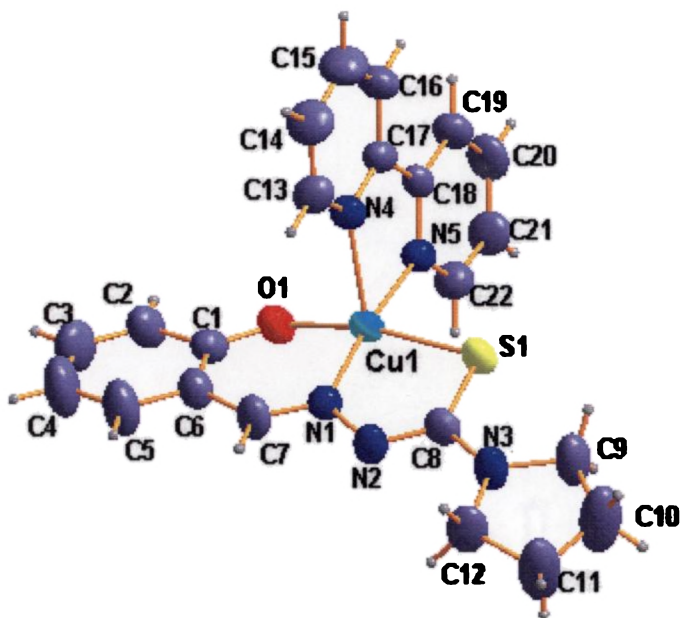


Figure 3.1. Structure and labeling scheme for $[\text{CuL}^4\text{bipy}]$ (10)

The unit cell is viewed along the c axis and four molecules are arranged in the unit volume cell (Figure 3.2). The packing of the molecules is stabilized by intermolecular hydrogen bonding, π - π and $\text{CH}\dots\pi$ interactions. These interactions are given in Table 3.4. The centroid $\text{Cg}(5)$ is involved in π - π interactions with pyridyl ring of the neighbouring unit at a distance of 3.5912 Å. The intermolecular hydrogen bonding involving atoms H13 and H14 with N2, H15 with S1 and H16, H19, H21 and H22 with O1 respectively, reinforce crystal structure cohesion in the close packing. In addition to the intermolecular hydrogen bonding, the $\text{CH}\dots\pi$ interactions of the pyridyl hydrogen of the bipyridine with the metal chelate rings of the neighbouring molecules contributes to the stability of the unit cell packing.

Table 3.4. Interaction parameters of the compound 10

 π - π interactions

Cg(I)-Res(1)⋯Cg(J)	Cg-Cg (Å)	α°	β°
Cg(5) [1] -> Cg(6) ^a	3.5912	3.72	21.17
Cg(6) [1] -> Cg(5) ^a	3.5912	3.72	23.11

Equivalent position code: a= -x, -y, -z

Cg(5)= N4, C13, C14, C15, C16, C17; Cg(6)= N5, C18, C19, C20, C21, C22

CH- π interactions

X-H(I)⋯Cg(J)	H...Cg (Å)	X-H...Cg (°)	X...Cg (Å)
C15-H15 [1] -> Cg(1) ^a	2.73	146	3.5377

Equivalent position code: a= -1+x, y, z

Cg(1)= Cu1, N1, N2, C8, S1

H-bonding

D-H...A	D...H (Å)	H...A (Å)	D...A (Å)	D-H...A (°)
C13-H13...N2 ^a	0.930	2.649(1)	3.555(1)	164.88(1)
C14-H14...N2 ^b	0.930	2.927	3.616	132(2)
C15-H15...S1 ^b	0.930	2.785	3.699	167.70(1)
C16-H16...O1 ^c	0.930	2.855(1)	3.690(1)	150.12(2)
C19-H19...O1 ^c	0.930	2.739	3.587	152.07(2)
C21-H21...O1 ^d	0.930	2.876	3.443	120.60(2)
C22-H22...O1 ^d	0.930	2.671	3.360	131.50(2)

D=donor, A=acceptor, Equivalent position code: a= -x+1, -y, -z+1; b= x-1, +y,+z; c= -x,-y,-z; d= -x+1,-y,-z

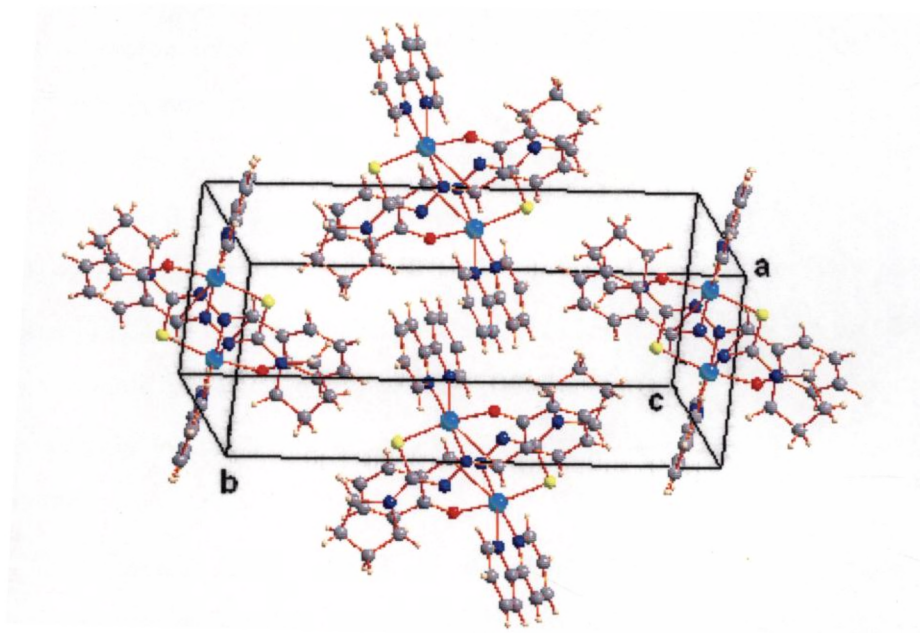


Figure 3.2. Unit cell packing diagram of the compound 10

3.3.2. IR spectra

The significant IR bands of the complexes 1–10 with their tentative assignments are presented in Table 3.5.

The IR spectra of the ligands H_2L^2 and H_2L^4 showed an intermolecular hydrogen bonded $\nu(OH)$ vibrations at 3315 and 3232 cm^{-1} respectively, which disappeared in the spectra of complexes except in 1 and 7. It is further corroborated with the downward shift of 60–80 cm^{-1} for $\nu(CO)$ as well as an appearance of a band at 390–430 cm^{-1} region due to a $\nu(Cu-O)$ stretch in the spectra of complexes [18, 19, 20]. It indicates coordination *via* phenolic oxygen.

Azomethine nitrogen bands ~ 1600 cm^{-1} in the uncomplexed thiosemicarbazones undergo a shift towards the lower energy side by 10–40 cm^{-1} in the spectra of complexes [13] due to the conjugation of the p-orbital on the double

bond with the d-orbital on the metal ion with the reduction of force constant, but with loss of proton from N, another strong band is found in the region of 1530–1555 cm^{-1} which may be due to the newly formed $\nu(\text{C}=\text{N})$ bond, resulting from enolization of the principal thiosemicarbazone ligands in the spectra for these complexes except **3** and **8**. Coordination of azomethine nitrogen is consistent with the presence of a band in the 430–480 cm^{-1} region, assignable to $\nu(\text{Cu}-\text{N})$ for these complexes [21, 22]. The increase in $\nu(\text{NN})$ in the spectra of complexes is due to enhanced double bond character through chelation, thus offsetting the loss of electron density *via* donation to the metal ion, and is supportive of azomethine coordination.

The spectral band $\nu(\text{NH})$ of thiosemicarbazones disappeared in the complexes except in **3** and **8**, indicating the deprotonation of the $-\text{NH}$ proton and coordination *via* thiolate sulfur is indicated by a decrease in stretching and bending frequencies (30–80 cm^{-1}) of the thioamide band, which is partly $\nu(\text{CS})$, and found at ~ 1320 and 840 cm^{-1} in the uncomplexed thiosemicarbazones to ~ 1270 and 750 cm^{-1} in the spectra of complexes. In complexes **3** and **8**, coordination takes place *via* thione sulfur atom. The negative shift of $\nu(\text{CS})$ in the complexes is already indicated by Campbell [2]. The $\nu(\text{CuS})$ vibration in the range 340–380 cm^{-1} further corroborates the sulfur bonding [23-25]. IR spectra of the complexes **4**, **5**, **6**, **9** and **10** exhibit bands characteristic of coordinated heterocyclic bases [26].

IR spectra of the complexes **2**, **5**, **6** and **9** are presented in Figures 3.3-3.6.

Table 3.5. Selected IR bands (cm^{-1}) with tentative assignments of the ligands and its Cu(II) complexes

Compound	$\nu(\text{OH})$	$\nu(\text{C}=\text{N}_{\text{azo}})$	$\nu(\text{C}=\text{N})$	$\nu(\text{N}-\text{N})$	$\nu/\delta[(\text{C}=\text{S})/(\text{C}-\text{S})]$	$\nu(\text{C}-\text{O})$	$\nu(\text{Cu}-\text{N})$	Bands due to heterocyclic bases
HL^1		1624	----	1066	1334, 837	----	----	----
$[\text{CuL}^1]_2 \cdot \text{H}_2\text{O}$ (1)		1587	1549	1072	1271, 753	----	463	----
H_2L^2	3315	1612	----	1037	1324, 861	1271	----	----
$[(\text{CuL}^2)_2]$ (2)		1594	1554	1083	1273, 751	1208	477	----
$[\text{Cu}(\text{HL}^2)_2]$ (3)		1585	----	1068	1310, 856	1198	453	----
$[\text{CuL}^2 \text{bipy}]$ (4)		1594	1536	1073	1271, 759	1201	461	1439, 736
$[\text{CuL}^2 \text{phen}]$ (5)		1593	1535	1082	1265, 754	1194	466	1444, 727
$[\text{CuL}^2 \gamma\text{-pic}] \cdot 2\text{H}_2\text{O}$ (6)		1596	1555	1082	1273, 751	1208	488	1437, 622
HL^3		1607	----	1064	1312, 821	----	----	----
$[\text{CuL}^3]_2 \cdot 0.5\text{H}_2\text{O}$ (7)		1595	1549	1076	1266, 730	----	453	----
H_2L^4	3442	1622	----	1034	1338, 839	1288	----	----
$[\text{Cu}(\text{HL}^4)_2]$ (8)		1605	----	1067	1325, 830	1230	437	----
$[\text{CuL}^4 \text{py}] \cdot 3\text{H}_2\text{O}$ (9)		1595	1552	1076	1260, 753	1208	486	1437, 657
$[\text{CuL}^4 \text{bipy}]$ (10)		1594	1535	1069	1276, 766	1248	440	1451, 648

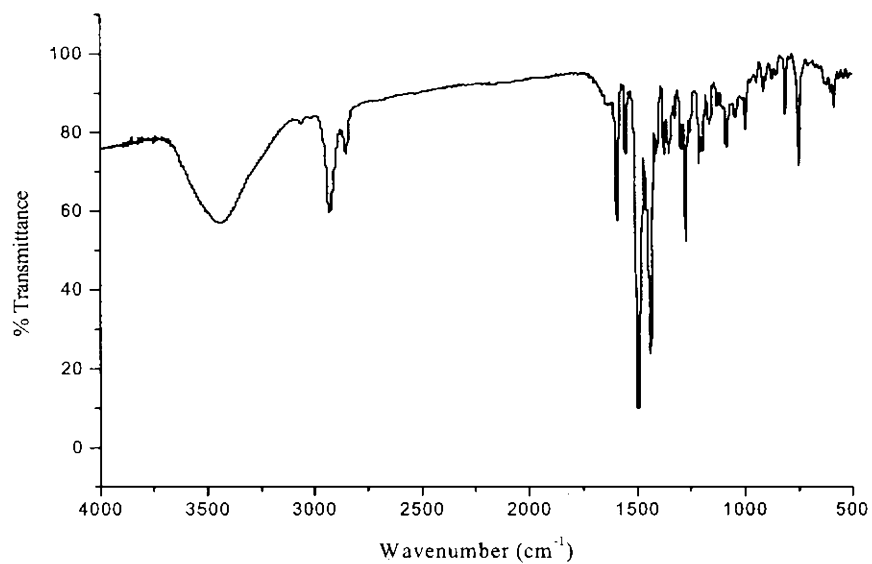


Figure 3.3. IR spectrum of the compound [(CuL²)₂] (2)

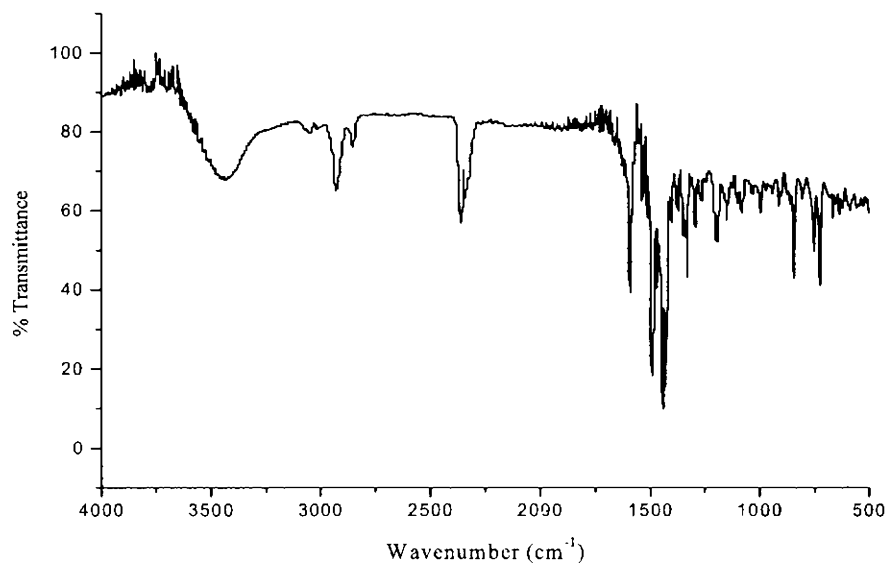


Figure 3.4. IR spectrum of the compound [CuL²phen] (5)

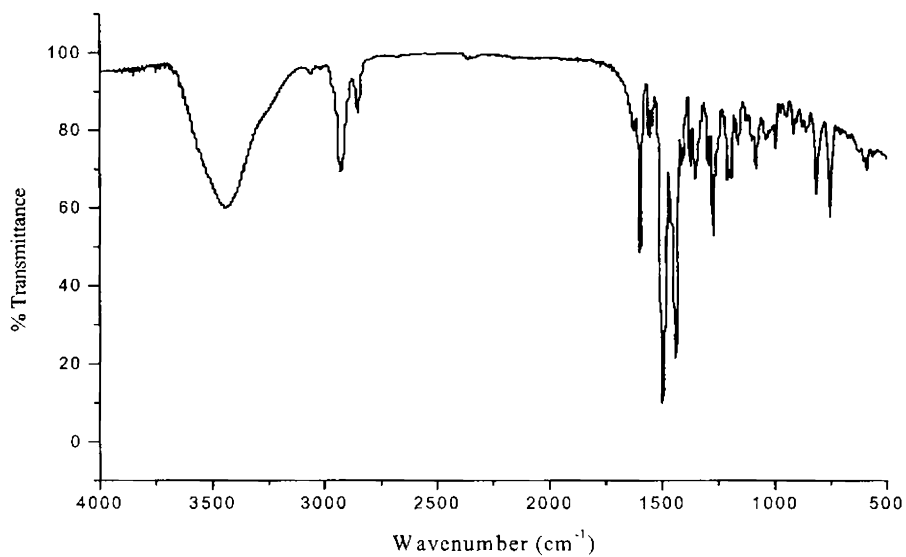


Figure 3.5. IR spectrum of the compound $[\text{CuL}^2\gamma\text{-pic}]\cdot 2\text{H}_2\text{O}$ (6)

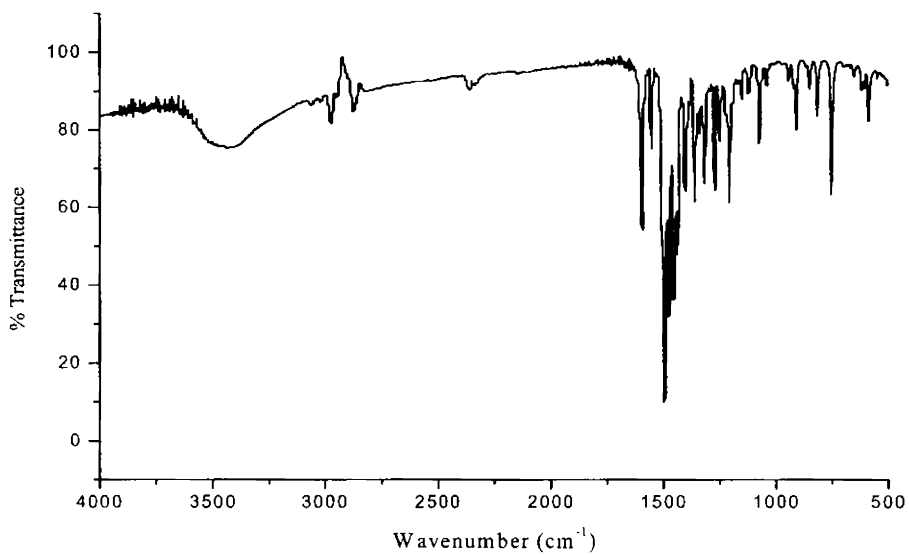


Figure 3.6. IR spectrum of the compound $[\text{CuL}^4\text{py}]\cdot 3\text{H}_2\text{O}$ (9)

3.3.3. Electronic spectra

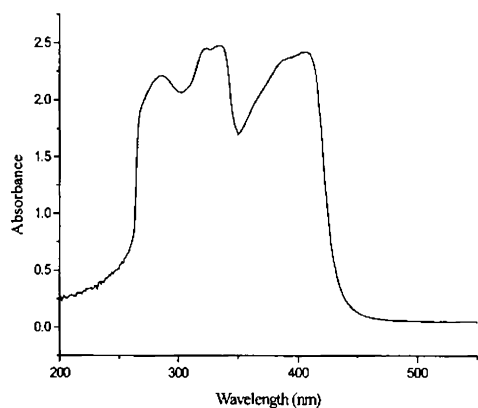
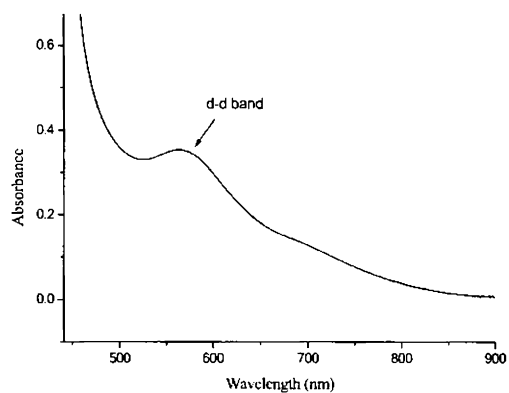
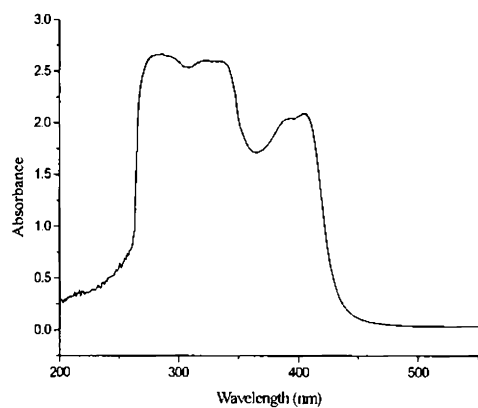
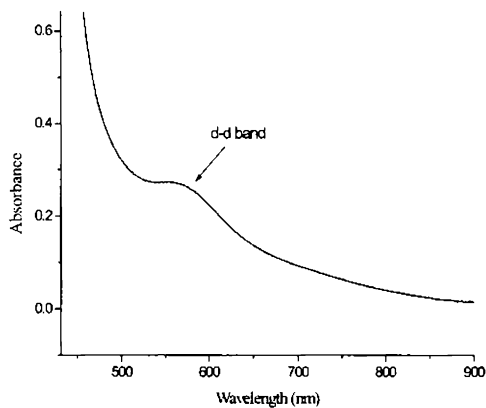
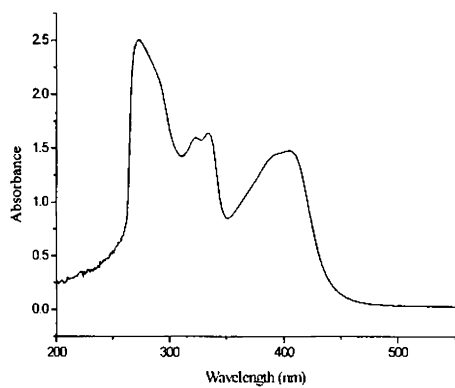
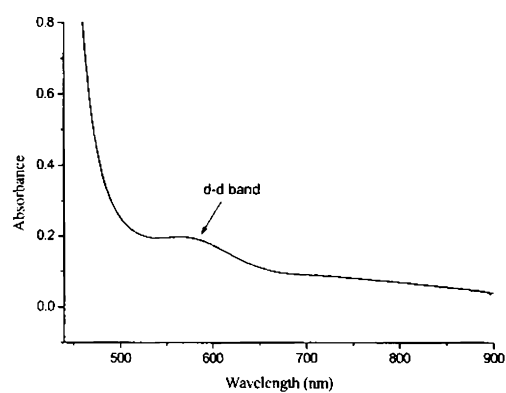
The significant electronic spectral bands for all the ligands and complexes in DMF are depicted in Table 3.6. The electronic spectra of thiosemicarbazones and its complexes show bands in the ranges 35000–37000 and 28000–32000 cm^{-1} assignable to $\pi \rightarrow \pi^*$ and $n \rightarrow \pi^*$ transitions respectively [25]. These bands are slightly shifted upon complexation. The shift of the $\pi \rightarrow \pi^*$ bands to longer wavelength region in complexes is the result of the C=S bond being weakened and the conjugation system enhanced on complexation [27, 28]. The $n \rightarrow \pi^*$ bands in the complexes have shown a blue shift due to donation of lone pair of electrons to the metal and hence the coordination of azomethine with a reduction of intensity. In the case of complexes having ONS donor ligands, the shift of two ligand to metal charge transfer bands are found in the 25000–27000 and 23000–24500 cm^{-1} ranges. In accordance with studies of previous copper(II) thiosemicarbazone complexes [29], the higher energy band is assigned to S→Cu(II) transitions. Complexes having NS donor ligands show only S→Cu(II) transitions. Its position is dependent on the steric requirements of the N(4) substituents. That is, thiosemicarbazones with bulkier N(4)-substituents have this band at somewhat higher energies. In most of the dianionic complexes, LMCT maxima of the phenolato complexes show line broadening with a tail running into the visible part of the spectrum. This may result from a phenolate to M(II) LMCT band being superimposed on the low energy side of S→M(II) LMCT. The band in the 21000–23000 cm^{-1} range involves bridging phenoxy O→Cu(II) transitions [30]. Each complex has a broad *d-d* combination band in the range 15000–17000 cm^{-1} and appears as a shoulder on the intraligand and charge transfer bands. For a square planar complex with $d_{x^2-y^2}$ ground state, three transitions are possible *viz*,

$$d_{x^2-y^2} \rightarrow d_{xy}, d_{z^2} \text{ and } d_{x^2-y^2} \rightarrow d_{xz}, d_{yz} \quad ({}^2A_{1g} \leftarrow {}^2B_{1g}, {}^2B_{2g} \leftarrow {}^2B_{1g} \text{ and } {}^2E_g \leftarrow {}^2B_{1g})$$

and square pyramidal complexes have the $d_{x^2-y^2} \rightarrow d_{xz}, d_{yz}$ and $d_{x^2-y^2} \rightarrow d_{z^2}$ transitions [31, 32]. Representative spectra of the complexes **2**, **3** and **5** are presented in Figure 3.7.

Table 3.6. Electronic spectral assignments (cm^{-1}) of the ligands and its Cu(II) complexes

Compound	$\pi - \pi^*$	$n - \pi^*$	LMCT	d - d
HL ¹	36900	28250	----	----
[CuL ¹] ₂ ·H ₂ O (1)	36360	30490	26170	15180
H ₂ L ²	36110	29500	----	----
[(CuL ²) ₂] (2)	35210	29670,31450	22330,25910	15820
[Cu(HL ²) ₂] (3)	35970	29670,31850	24330,25970	15630
[CuL ² bipy] (4)	35090	29850,31250	24330,25640	17420
[CuL ² phen] (5)	35120	29670,31200	24330,25770	17120
[CuL ² γ -pic]·2H ₂ O (6)	35210	29790,31250	24270,25990	17300
HL ³	35340	31150	----	----
[CuL ³] ₂ ·0.5H ₂ O (7)	35250	31210	25900	16640
H ₂ L ⁴	36490	30210	-----	-----
[Cu(HL ⁴) ₂] (8)	36100	31460	25380	14160
[CuL ⁴ py]·3H ₂ O (9)	35590	31450	25320	17510
[CuL ⁴ bipy] (10)	35560	31640	25250	17180

 $[(\text{CuL}^2)_2] (2)$  $[(\text{CuL}^2)_2] (2)$  $[\text{Cu}(\text{HL}^2)_2] (3)$  $[\text{Cu}(\text{HL}^2)_2] (3)$  $[\text{CuL}^2 \text{ phen}] (5)$  $[\text{CuL}^2 \text{ phen}] (5)$ **Figure 3.7.** Electronic spectra of the compounds 2, 3 and 5 in DMF solutions

3.3.4. EPR spectra

EPR spectra of the complexes in the polycrystalline state at 298 K and in DMF at 77 K were recorded in the X-band and the g factors were quoted relative to the standard marker TCNE ($g=2.00277$). The EPR parameters of Cu(II) complexes obtained for the polycrystalline state at 298 K and in DMF at 77 K are presented in Tables 3.7 and 3.8.

EPR spectra of the complexes recorded in polycrystalline state at room temperature also provide information about the coordination environment around Cu(II) in these complexes. EPR studies of Cu(II) complexes of some salicylaldehyde thiosemicarbazones were reported earlier [25, 33]. The EPR spectra of compounds **2**, **3**, **6**, **9** and **10** in the polycrystalline state (298 K) show only one broad signal, which is attributable to enhanced spin lattice relaxation due to dipolar interaction. These type of spectra do not give any information on the electronic ground state of Cu(II) ion present in the complexes. The spectrum of compound **4** gave three g values viz. g_1 , g_2 and g_3 , which indicate rhombic distortion in their geometry. The values g_1 and g_2 are very close to each other in the compounds, which mean that rhombic distortion is very small. The lowest g value (g_1) is >2.04 indicating a rhombic, distorted square based pyramidal geometry. The spectra of compounds **1**, **5**, **7** and **8** show typical axial spectra with well-defined g_{\parallel} and g_{\perp} values. The geometric parameter G , which is a measure of the exchange interaction between the copper centers in the polycrystalline compound is calculated using the equation, $G = g_{\parallel} - 2.0023 / g_{\perp} - 2.0023$ for axial spectra and for rhombic spectra $G = g_3 - 2.0023 / g_{\perp} - 2.0023$, where $g_{\perp} = (g_1 + g_2) / 2$. If $G > 4.4$, exchange interaction is negligible and if it is less than 4.4, considerable exchange interaction is indicated in the solid complex [33, 34]. In all the Cu(II) complexes $g_{\parallel} > g_{\perp} > 2.0023$ and G value within the range 2.5–3.5 are consistent with a

$d_{x^2-y^2}$ ground state [35, 36]. The parameter R $\{R = (g_2 - g_1)/(g_3 - g_2)$ for rhombic systems $\}$ calculated for the compound **4** is around 0.326, *i.e.*, $R < 1$, indicating a $d_{x^2-y^2}$ ground state of the copper(II) ion [37, 38].

Table 3.7. EPR spectral assignments for Cu(II) complexes in polycrystalline state at 298 K and in DMF at 77 K

Compound	Polycrystalline state (298 K)	DMF solution (77 K)					
		g_{\parallel}	g_{\perp}	g_{av}	A_{\parallel}^a	A_{\perp}^a	A_{av}^a
[CuL ₂] \cdot H ₂ O (1)	2.141/2.050 (g_{\parallel}/g_{\perp})	2.113	2.040	2.064	164.4	25.4	70.7
[(CuL ₂) ₂] (2)	2.040 (g_{iso})	2.162	2.045	2.084	191.8	22.2	76.9
[Cu(HL ²) ₂] (3)	2.053 (g_{iso})	2.134	2.037	2.069	179.3	22.2	72.9
[CuL ² bipy] (4)	2.177/2.079/2.047 ($g_3/g_2/g_1$)	2.168	2.045	2.086	190.6	14.2	70.9
[CuL ² phen] (5)	2.192/2.059 (g_{\parallel}/g_{\perp})	2.184	2.059	2.101	----	----	----
[CuL ² γ -pic] \cdot 2H ₂ O (6)	2.067 (g_{iso})	2.169	2.047	2.088	202.5	22.3	80.1
[CuL ³ ₂] \cdot 0.5H ₂ O (7)	2.199/2.061 (g_{\parallel}/g_{\perp})	2.194	2.055	2.107	196.2	15.9	73.7
[Cu(HL ⁴) ₂] (8)	2.141/2.053 (g_{\parallel}/g_{\perp})	2.117	2.047	2.070	174.6	----	----
[CuL ⁴ py] \cdot 3H ₂ O (9)	2.047 (g_{iso})	2.155	2.042	2.080	194.5	27.0	80.9
[CuL ⁴ bipy] (10)	2.053 (g_{iso})	2.170	2.052	2.091	189.1	20.7	74.8

^a Expressed in units of cm^{-1} multiplied by a factor of 10^{-4} .

The spectra of all the complexes in DMF at 77 K are axial. The solution spectra of complexes except **5**, at 77 K in DMF show four hyperfine lines characteristic of monomeric Cu(II) complexes corresponding to $-3/2, -1/2, 1/2$ and $3/2$ transitions, which arise from the coupling of the odd electron with Cu nuclei (^{65}Cu , $I=3/2$) and spectrum of compound **5** is axial without any super or hyperfine lines. The third copper hyperfine line is expected to overlap with the high field component (g_{\perp}) in **1** and **8**. However, the half field signal corresponding to the dimer was not observed for the compound **2** [39]. The spectra of compounds **1**, **3** and **7** gave five superhyperfine lines, which arise from the coupling of the electron spin with the nuclear spin of the two nitrogen atoms in the g_{\parallel} features indicating the

coordination of two coplanar nitrogen atoms *i.e.* in each complex two azomethine nitrogens coordinate to the metal centre. The spectrum of complex **2** gave three superhyperfine lines, indicating that only azomethine nitrogen is involved in bonding in the monomer unit. This confirms the binuclear nature of the complex. In the spectra of compounds **6** and **9**, all the signals show five superhyperfine lines in the low field and five splittings in the high field region. This splitting may be due to the presence of heterocyclic bases present in the molecule *i.e.* two nitrogens involved are coplanar. The g_{\parallel} values in all these complexes are less than 2.3 is an indication of significant covalent bonding in these complexes [40, 41]. The $g_{\parallel} > g_{\perp}$ values accounts to the distorted square based pyramid structure in five coordinated complexes and rules out the possibility of a trigonal bipyramidal structure, which would be expected to have $g_{\parallel} < g_{\perp}$. For complexes **4** and **10** having bipyridine as coligand, g_{\parallel} value of **4** is smaller compared to **10** indicating that H_2L^2 is stronger ligand than H_2L^4 .

Table 3.8. EPR bonding parameters for compounds 1-10

Compound	G	R	DMF solution (77 K)							
	(298 K)		α^2	β^2	γ^2	K	K_{\parallel}	K_{\perp}	f^a	P
[CuL ¹ ₂]-H ₂ O (1)	2.94	----	0.62	0.81	0.94	0.32	0.50	0.58	128	0.0183
[(CuL ²) ₂] (2)	----	----	0.76	0.81	0.83	0.37	0.62	0.63	112.7	0.0239
[Cu(HL ²) ₂] (3)	----	----	0.68	0.81	0.83	0.33	0.55	0.57	119	0.0213
[CuL ² bipy] (4)	2.89	0.326	0.75	0.88	0.89	0.32	0.66	0.67	113.7	0.0253
[CuL ² phen] (5)	3.31	----	----	----	----	----	----	----	----	----
[CuL ² γ -pic]-2H ₂ O (6)	----	----	0.79	0.83	0.86	0.36	0.66	0.68	107	0.0256
[CuL ³]-0.5H ₂ O (7)	----	----	0.69	0.83	0.86	0.30	0.57	0.59	116.8	0.0214
[Cu(HL ⁴) ₂] (8)	2.50	----	0.66	0.77	0.95	----	0.51	0.63	121.3	----
[CuL ⁴ py]-3H ₂ O (9)	----	----	0.75	0.85	0.86	0.35	0.63	0.64	110.8	0.0236
[CuL ⁴ bipy] (10)	----	----	0.75	0.88	0.95	0.34	0.66	0.72	114.8	0.0239

^a Expressed in units of cm.

The EPR parameters g_{\parallel} , g_{\perp} , g_{av} , $A_{\parallel}(\text{Cu})$, $A_{\perp}(\text{Cu})$ and energies of $d-d$ transitions were used to evaluate the bonding parameters α^2 , β^2 and γ^2 , which may be regarded as measures of covalency of the in-plane σ -bonds, in-plane π -bonds and out-of-plane π -bonds respectively [40].

The value of in-plane σ -bonding parameter α^2 was estimated from the expression,

$$\alpha^2 = -A_{\parallel}/0.036 + (g_{\parallel} - 2.00277) + 3/7 (g_{\perp} - 2.00277) + 0.04$$

The orbital reduction factors, $K_{\parallel}^2 = \alpha^2\beta^2$ and $K_{\perp}^2 = \alpha^2\gamma^2$ were calculated using the following expressions [40, 42],

$$K_{\parallel}^2 = (g_{\parallel} - 2.00277) E_{d-d}/8\lambda_0$$

$$K_{\perp}^2 = (g_{\perp} - 2.00277) E_{d-d}/2\lambda_0$$

Where λ_0 is the spin orbit coupling constant with a value of -828 cm^{-1} for Cu(II) d^9 system.

According to Hathaway [43], for pure σ -bonding $K_{\parallel} \approx K_{\perp} \approx 0.77$, and for in-plane π -bonding, $K_{\parallel} < K_{\perp}$; while for out-of-plane π -bonding $K_{\perp} < K_{\parallel}$. In all the complexes it is observed that $K_{\parallel} < K_{\perp}$, which indicates the presence of significant in-plane π -bonding. The values of the bonding parameters α^2 , β^2 and $\gamma^2 < 1.0$ (value of 1.0 for 100% ionic character) indicate significant in-plane π -bonding and in-plane σ -bonding.

The Fermi contact hyperfine interaction term K , which is a dimensionless quantity and is generally found to have a value of 0.36, which is a measure of the contribution of 's' electrons to the hyperfine interaction can be calculated from the expression [43],

$$K = A_{iso}/P\beta^2 + (g_{av} - 2.00277) / \beta^2$$

Where P is the free ion dipolar term and its value is 0.036. The K values obtained for all the complexes are in good agreement with those estimated by Assour [44] and Abragam and Pryce [45]. The empirical factor $f = g_{\parallel} / A_{\parallel} (\text{cm}^{-1})$ is an index of tetragonal distortion. The value may vary from 105–135 for small to extreme distortion and that depends on the nature of the coordinated atom. In all the compounds except **1** and **8**, f falls in the range 105–135 corresponding to a copper(II) center with medium distortion [12]. High distortion occurs for the complexes **1** and **8** which are evidenced from the f value. Representative EPR spectra of the compounds **3**, **4** and **5** in polycrystalline state at 298 K (Figures 3.8–3.10) and **2**, **3**, **6** and **9** in DMF at 77 K are presented in Figures 3.11–3.14.

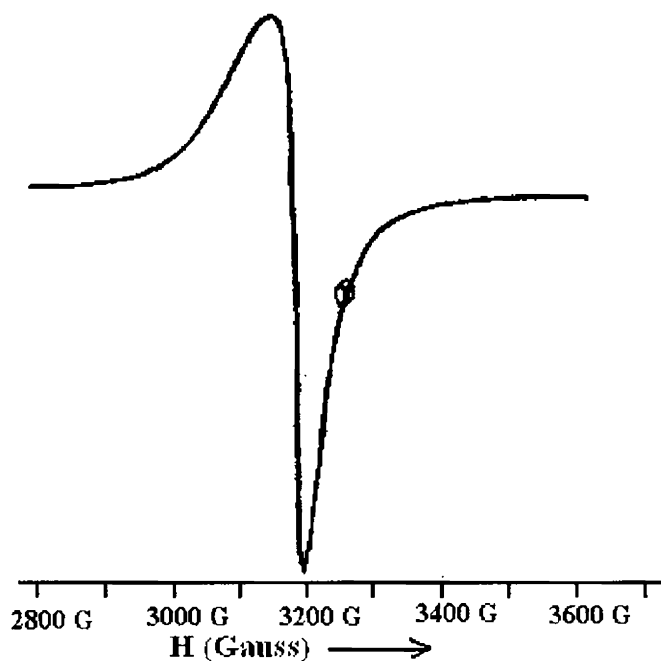


Figure 3.8. EPR spectrum of the compound $[\text{Cu}(\text{HL}^2)_2]$ (**3**) in polycrystalline state at 298 K

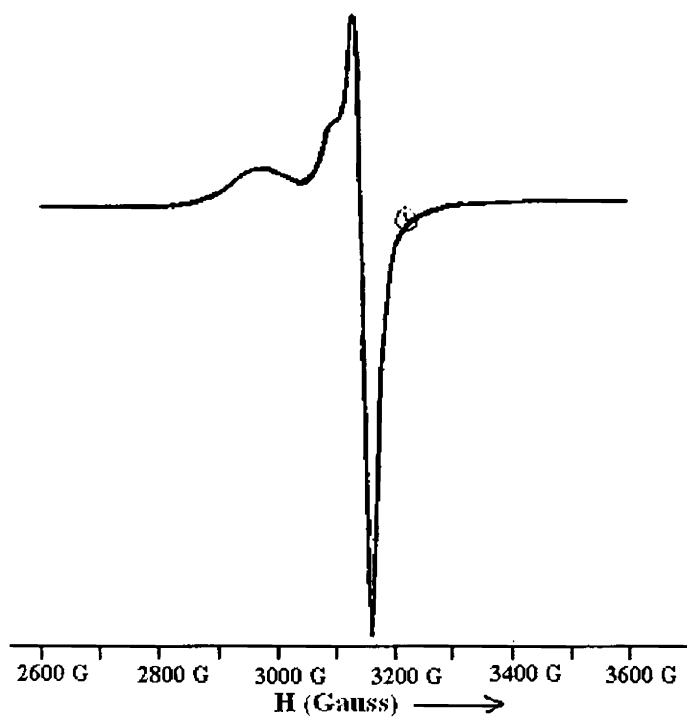


Figure 3.9. EPR spectrum of the compound $[\text{CuL}^2\text{bipy}]$ (4) in polycrystalline state at 298 K

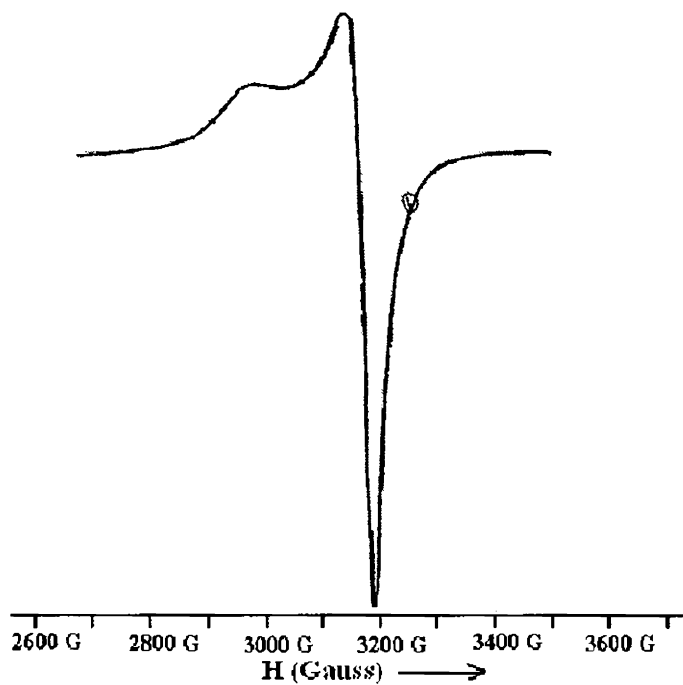


Figure 3.10. EPR spectrum of the compound $[\text{CuL}^2\text{phen}]$ (5) in polycrystalline state at 298 K

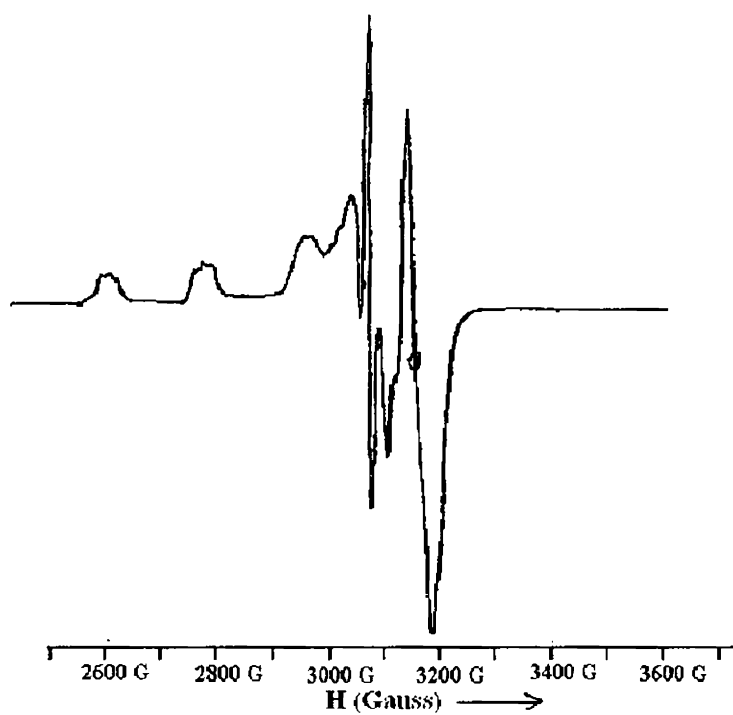


Figure 3.11. EPR spectrum of the compound $[(\text{CuL}^2)_2]$ (2) in DMF at 77 K.

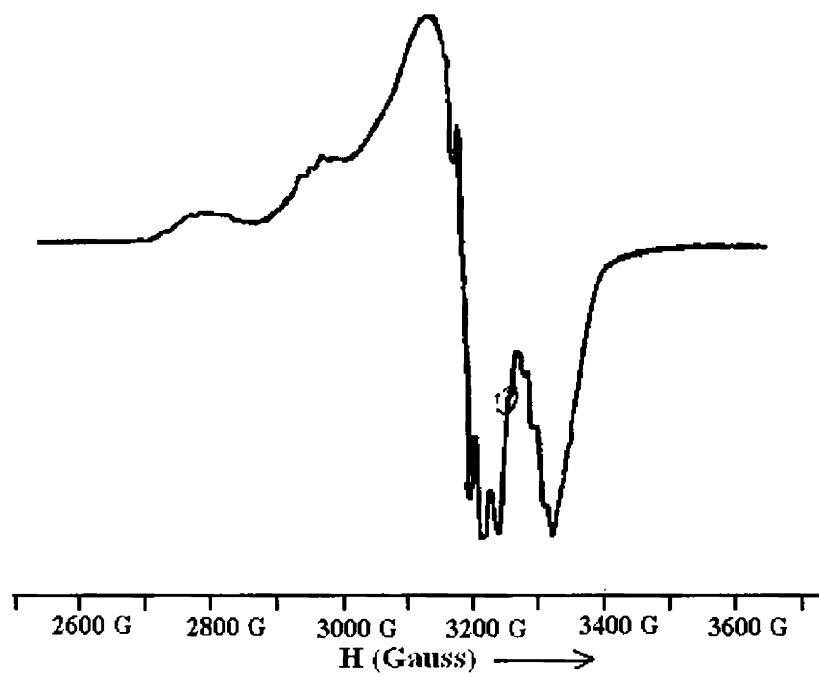


Figure 3.12. EPR spectrum of the compound $[\text{Cu}(\text{HL}^2)_2]$ (3) in DMF at 77 K.

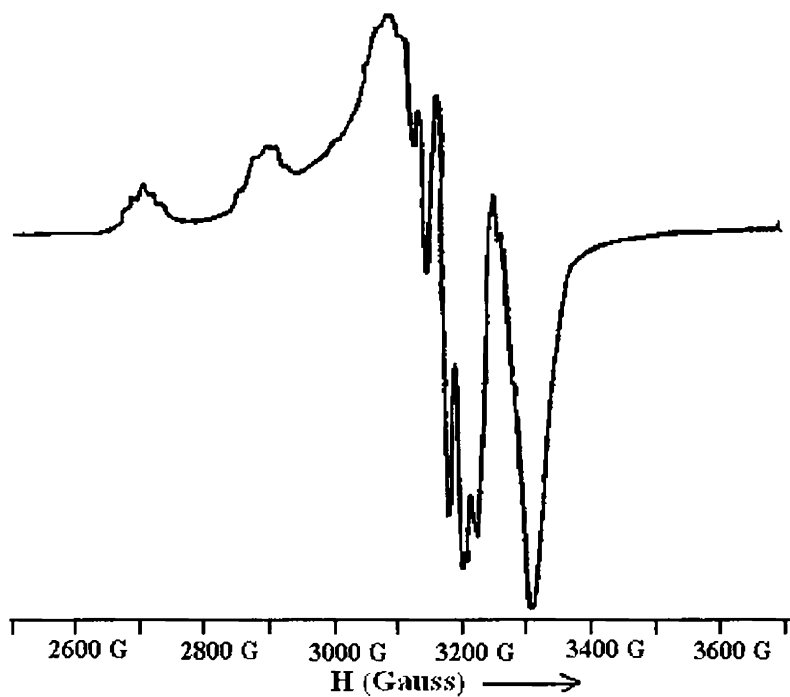


Figure 3.13. EPR spectrum of the compound $[\text{CuL}^2\gamma\text{-pic}]\cdot 2\text{H}_2\text{O}$ (6) in DMF at 77 K

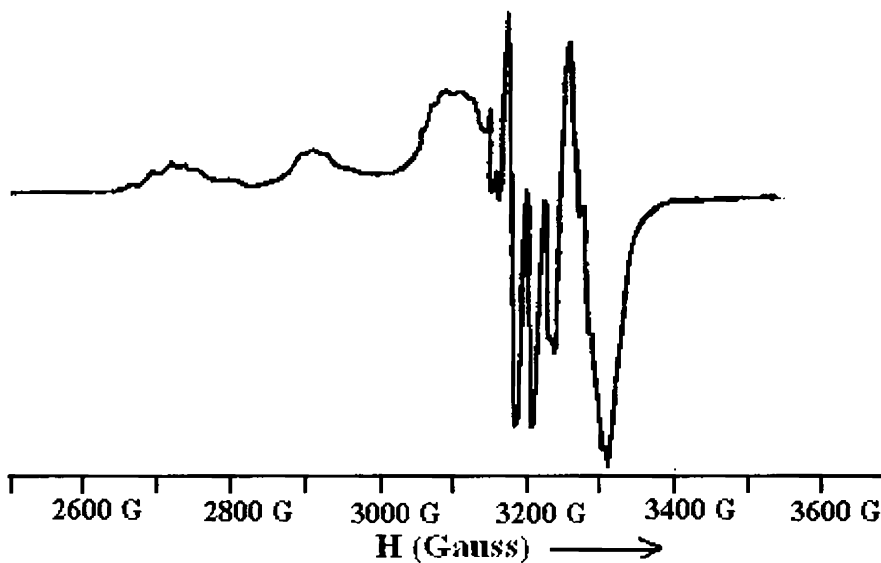


Figure 3.14. EPR spectrum of the compound $[\text{CuL}^4\text{py}]\cdot 3\text{H}_2\text{O}$ (9) in DMF at 77 K

Based on the elemental analyses and spectral investigations, following tentative structures were assigned for the complexes for which, single crystals suitable for crystallographic studies could not be isolated (Figure 3.15).

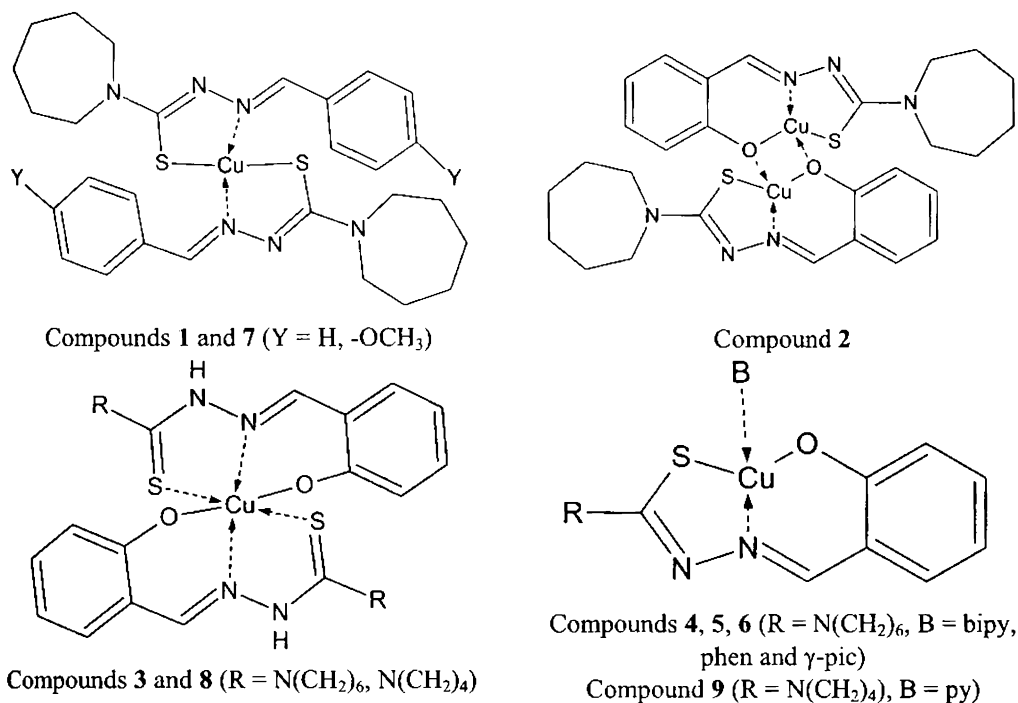


Figure 3.15. Tentative structures of the compounds

References

1. E.S. Raper, *Coord. Chem. Rev.* 153 (1996) 199.
2. M.J.M. Campbell, *Coord. Chem. Rev.* 15 (1975) 279.
3. S.B. Padhye, G.B. Kauffman, *Coord. Chem. Rev.* 63 (1985) 127.
4. D.X. West, A.E. Liberta, S.B. Padhye, R.C. Chikate, P.B. Sonawane, A.S. Kumbhar, R.G. Yerande, *Coord. Chem. Rev.* 123 (1993) 49.
5. M.B. Ferrari, S. Capacchi, G. Pelosi, G. Reffo, P. Tarasconi, R. Albertini, S. Pinelli, P. Lunghi, *Inorg. Chim. Acta* 286 (1999) 134.
6. M. A. Ali, D.A. Chowdhury, M. Nazimuddin, *Polyhedron* 3 (1984) 595.

7. Nonius (1997) MACH3 software, B.V. Nonius, Delft, The Netherlands.
8. G.M. Sheldrick, *Acta Crystallogr.* A46 (1990) 467.
9. G.M. Sheldrick, SHELXL-97 and SHELXS-97 Program for the solution of Crystal Structures, University of Göttingen, Germany, 1997.
10. K. Brandenburg, DIAMOND version 3.1d, Crystal Impact GbR, Bonn, Germany, 2006.
11. G. Plesch, C. Friebel, *Polyhedron* 14 (1995) 1185.
12. R.P. John, A. Sreekanth, V. Rajakannan, T.A. Ajith, M.R.P. Kurup, *Polyhedron* 23 (2004) 2549.
13. E.B. Seena, M.R.P. Kurup, *Polyhedron* 26 (2007) 829.
14. C.B. Castellani, G. Gatti, R. Millini, *Inorg.Chem.* 23 (1983) 4004.
15. N.J. Ray, B.J.Hathaway, *Acta Crystallogr.* B34 (1978) 3224.
16. G. Druhan, B.J.Hathaway, *Acta Crystallogr.* B35 (1979) 344.
17. A.W. Addison, T.N. Rao, J. Reedijk, J. Van Rijn, G.C. Verschoor, *J.Chem.Soc., Dalton Trans.* (1984) 1349.
18. R.C. Chikate, A.R. Belapure, S.B. Padhye, D.X. West, *Polyhedron* 24 (2005) 889.
19. V.D. Khanolkar, D.D. Khanolkar, *Indian J. Chem.* 18A (1979) 315.
20. J. Jezierska, B. Jezowska-Trzebiatowska, G. Petrova, *Inorg. Chim. Acta* 50 (1981) 153.
21. Z. Afrasiabi, E. Sinn, J. Chen, Y. Ma, A.L. Rheingold, L.N. Zakharov, N. Rath, S. Padhye, *Inorg. Chim. Acta* 357 (2004) 271.
22. R.P. John, A. Sreekanth, M.R.P. Kurup, A. Usman, I.A. Razak, H.-K. Fun, *Spectrochim. Acta* 59A (2003) 1349.
23. S.K. Sengupta, S.K. Sahni, R.N. Kapoor, *Acta. Chim. Acad. Sci. Hungary* 104 (1980) 89.

24. M. Joseph, M. Kuriakose, M.R.P. Kurup, E. Suresh, A. Kishore, S.G. Bhat, *Polyhedron* 25 (2006) 61.
25. P. Bindu, M.R.P. Kurup, T.R. Satyakeerty, *Polyhedron* 18 (1998) 321.
26. P.B. Sreeja, M.R.P. Kurup, *Spectrochim. Acta* 61A (2005) 331.
27. V. Philip, V. Suni, M.R.P. Kurup, *Polyhedron* 25 (2006) 1931.
28. I.-X. Li, H.A. Tang, Yi-Zhi Li, M. Wang, L.-F. Wang, C.-G. Xia, *J. Inorg. Biochem.* 78 (2000) 167.
29. M. Mikuriya, H. Okawa, S. Kida, *Inorg. Chim. Acta* 34 (1979) 13.
30. M. Mikuriya, H. Okawa, S. Kida, *Bull. Chem. Soc. Japan* 53 (1980) 3717.
31. P. Bindu, M.R.P. Kurup, *Trans. Met. Chem.* 22 (1997) 578.
32. I.M. Proctor, B.J. Hathaway, P. Nicholis, *J. Chem. Soc.* (1968) 1678.
33. B.J. Hathaway, D.E. Billing, *Coord. Chem. Rev.* 5 (1970) 1949.
34. A. Sreekanth, M.R.P. Kurup, *Polyhedron* 22 (2003) 3321.
35. M.J. Bew, B.J. Hathaway, R.R. Faraday, *J.Chem.Soc., Dalton Trans.* (1972) 1229.
36. S.S. Kandil, A. El-Dissouky, G.Y. Ali, *J. Coord. Chem.* 57 (2004) 105.
37. M.F. El-Shazly, A. El-Dissouky, T.M. Salem, M.M. Osman, *Inorg. Chim. Acta* 40 (1980) 1.
38. A.H. Maki, B.R. McGarvey, *J. Chem. Phys.* 29 (1958) 35.
39. P.F. Raphel, E. Manoj, M.R.P. Kurup, *Polyhedron* 26 (2007) 818.
40. J.R. Wasson, C. Trapp, *J. Phys. Chem.* 73 (1969) 3763.
41. D. Kivelson, R. Neiman, *J.Chem.Soc., Dalton Trans.* 35 (1961) 149.
42. B.J. Hathaway, *Structure and Bonding*, Springer Verlag, Heidelberg, (1973) 60.
43. R.S. Nicholson, *Anal. Chem.* 37 (1965) 1351.
44. M. Assour, *J. Chem. Phys.* 43 (1965) 2477.
45. A. Abragam, M.H.L. Pryce, *Proc. R. Soc. London A206* (1961) 164.

Synthesis, spectral and structural studies of Ni(II) complexes of N(4)-ring incorporated thiosemicarbazones of aromatic aldehydes

4.1. Introduction

Nickel is the twenty-second most abundant element by weight in the earth's crust. Nickel is one of the most toxic metals among transition metals. It shows the toxicity even in low doses to both plants and animals [1, 2]. Excess nasal and lung cancers are known to be associated with the refining of nickel. Epidemiological data and animal study confirm that crystalline nickel compounds are carcinogenic, while amorphous nickel compounds are weak or non-carcinogenic. Nickel is also involved in transport of metal in eukaryotic algae.

Nickel shows a range of oxidation states from (0) to (+IV), but its chemistry is predominantly that of the (+II) state. It is predominantly divalent and ionic in simple compounds, and exists as Ni(II) in most of its complexes. Nickel forms four, five and six coordinate complexes *viz*, square planar, tetrahedral, trigonal bipyramidal, square pyramidal and octahedral geometries. Five coordinate nickel complexes are rather unusual.

Ni(II) complexes derived from the thiosemicarbazones of aromatic *o*-hydroxyaldehydes, in particular salicylaldehyde, have recently attracted considerable attention as homogeneous catalysts. Complexes between metals and thiosemicarbazone ligands exhibit a broad spectrum of biological properties, including antibacterial, antimalarial, antiviral and antineoplastic activities [3]. In

the last few years, nickel(II) complexes containing sulfur donors have received considerable attention due to the identification of a sulfur rich coordination environment in biological nickel centers such as at the active sites of certain ureases, methyl-S-coenzyme-M-methyl reductase, hydrogenases and may play a role in the supposed mutagenicity of nickel compounds. Several aspects of the chemistry of these biological nickel ions are unusual in the context of the known coordination chemistry of nickel [4].

This chapter deals with the synthesis, structural and spectral characterization of Ni(II) complexes with different N(4)-ring incorporated thiosemicarbazone ligands. The structures of four of the compounds have been solved by single crystal X-ray crystallography.

4.2. Experimental

4.2.1. Materials

The synthesis of ligands HL^1 , H_2L^2 , HL^3 and H_2L^4 are discussed in Chapter 2. $Ni(OAc)_2 \cdot 4H_2O$ (Central drug house), pyridine, $\alpha/\beta/\gamma$ -picoline, 2,2'-bipyridine (bipy) (Central drug house) and 1,10-phenanthroline (phen) (Ranbaxy fine chemicals) were used as received. The reagents used were of Analar grade and used without further purification.

4.2.2. Synthesis of the complexes

$[NiL^1_2]$ (11): This complex was synthesized by refluxing an ethanolic solution of HL^1 (2 mmol, 0.522 g) with methanolic solution of $Ni(OAc)_2 \cdot 4H_2O$ (1 mmol, 0.248 g) for 4 h. The brown colored complex formed was filtered, washed with ethanol and finally with ether and dried over P_4O_{10} *in vacuo*.

$[Ni(HL^2)_2]$ (12): Ethanolic solution of the ligand H_2L^2 (2 mmol, 0.554 g) and hot methanolic solution of $Ni(OAc)_2 \cdot 4H_2O$ (1 mmol, 0.248 g) in 2:1 ratio was refluxed

for 2 h. The brown colored product formed was filtered, washed with ethanol and finally with ether and dried over P_4O_{10} *in vacuo*.

[NiL²py] (13): To a hot ethanolic solution of the ligand H_2L^2 (1 mmol, 0.277 g), added hot methanolic solution of $Ni(OAc)_2 \cdot 4H_2O$ (1 mmol, 0.248 g) with constant stirring. This was followed by the addition of slight excess of the base pyridine (2 mmol, 0.158 g). The above brown solution was refluxed for about 4 h and allowed to cool, when reddish brown crystals were formed. The complex formed was filtered, washed with ethanol and ether and dried *in vacuo* over P_4O_{10} .

[NiL² α -pic] (14): $Ni(OAc)_2 \cdot 4H_2O$ (1 mmol, 0.248 g) dissolved in methanol was added to a solution of H_2L^2 (1 mmol, 0.277 g) in hot ethanol and slight excess of heterocyclic base α -picoline (2 mmol, 0.186 g) with constant stirring. The solution was then refluxed for 2 h. The reddish brown crystals formed was filtered, washed with ethanol and finally with ether and dried over P_4O_{10} *in vacuo*.

[NiL² β -pic] (15): An ethanolic solution of H_2L^2 (1 mmol, 0.277 g) was mixed with hot methanolic solution of $Ni(OAc)_2 \cdot 4H_2O$ (1 mmol, 0.248 g) and this was followed by the addition of the base β -picoline (2 mmol, 0.186 g). The resulting solution was then refluxed for 3h, when reddish brown shining crystals began to separate. This was filtered, washed with ethanol and ether and dried *in vacuo* over P_4O_{10} .

[NiL² γ -pic]·H₂O (16): Solutions of H_2L^2 (1 mmol, 0.277 g) in ethanol and heterocyclic base γ -picoline (2 mmol, 0.186 g) were mixed and to this was added hot methanolic solution of $Ni(OAc)_2 \cdot 4H_2O$ (1 mmol, 0.248 g). The solution was then refluxed for 3-4 h and allowed to cool, when reddish brown crystalline compound was formed. The complex formed was filtered, washed with ethanol and finally with ether and dried over P_4O_{10} *in vacuo*.

[Ni₂L²₂phen] (17): To a hot ethanolic solution of the ligand H₂L² (2 mmol, 0.554 g), added hot methanolic solution of Ni(OAc)₂·4H₂O (2 mmol, 0.496 g) with constant stirring. This was followed by the addition of the base 1,10-phenanthroline (1 mmol, 0.198 g). The above brown solution was refluxed for about 4 h and allowed to cool, when brown crystals were formed. The complex formed was filtered, washed with ethanol and ether and dried *in vacuo* over P₄O₁₀.

[NiL³]₂ (18): This complex was synthesized by refluxing an ethanolic solution of HL³ (2 mmol, 0.582 g) with hot methanolic solution of Ni(OAc)₂·4H₂O (1 mmol, 0.248 g) for 4 h. The brown colored complex formed was filtered, washed with ethanol and finally with ether and dried over P₄O₁₀ *in vacuo*.

[NiL⁴py] (19): The H₂L⁴ (1 mmol, 0.249 g) was dissolved in ethanol, to which was added hot methanolic solution of Ni(OAc)₂·4H₂O (1 mmol, 0.248 g) with constant stirring. This was followed by the addition of the base 2,2'-bipyridine (1 mmol, 0.156 g) in the solid form. The stirring was continued for about an hour when reddish brown compound began to separate. This was filtered, washed with ethanol and ether and dried *in vacuo* over P₄O₁₀.

[NiL⁴γ-pic] (20): To a hot ethanolic solution of the ligand H₂L⁴ (1 mmol, 0.249 g), added hot methanolic solution of Ni(OAc)₂·4H₂O (1 mmol, 0.248 g) with constant stirring. This was followed by the addition of slight excess of the base γ-picoline (2 mmol, 0.186 g) and the resulting solution was then refluxed for about 2-3 h and allowed to cool when reddish brown crystalline compound was formed. The complex formed was filtered, washed with ethanol and ether and dried *in vacuo* over P₄O₁₀.

4.2.3. Physical measurements

Details regarding physical measurements are presented in Chapter 3.

4.2.4. X-ray crystallography

Reddish brown crystals of the compounds **13**, **14**, **15** and a brown block crystal of the compound **17** having approximate dimensions of 0.26 x 0.21 x 0.17, 0.35 x 0.30 x 0.20, 0.24 x 0.18 x 0.10 and 0.33 x 0.16 x 0.11 mm³ respectively were selected. Compounds **13**, **14** and **17** were diffracted by CrysAlis CCD, Oxford Diffraction Ltd. with graphite-monochromated Mo K α ($\lambda=0.71073$ Å) radiation. In compound **13**, the atom C10 in the ring containing N3 is disordered as this carbon splits over two sets of positions. The ratio of major to minor disorder component is 54: 46. In compounds **13** and **14**, restraints were applied to assist the geometry of the disordered atom. The data of **15** was collected using a Bruker Smart Apex CCD diffractometer equipped with graphite-monochromated Mo K α ($\lambda=0.71073$ Å) radiation. The trial structure was solved using SHELXS-97 [5] and refinement was carried out by full-matrix least squares on F^2 (SHELXL) [5]. The graphical tool used was DIAMOND version 3.1d [6], and MERCURY [7]. All non-hydrogen atoms were refined anisotropically and hydrogen atoms were geometrically fixed at calculated positions. X-ray quality single crystals of the complex **13** were obtained from its solution in DMF over a period of 14 days and single crystals of the complexes **14**, **15** and **17** were obtained from the reaction mixture. The crystallographic data and structure refinement parameters for the complexes **13**, **14**, **15** are given in Table 4.1 and **17** in Table 4.2.

Table 4.1. Crystal data and experimental parameters for the compounds 13, 14 and 15

	13	14	15
Empirical formula	C ₁₉ H ₂₂ N ₄ NiOS	C ₂₀ H ₂₄ N ₄ Ni OS	C ₂₀ H ₂₄ N ₄ Ni OS
Formula weight	826.35	427.20	427.20
Temperature	293(2) K	293(2) K	296(2) K
Wavelength	0.71073 Å	0.71073 Å	0.71073 Å
Crystal system	Orthorhombic	Monoclinic	Triclinic
Space group	<i>Pbca</i>	<i>P2₁/a</i>	<i>Pt</i>
Unit cell dimensions	a = 13.7965(19) Å b = 21.954(4) Å c = 25.410(5) Å α = 90° β = 90° γ = 90°	a = 9.519(2) Å b = 10.726(2) Å c = 11.300(2) Å α = 67.191(3)° β = 74.416(3)° γ = 68.981(3)°	a = 8.7464(16) Å b = 10.879(3) Å c = 11.098(2) Å α = 95.178(19)° β = 100.563(16)° γ = 103.999(19)°
Volume	7696(2) Å ³	1981.5(10) Å ³	981.5(4) Å ³
Z	16	4	2
Density (calculated)	1.426 g/cm ³	1.432 g/cm ³	1.445 g/cm ³
Absorption coefficient	1.132 mm ⁻¹	1.102 mm ⁻¹	1.112 mm ⁻¹
F(000)	3456	896	448
Crystal size	0.26 x 0.21 x 0.17 mm ³	0.35 x 0.30 x 0.20 mm ³	0.24 x 0.18 x 0.10 mm ³
θ range for data collection	2.95 to 25°	3.02 to 27.50°	1.98 to 28.34°
Index ranges	-16 ≤ h ≤ 16, -26 ≤ k ≤ 25, -30 ≤ l ≤ 19	-13 ≤ h ≤ 13, -14 ≤ k ≤ 14, -22 ≤ l ≤ 22	-12 ≤ h ≤ 12, -13 ≤ k ≤ 14, -15 ≤ l ≤ 15
Reflections collected	37350	20726	8283
Independent reflections	6769 [R(int) = 0.0865]	4539 [R(int) = 0.1259]	4394 [R(int) = 0.0205]
Refinement method	Full-matrix on F ²	Full-matrix on F ²	Full-matrix on F ²
Data / restraints/parameters	6769 / 0 / 469	4539 / 0 / 232	4394 / 0 / 245
Goodness-of-fit on F ²	0.759	0.706	1.107
Final R indices [I > 2σ(I)]	R ₁ = 0.0368, wR ₂ = 0.0669	R ₁ = 0.0599, wR ₂ = 0.1407	R ₁ = 0.0569, wR ₂ = 0.1536
R indices (all data)	R ₁ = 0.1034, wR ₂ = 0.0771	R ₁ = 0.2402, wR ₂ = 0.1791	R ₁ = 0.0638, wR ₂ = 0.1611

Table 4.2. Crystal data and experimental parameters for compound 17

Empirical formula	C ₄₀ H ₄₂ N ₈ Ni ₂ O ₂ S ₂
Temperature	150(2) K
Formula weight	848.35
Wavelength	0.71073 Å
Crystal system	Triclinic
Space group	<i>P</i> $\bar{1}$
Unit cell dimensions	a = 12.3730(12) Å b = 12.573(2) Å c = 14.181(2) Å α = 73.639(15) $^\circ$ β = 79.832(11) $^\circ$ γ = 63.324(14) $^\circ$
Volume	1888.2(5) Å ³
Z	2
Calculated density	1.492 g/cm ³
Absorption coefficient	1.156 mm ⁻¹
F(000)	884
Crystal size	0.33 x 0.16 x 0.11 mm ³
θ range for data collection	2.9995 to 32.0746 $^\circ$
Index ranges	-14 \leq h \leq 14, -14 \leq k \leq 14, -16 \leq l \leq 16
Reflections collected	14670
Independent reflections	6350 [R(int) = 0.0423]
Refinement method	Full-matrix least-squares on F ²
Data / restraints / parameters	6350/ 0 / 487
Goodness-of-fit on F ²	1.110
Final R indices [I > 2 σ (I)]	R1 = 0.0565, wR2 = 0.1341
R indices (all data)	R1 = 0.0773, wR2 = 0.1425

4.3. Results and discussion

The analytical data of the complexes are presented in Table 4.3. The elemental analyses data are consistent with the general empirical formula ML₂ for **11** and **18**, [M(HL)₂] for **12**, MLB for the **13**, **14**, **15** and **16** and [M₂L₂B] for the compound **17**, where M is the nickel atom, L is the doubly deprotonated thiosemicarbazone ligand and B are the heterocyclic bases *viz.* py, phen and $\alpha/\beta/\gamma$ pic. All the nickel complexes are brown or reddish brown colored, which are common to the complexes involving thiosemicarbazone coordination, resulting

from the sulfur to metal charge transfer bands [8, 9]. The complexes are soluble in DMF, CHCl₃ and DMSO.

Table 4.3. Analytical data

Compound	color	μ_{eff} (B.M)	Anal: Found (Calcd.) %		
			C	H	N
[NiL ¹] ₂ (11)	brown	diamagnetic	57.30(58.04)	6.83(6.26)	14.28(14.50)
[Ni(HL ²) ₂] (12)	brown	diamagnetic	55.9(55.30)	6.36(5.93)	14.04(13.74)
[NiL ² py] (13)	reddish brown	diamagnetic	55.20(55.23)	5.35(5.37)	13.55(13.56)
[NiL ² α -pic] (14)	reddish brown	diamagnetic	56.21(56.23)	5.63(5.66)	13.11(13.12)
[NiL ² β -pic] (15)	reddish brown	diamagnetic	56.09(56.23)	6.12(5.66)	13.04(13.12)
[NiL ² γ -pic]·H ₂ O (16)	reddish brown	diamagnetic	54.11(53.90)	6.02(5.89)	12.59(12.58)
[Ni ₂ L ² ₂ phen] (17)	brown	2.25	56.32(56.63)	5.29(4.99)	13.16(13.64)
[NiL ³] ₂ (18)	brown	diamagnetic	56.09(56.34)	6.62(6.30)	13.01(13.14)
[NiL ⁴ py] (19)	reddish brown	diamagnetic	53.12(53.02)	4.57(4.71)	14.42(14.55)
[NiL ⁴ γ -pic] (20)	reddish brown	diamagnetic	54.02(54.16)	5.70(5.05)	14.16(14.04)

Magnetic susceptibility measurements at 293 K suggest that all the compounds except **17** are diamagnetic. The diamagnetism of the Ni(II) complex is strong evidence that coordination occurs through the thiolato sulfur atom and not through the thioether sulfur, since thiols but not thioethers cause spin pairing in complexes of Ni(II). Its diamagnetism and the presence of a single band at 600 nm in its electronic spectrum suggest that it has a square planar structure [10]. The magnetic susceptibility of **17** is 2.25 B.M, which is lower than that found for octahedral Ni(II) complexes (2.94–3.04 B.M). Some of the magnetic moments may be cancelled due to low spin Ni(II) coordination in the binuclear complex.

4.3.1. Crystal structures of the compounds $[\text{NiL}^2\text{py}]$, $[\text{NiL}^2\alpha\text{-pic}]$ and $[\text{NiL}^2\beta\text{-pic}]$

The molecular structures of $[\text{NiL}^2\text{py}]$ (**13**), $[\text{NiL}^2\alpha\text{-pic}]$ (**14**) and $[\text{NiL}^2\beta\text{-pic}]$ (**15**) along with atom labeling schemes are shown in Figures 4.1, 4.2 and 4.3, and selected bond lengths and bond angles are summarized in Table 4.4. The ligand H_2L^2 gets double deprotonated to behave as ONS tridentate, coordinating *via* its phenolato oxygen, azomethine nitrogen and thiolate sulfur atom of the deprotonated form after thiol formation giving a distorted square planar geometry around the nickel atom. The fourth coordination site is occupied by the nitrogen atom from the heterocyclic bases. The *E* configuration of the thiosemicarbazone chain about C7–N1 bond retains to facilitate the coordination of the thiolate sulfur to Ni in all of the three complexes. This reveals that no rotation has occurred about the azomethine bond for coordination. The coordination results one five membered and one six membered chelate rings in all the three complexes.

The compound **13** crystallized with two monomers per asymmetric unit into orthorhombic crystal system. The two molecules in the asymmetric unit are almost identical. So the discussion can be limited to one of the molecule. The Ni(II) ion is found to be displaced by 0.0022 Å from the plane constituted by the atoms O1, N1, S1, N4 with the maximum least square plane deviation at N4 by 0.010(3) Å. The thiosemicarbazonato moiety, C7–N1–N2–C8–S1–N3, also is almost planar has a maximum least square plane deviation of 0.037(4) Å and is at an angle of 2.86(6)° to the plane of the four donor atoms, while the phenyl ring has an angle of 6.29(10)° to the donor plane of the compound **13** indicating that the thiosemicarbazone moieties are close to coplanar with the nickel's coordination plane. Ring puckering analysis and least-square plane calculations show that the Cg(5) ring comprising of N3, C9, C10, C11, C12, C13 and C14 and Cg(10) ring comprising atoms

N7, C28, C29, C30, C31, C32 and C33 adopts chair conformation [$Q_T = 0.696(6)$ Å, $Cg(5)$ and $Q_T = 0.650(6)$ Å, $Cg(10)$].

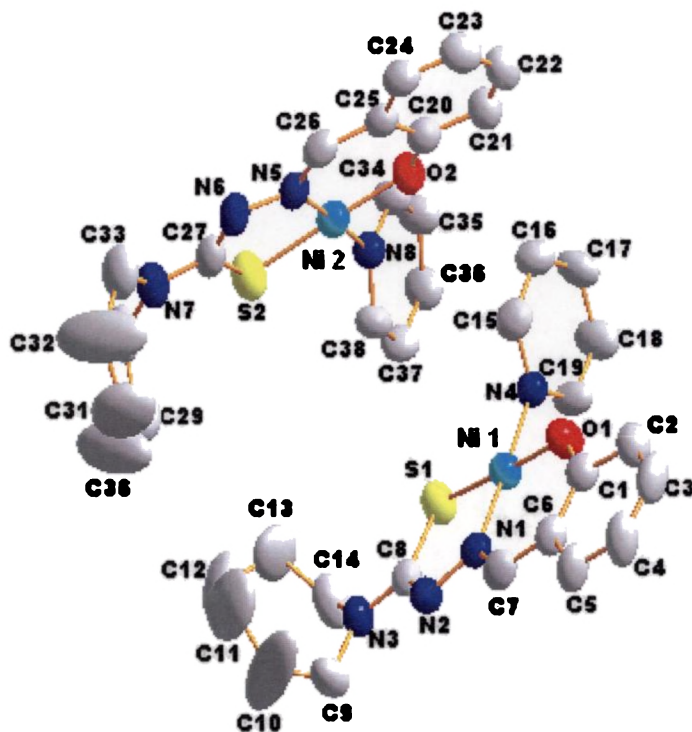


Figure 4.1. Structure and labeling diagram of the compound 13

The bond angles, O1–Ni1–N1 [$96.16(12)^\circ$], O1–Ni1–N4 [$85.35(11)^\circ$] and N1–Ni1–S1 [$87.08(10)^\circ$] also reveal the distortion of the square planes comprising of Ni1, O1, S1, N1 and N4. The dihedral angle formed by the least square planes $Cg(1)$ comprising atoms [Ni1, S1, N1, N2, C8] and $Cg(2)$ comprising atoms [Ni1, O1, N1, C1, C6, C7] is $3.47(12)^\circ$. The C7–N1 bond distance observed at $1.305(4)$ Å lengthens compared to the corresponding C7–N1 [$1.269(3)$ Å] bond distance in the ligand. The delocalization of electron density from the coordinating nitrogen onto the central metal atom gives rise to an elongated N1–N2 bond length [$1.406(3)$ Å] compared to the uncomplexed thiosemicarbazone [$1.356(3)$ Å]. Also, C7–N1–N2 bond angle decreased considerably compared to the ligand H_2L^1 . The

loss of the proton bound to N2 in H₂L¹ produces a negative charge, which is delocalized on the N1–N2–C8 system. This is indicated by the lengthening of the bond C8–S1, 1.753(4) Å compared to the value of 1.684(3) Å in the ligand. This thiolate formation is also supported by the decrease in bond length of N2–C8, 1.304(4) Å from the value of 1.362(3) Å found in uncomplexed thiosemicarbazone. The bond angles O1–Ni1–N4 [85.35(11)°] and S1–Ni1–N1 [87.08(10)°] are also analogous, as expected on the basis of the similar square planar nature for all complexes. Coordination of O1 results in O1–C1 decreasing by approximately 0.04–0.05 Å.

The compound **14** crystallized with only one monomer per asymmetric unit into monoclinic crystal system. The bond angles N1–Ni1–O1 [96.5(2)°], O1–Ni1–N4 [87.56(19)°] and N1–Ni1–S1 [86.77(19)°] reveal the distortion of the square planar geometry. The dihedral angle formed by the least square planes Cg(1) comprising atoms [Ni1, S1, N1, N2, C8] and Cg(2) comprising atoms [Ni1, O1, N1, C1, C6, C7] is 0.6(2)°. Similar to compound **13**, the C7–N1 bond length increases compared to the ligand. Thus on complexation, the azomethine C=N bond lengthens, because of coordination of the azomethine nitrogen. Coordination lengthens the thiosemicarbazone moiety's C8–S1 bond length to 1.759(6) Å and shortens the N2–C(8) to 1.302(7) Å.

The maximum deviation from the least square coordination planes around the Ni(II) ion is –0.026(5) Å at N1 for compound **14**. The thiosemicarbazonato moiety, C7–N1–N2–C8–S1–N3, is almost planar with a maximum mean deviation of 0.029(8) Å for N2 and are at an angle of 1.46(8)° to the plane of the four donor atoms, while the dihedral angle formed by the phenyl ring is 1.95° to the donor plane. The hexamethyleneiminyl ring adopts chair conformation [$Q_T = 0.7269$ Å].

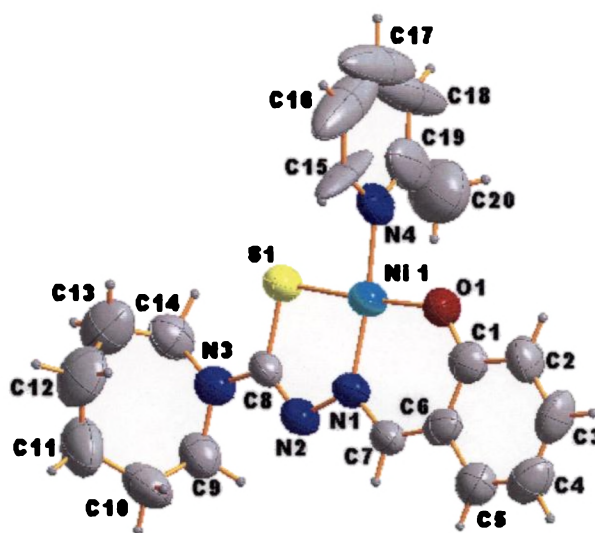


Figure 4.2. Structure and labeling diagram of the compound 14

In compound 15, the asymmetric unit contains only one molecule and is having a triclinic crystal system. In this complex also the environment around the Ni(II) ion is distorted square planar which is evident from the bond angles given in Table 4.4. The dihedral angles formed by the least square planes Cg(1) and Cg(2) is 2.11° . This supports the distorted square planar conformation for these complexes where greater distortion is observed for compound 13. This small deviation from coplanarity would certainly not hinder the delocalization of electrons in the coordination sphere, and the stability of the complex is sustained. The increase in bond length of C7–N1 to $1.305(4)$ Å, confirms the coordination of azomethine nitrogen. Similar to compounds 13 and 14, there occurs elongation of the C8–S1 and compression of the N2–C8 bond length. The Ni(II) ion is found to be displaced by $-0.007(2)$ Å from the plane constituting atoms N1, S1, O1, N4 with a maximum least square plane deviation at O1 by $0.045(2)$ Å. The dihedral angle formed by the thiosemicarbazate moiety with the plane containing coordinating atoms is 3.14° while the phenyl ring has an angle of 4.38° to the donor plane indicating that the thiosemicarbazone moieties are close to coplanar with the

nickel's coordination plane. The bond lengths and bond angles indicates distortion from the square planar geometry.

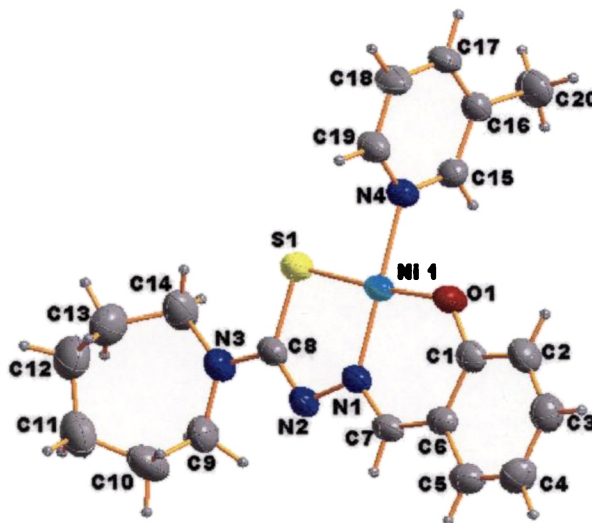


Figure 4.3. Structure and labeling diagram of the compound 15

Ring puckering and least square plane calculations indicates that the hexamethyleneiminyl ring adopts chair conformation [$Q_T = 0.7957 \text{ \AA}$]. The adjacent molecules are packed in an opposite manner within the unit cell.

The Ni–N_{azomethine} bond lengths are shorter compared to Ni–N_{base} bond lengths, indicating the greater strength of former bonds compared to the latter in all the three complexes. The O1–Ni1–N1 bond angles are slightly greater compared to similar Ni(II) ONS donor complexes of [Ni(PTSC)(PPh₃), 95.32(9)°] and [Ni(PTSC)(PPh₃)]·CHCl₃, 95.4(1)° [11] and N1–Ni1–S1 bond angles are comparable. N1–Ni1–S1 bond angles are greater compared to [Ni(Et-fbt)₂, 85.35(11)], [Ni(fbt)₂, 84.90(10)] [12] and [Ni(NQTS)₂]-2DMSO 81.47(16)] [13]. The C–N_{azo} bond length is shorter compared to other C–N_{py} bond lengths in the complexes. This indicates that the bonding is dominated by thiosemicarbazone moiety.

In compound **13**, the adjacent molecules are arranged in an offset manner within the unit cell when viewed along the a axis, as seen in Figure 4.4, as a result of diverse π - π stacking, CH... π and hydrogen bonding interactions (Table 4.5).

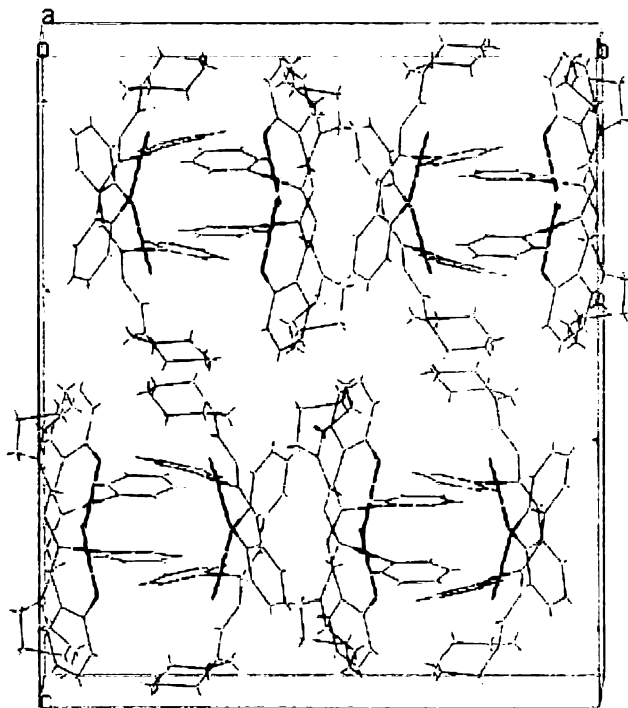


Figure 4.4. Unit cell packing diagram of the compound **13**

The molecules of **14** are connected by various hydrogen bonding interactions and are packed in the lattice in an offset manner (Figure 4.5). Though π - π interactions exist in the lattice of this compound, they are observed at distances greater than 4.0 Å also no effective CH... π interactions (Table 4.6). The adjacent molecules are arranged in an opposite direction within the unit cell.

In compound **15**, the assemblage of molecules in the respective manner in the unit cell (Figure 4.6) is resulted by the diverse π - π stacking, CH... π , hydrogen bonding and ring-metal interactions are depicted in Table 4.7. Short ring-metal interaction of the chelate ring Cg(1) is observed at a distance of 3.994 Å from the

Ni centre. These interactions point out the possibility for metalloaromaticity, a classic concept recently reviewed by Masui [14].

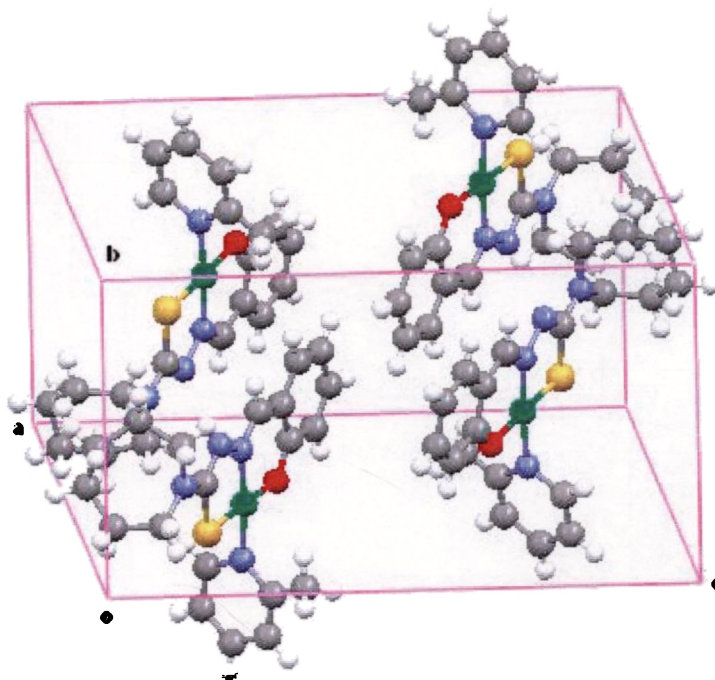


Figure 4.5. Unit cell packing diagram of the compound 14

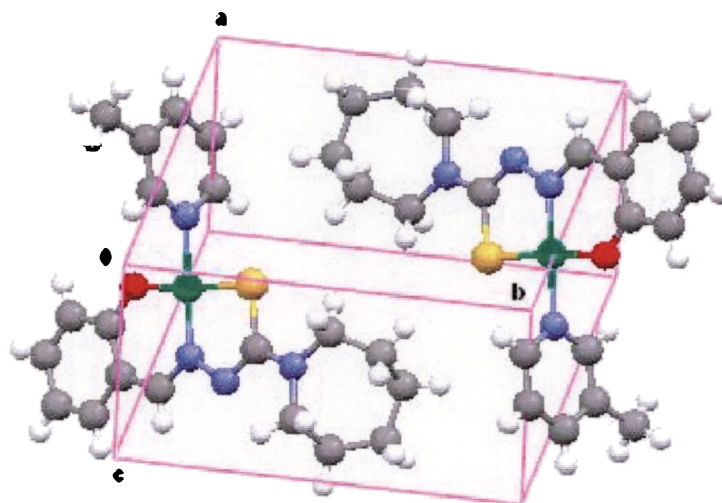


Figure 4.6. Unit cell packing diagram of the compound 15

Table 4.4. Selected bond lengths (Å) and bond angles (°) for **13**, **14** and **15**

	13	14	15
Bond lengths (Å)			
Ni1–O1	1.837(2)	1.859(4)	1.845(2)
Ni1–N1	1.848(3)	1.847(5)	1.851(3)
Ni1–N4	1.907(3)	1.906(4)	1.915(3)
Ni1–S1	2.134(11)	2.151(2)	2.131(10)
Ni2–O2	1.848(2)		
Ni2–N5	1.859(3)		
Ni2–N8	1.925(3)		
Ni2–S2	2.132(11)		
S1–C8	1.753(4)	1.759(6)	1.750(3)
S2–C27	1.752(4)		
N1–C7	1.305(4)	1.320(7)	1.305(4)
N1–N2	1.406(3)	1.393(6)	1.397(4)
N2–C8	1.304(4)	1.302(7)	1.313(5)
N3–C8	1.350(4)	1.362(7)	1.353(5)
N4–C19	1.326(4)	1.388	1.337(5)
N4–C15	1.327(4)	1.392	1.343(4)
N5–C26	1.302(4)		
N5–N6	1.400(4)		
N6–C27	1.293(4)		
N7–C27	1.357(4)		
N8–C34	1.340(4)		
N8–C38	1.343(4)		
Bond angles (°)			
O1–Ni1–N1	96.56(12)	96.5(2)	96.83(11)
O1–Ni1–N4	85.35(11)	87.56(19)	86.28(11)
N1–Ni1–N4	177.87(12)	174.4(2)	175.49(11)
O1–Ni1–S1	176.35(8)	176.71(14)	175.24(8)
N1–Ni1–S1	87.08(10)	86.77(19)	87.39(9)
N4–Ni1–S1	91.01(8)	89.17(15)	89.64(9)
O2–Ni2–N5	95.75(12)		
O2–Ni2–N8	86.96(11)		
N5–Ni2–N8	177.26(14)		
O2–Ni2–S2	176.83(8)		
N5–Ni2–S2	87.15(11)		
N8–Ni2–S2	90.16(9)		
C8–S1–Ni1	96.57(13)	95.8(3)	96.44(12)
C27–S2–Ni2	96.11(16)		
C7–N1–N2	113.3(3)	112.4(5)	113.1(3)
N2–N1–Ni1	122.8(2)	123.8(4)	122.6(2)
C26–N5–N6	113.6(3)		
C26–N5–Ni2	124.0(3)		
C26–N5–N6	113.6(3)		

Table 4.5. Interaction parameters of the compound 13

 π - π interactions

Cg(I)-Res(1)···Cg(J)	Cg-Cg (Å)	α°	β°
Cg(1) [1] -> Cg(9) ^a	3.7468	3.28	25.77
Cg(2) [1] -> Cg(9) ^a	3.6244	6.74	24.05
Cg(3) [1] -> Cg(8) ^b	3.8557	17.19	27.64
Cg(8) [1] -> Cg(3) ^b	3.8557	17.19	12.31
Cg(9) [1] -> Cg(1) ^c	3.7468	3.28	22.53
Cg(9) [1] -> Cg(2) ^c	3.6244	6.74	24.30

Equivalent position code: a= 1/2-x, 1/2+y, z; b= 1/2+x, y, 1/2-z; c= 1/2-x, -1/2+y, z

Cg(1)= Ni1, S1, C8, N2, N1; Cg(2)= Ni1, O1, C1, C6, C7, N1; Cg(3)= N4, C15, C16, C17, C18, C19; Cg(8)= N8, C34, C35, C36, C37, C38; Cg(9)= C20, C21, C22, C23, C24, C25

CH- π interactions

X-H(I)···Cg(J)	H...Cg (Å)	X-H...Cg (°)	X...Cg (Å)
C17-H17 [1] -> Cg(6) ^a	2.69	144	3.4857
C18-H18 [1] -> Cg(1) ^a	2.69	139	3.4420
C35-H35 [1] -> Cg(9) ^a	2.67	153	3.5223
C37-H37 [1] -> Cg(4) ^a	2.90	141	3.6669

Equivalent position code: a= 1/2+x, y, 1/2-z

Cg(1)= Ni1, S1, C8, N2, N1; Cg(4)= C1, C2, C3, C4, C5, C6; Cg(6)= Ni2, S2, C27, N6, N5; Cg(9)= C20, C21, C22, C23, C24, C25

H-bonding

D-H...A	D...H (Å)	H...A (Å)	D...A (Å)	D-H...A (°)
C15-H15...O(2) ^a	0.930	2.967(2)	3.539(5)	121.23(25)
C16-H16...O(2) ^a	0.930	2.827(2)	3.460(5)	126.33(26)
C3-H3...N7 ^b	0.930	2.895(3)	3.589(5)	132.41(26)
C17-H17...N5 ^c	0.930	2.755(3)	3.530(6)	141.42(29)
C18-H18...N1 ^c	0.930	2.962(3)	3.445(5)	113.90(27)
C18-H18...N2 ^c	0.930	2.859(3)	3.424(5)	120.36(28)
C36-H36...O1 ^c	0.930	2.863(2)	3.723(5)	154.33(25)
C19-H19...N2 ^c	0.930	2.699(3)	3.358(5)	128.52(24)

D=donor, A=acceptor, Equivalent position code: a= x, y, z; b= x, 1/2-y, 1/2+z; c= 1/2+x, +y, -z+1/2+1

Table 4.6. Interaction parameters of the compound 14 **π - π interactions**

Cg(I)-Res(1)···Cg(J)	Cg-Cg (Å)	α°	β°
Cg(1) [1] -> Cg(4) ^a	4.0511	3.48	28.16
Cg(4) [1] -> Cg(1) ^b	4.0511	3.48	31.41

Equivalent position code: a= -1/2+x, 1/2-y, z; b= 1/2+x, 1/2-y, z

Cg(1)= Ni1, S1, C8, N2, N1; Cg(4)= C1, C1, C2, C3, C4, C5, C6

H-bonding

D-H...A	D...H (Å)	H...A (Å)	D...A (Å)	D-H...A (°)
C14-H14B....S1 ^a	0.970	2.517(2)	3.021(8)	112.25(47)
C14-H14A....N2 ^b	0.970	2.867(6)	3.540(11)	127.27(48)
C17-H17....N2 ^c	0.930	2.858(5)	3.771(7)	167.25(27)
C18-H18....O1 ^d	0.930	2.732(5)	3.596(9)	154.94(47)

D=donor, A=acceptor, Equivalent position code: a= x, y, z; b= x-1/2, -y+1/2, +z; c= x, y-1, z; d= x-1/2, -y-1/2, +z

Table 4.7. Interaction parameters of the compound 15 **π - π interactions**

Cg(I)-Res(1)···Cg(J)	Cg-Cg (Å)	α°	β°
Cg(1) [1] -> Cg(1) ^a	3.7819	0.00	26.39
Cg(1) [1] -> Cg(2) ^a	3.6927	2.11	21.69
Cg(2) [1] -> Cg(1) ^a	3.6927	2.11	22.65
Cg(3) [1] -> Cg(3) ^b	3.9463	0.02	23.88

Equivalent position code: a= -x, 1-y, 2-z; b= 1-x, -y, 2-z

Cg(1)= Ni1, S1, C8, N2, N1; Cg(2)= Ni1, O1, C1, C6, C7, N1; Cg(3)= N4, C15, C16, C17, C18, C19

CH- π interactions

X-H(I)···Cg(J)	H...Cg (Å)	X-H...Cg (°)	X...Cg (Å)
C14-H14A [1] -> Cg(4) ^a	2.81	147	3.6597
C18-H18 [1] -> Cg(2) ^b	2.95	137	3.6826

Equivalent position code: a= -x, 1-y, 2-z; b= -x, -y, 2-z

Cg(4)= C1, C2, C3, C4, C5, C6

H-bonding

D-H...A	D...H (Å)	H...A (Å)	D...A (Å)	D-H...A (°)
C15-H15....N2 ^a	0.930	2.979(1)	3.832(1)	153.25(2)
C9-H9A....O1 ^a	0.970	2.865	3.420(1)	117.35(2)
C19-H19....O1 ^b	0.970	2.772	3.466	132.19(2)

D=donor, A=acceptor, Equivalent position code: a= -x+2, -y+1, -z; b= -x+2, -y+2, -z

4.3.2. Crystal structure of the compound $[Ni_2L^2_2phen]$

The molecular structure of the compound along with atom numbering scheme is given in Figure 4.7 and selected bond lengths and bond angles are summarized in Table 4.8. In this complex, nickel centers adopt two different coordination environments. Ni1 adopts octahedral geometry defined by the tridentate ONS donor dianionic ligand, neutral bidentate phenanthroline ligand and one of the oxygen O2 coordinated to a second nickel centre, which bridge to occupy the sixth coordination site. The Ni–O, Ni–N and Ni–S bond lengths [Ni1–O1, 2.006(3); Ni1–O2, 2.236(3); Ni1–N1, 2.214(4); Ni1–N2, 2.082(4); Ni1–N3, 2.006(4); Ni1–S1, 2.388(13)] are in agreement with those found in the related Ni(II) complex [15, 16]. The Ni1–O1 bond length is shorter than Ni1–O2 indicates that the phenoxy oxygen O1 coordinates more strongly to the Ni1 center than the bridging phenoxy oxygen O2. Ni2–S1 distance is shorter compared to Ni1–S1, indicating that the bridging S1 atom is near to the Ni2 atom in this complex, whereas the bridging O2 atom is at a greater distance from the Ni1 atom. The high spin nature of Ni1 is nicely reflected by its comparatively long bond distances to O1, S1 and N3. For example, the “intramolecular” distance Ni1–S1 [2.3876(13)Å] even exceeds the ‘intermolecular’ distance Ni2–S1 [2.2424(13)Å]. These values are in agreement with the trimeric nickel thiosemicarbazone complex [17] but compared to the previous reports [17, 18], the complex shows paramagnetism lower than that found for octahedral complexes. The paramagnetism may be due to the presence of phenanthroline coligand present in the molecule. Ni1–O2 distance is larger compared to the previous binuclear Ni(II) complexes [18, 19].

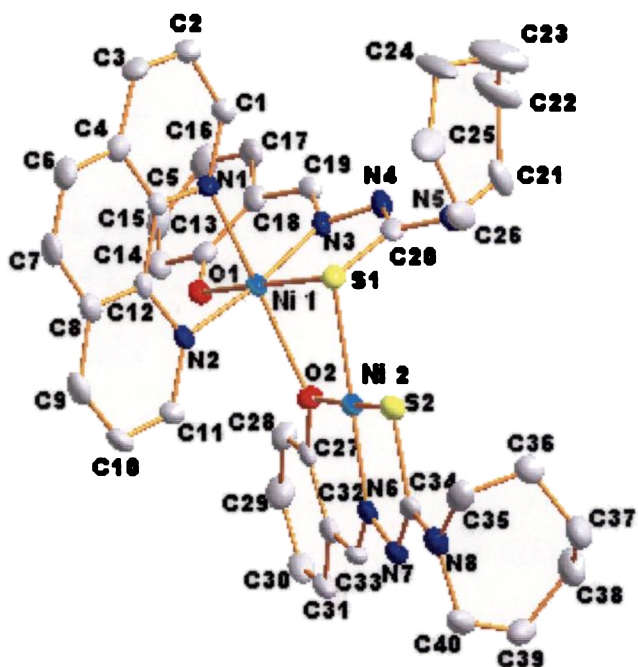


Figure 4.7. Structure and labeling diagram of the compound 17

The planes defined by atoms Ni1–O2–Ni2 and Ni1–S1–Ni2 intersect at an angle of $156.54(10)^\circ$. This structural feature is due to the greater steric effect between the phenyl rings of the monomeric subunit bound to Ni1, sp^3 like character of O2 and S1 and also due to the coordination of the bulkier phenanthroline coligand. The C=N bond distances in the complex are observed to be at $1.300(6)$ Å and compared to the ligand [20], the bond distance of C=N lengthens. Thus on complexation the azomethine C=N bond lengthens, because of coordination of the azomethine nitrogen. The delocalization of electron density from the coordinating nitrogen onto the central metal atom gives rise to an elongated N–N bond length [N3–N4 = $1.404(5)$ Å, and N6–N7 = $1.411(5)$ Å, and $1.356(3)$ Å for compound and H_2L^1] compared to the uncomplexed thiosemicarbazone. The loss of protons bound to N4 and N7 in the ligand produces a negative charge, which is delocalized on the N3–N4–C20 and N6–N7–C34 system. This is indicated by the lengthening of the

bond C–S, 1.801(5) [C20–S1] and 1.773(4) Å [C34–S2] in the complex, compared to the value of 1.684(3) Å seen in the thiosemicarbazone ligand. The C20–S1 bond length is larger and almost equal to the C–S single bond length. This is due to the bridging nature of the S1 atom compared to S2. This thiolate formation is also supported by the decrease in bond length of N4–C20, 1.308(6) Å and N7–C34, 1.307(6) Å in the Ni(II) binuclear complex, from the value of 1.362(3) Å of the thiosemicarbazone. The Ni–N_{bipyridyl} bonds are longer than Ni–N_{azomethine} bonds, denoting the strength of the azomethine nitrogen coordination. The N–N–C bond angle of the ligand (H_2L^2) [N1–N2–C8, 119.3(3)°] is reduced by few degrees [N3–N4–C20, 115.8(4)° and N6–N7–C34, 112.7(4)°] on complex formation. These changes are directly due to coordination of the ligand to the Ni(II) moiety when it becomes a delocalized system. The bond angles O1–Ni1–S1 = 174.51(10)° and O1–Ni1–N2 = 88.05(14)° indicate distortion from octahedral geometry. The Ni2 adopts a square-planar geometry in which coordination occurs through deprotonated ligand and the fourth position by bridging sulfur S1. The Ni2 deviates from the basal plane N6–O2–S2–S1 by 0.056(7) Å. The Ni2–S2 bond length is 2.1520(14) Å, which is slightly shorter than Ni2–S1 suggests the weakening of sulfur bridging. The O2–Ni2–S2 bond angle in [Ni₂L²₂phen], 174.88(11)° is a measure of distortion from regular stereochemistry for complexes with tridentate thiosemicarbazonato ligands. These angles are comparable to [Ni(Ap4DM)]₂, 174.3(1)° [17], [Ni(DMAp4DM)]₂, 173.5(1)°, 173.1(1)° [21] found for nickel(II) complexes with ONS tridentate thiosemicarbazones.

The distance between the Ni–Ni atoms in the complex is 3.247 Å, which is greater than the 2.721(1) Å found for [Ni(Ap4DM)]₂ [19], 2.728(1) Å found for [Ni(5Map4DM)]₂ [21] and 2.729 Å found for [Ni(tmtssA)]₂ [19]. The four membered metal chelate ring Cg(1) [Ni1–S1–Ni2–O2] having maximum deviation of 0.451(3) Å at O2. This indicates large tetrahedral distortion in this complex.

Table 4.8. Selected bond lengths (Å) and bond angles (°) of 17

<i>Bond lengths (Å)</i>			
Ni1-N3	2.006(4)	C19-N3	1.300(6)
Ni1-O1	2.006(3)	N3-N4	1.404(5)
Ni1-N2	2.082(4)	C20-N4	1.308(6)
Ni1-N1	2.124(4)	C20-N5	1.371(6)
Ni1-O2	2.236(3)	C26-N5	1.468(7)
Ni1-S1	2.3876(13)	C21-N5	1.482(7)
Ni2-N6	1.882(4)	C33-N6	1.300(6)
Ni2-O2	1.910(3)	N6-N7	1.411(5)
Ni2-S2	2.1520(14)	C34-N7	1.307(6)
Ni2-S1	2.2424(13)	O1-C13	1.302(6)
C20-S1	1.801(5)	O2-C27	1.343(5)
C34-S2	1.773(4)		
<i>Bond angles (°)</i>			
N3-Ni1-O1	91.91(14)	N6-Ni2-S1	176.54(13)
N3-Ni1-N2	173.28(14)	O2-Ni2-S1	87.14(9)
O1-Ni1-N2	88.05(14)	S2-Ni2-S1	89.74(5)
N3-Ni1-N1	93.93(15)	Ni2-S1-C20	105.64(15)
O1-Ni1-N1	92.47(13)	Ni1-S1-C20	93.78(16)
N2-Ni1-N1	79.36(14)	Ni1-S1-Ni2	89.02(5)
N3-Ni1-O2	95.32(13)	Ni2-S2-C34	96.49(17)
O1-Ni1-O2	100.59(12)	C19-N3-N4	113.4(4)
N2-Ni1-O2	91.29(13)	C19-N3-Ni1	123.7(3)
N1-Ni1-O2	163.70(13)	N4-N3-Ni1	122.1(3)
N3-Ni1-S1	83.62(11)	N3-N4-C20	115.8(4)
O1-Ni1-S1	174.51(10)	C33-N6-N7	113.3(4)
N2-Ni1-S1	96.77(11)	C33-N6-Ni2	124.6(3)
N1-Ni1-S1	91.03(10)	N7-N6-Ni2	122.0(3)
O2-Ni1-S1	76.73(9)	N6-N7-C34	112.7(4)
N6-Ni2-O2	95.80(15)	C13-O1-Ni1	126.8(3)
N6-Ni2-S2	87.18(13)	C27-O2-Ni2	125.9(3)
N6-Ni2-S2	87.18(13)	C27-O2-Ni1	130.7(3)
O2-Ni2-S2	174.88(11)	Ni2-O2-Ni1	102.86(13)

The molecules are packed in an opposite manner within the unit cell when viewed along the *a* axis (Figure 4.8). The assemblage of molecules in the respective manner within the unit cell is resulted by the diverse π - π stacking, CH... π and ring metal interactions included in Table 4.9. The metal chelate ring Cg(2) comprising atoms Ni1, S1, C20, N4 and N3 is involved in π - π interactions

with metal chelate ring Cg(6) comprising of atoms Ni2, O2, C27, C32, C33 and N6 of the neighbouring unit with an average distance of 3.9967 Å. In addition to this, the CH... π interactions of the bipyridyl and phenyl hydrogens with the metal chelate rings of the neighbouring molecules and also other CH... π interactions contribute to the stability of the unit cell packing. Ring- metal interaction of the chelate ring Cg(11) is at a distance of 3.969 Å from the nickel centre in the packed molecules. These interactions point out the possibility for metalloaromaticity, a classic concept recently reviewed by Masui [14].

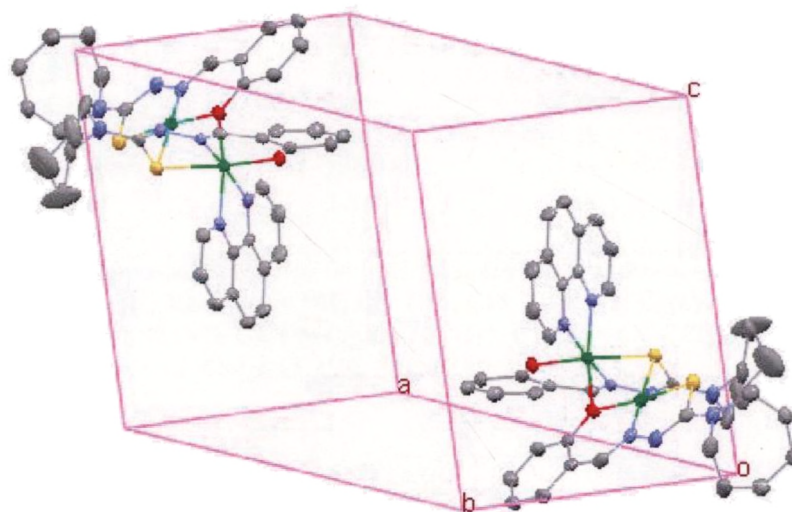


Figure 4.8. Unit cell packing diagram of the compound 17

Table 4.9. Interaction parameters of the compound 17

 π - π interactions

Cg(I)-Res(I)···Cg(J)	Cg-Cg (Å)	α°	β°
Cg(2) [1] -> Cg(6) ^a	3.9967	73.81	30.66
Cg(6) [1] -> Cg(11) ^b	3.4932	4.42	9.80
Cg(7) [1] -> Cg(7) ^c	3.7002	0.00	25.03
Cg(7) [1] -> Cg(9) ^c	3.7934	1.29	26.65
Cg(9) [1] -> Cg(7) ^c	3.7934	1.29	27.77
Cg(11) [1] -> Cg(6) ^b	3.4932	4.42	10.29

Equivalent position code: a= x, y, z; b= -x, 1-y, -z; c= 1-x, -y, 1-z

Cg(2)= Ni1, S1, C20, N4, N3; Cg(6)= Ni2, O2, C27, C32, C33, N6; Cg(7)= N1, C1, C2, C3, C4, C5; Cg(9)= C4, C5, C12, C8, C7, C6; Cg(11)= C27, C28, C29, C30, C31, C32

CH- π interactions

X-H(I)···Cg(J)	H...Cg (Å)	X-H...Cg ($^\circ$)	X...Cg (Å)
C6-H6 [1] -> Cg(10) ^a	2.53	172	3.4513
C9-H9 [1] -> Cg(4) ^b	2.68	167	3.5895
C11-H11 [1] -> Cg(6) ^c	2.99	142	3.7657
C25-H25A [1] -> Cg(7) ^d	2.77	156	3.6795
C25-H25A [1] -> Cg(9) ^d	2.98	143	3.8031
C28-H28 [1] -> Cg(5) ^c	2.65	148	3.4753
C36-H36A [1] -> Cg(8) ^e	2.96	155	3.8633

Equivalent position code: a= 1-x, -y, 1-z; b= -x, 1-y, 1-z; c= x, y, z; d= -x, -y, 1-z; e= -1+x, y, z

Cg(4)= Ni2, S2, C34, N7, N6; Cg(5)= Ni1, O1, C13, C18, C19, N3; Cg(6)= Ni2, O2, C27, C32, C33, N6; Cg(7)= N1, C1, C2, C3, C4, C5; Cg(8)= N2, C11, C10, C9, C8, C12; Cg(9)= C4, C5, C12, C8, C7, C6; and Cg(10)= C13, C14, C15, C16, C17, C18

H-bonding

D-H...A	D...H (Å)	H...A (Å)	D...A (Å)	D-H...A ($^\circ$)
C1-H1...N3 ^a	0.930(6)	2.765(3)	3.255(6)	113.99
C11-H11...O2 ^a	0.930(5)	2.678(4)	3.224(8)	118.26
C25-H25B...S1 ^a	0.970(8)	2.931(1)	3.457(8)	115.16
C26-H26B...S2 ^a	0.970(6)	2.763(1)	3.705(6)	164.02
C28-H28...O1 ^a	0.930(4)	2.377(3)	3.126(5)	137.52
C3-H3...O1 ^b	0.930(4)	2.860(4)	3.675(6)	146.98
C9-H9...S2 ^c	0.930(7)	2.947(2)	3.798(7)	152.66
C7-H7...N7 ^c	0.930(6)	2.612(5)	3.487(8)	157.02
C30-H30...N5 ^d	0.930(5)	2.829(4)	3.574(6)	137.86
C31-H31...N4 ^d	0.930(4)	2.931(4)	3.757(6)	148.67
C37-H37A...O1 ^c	0.970(8)	2.878(3)	3.656(8)	137.95

D=donor, A=acceptor, Equivalent position code: a= x, y, z; b= -x+1, -y, -z+1; c= -x, -y+1, -z+1; d= -x, -y+1, -z; e= x-1, y, z

4.3.3. IR spectra

The characteristic IR bands (50–4000 cm^{-1}) for the four free ligands differ from those of their complexes and provide significant indications regarding the bonding sites of the ligands. IR spectral assignments of the ligands and the complexes are listed in Table 4.10. A medium band in the range 3070–3160 cm^{-1} in the free ligands due to the $\nu(\text{NH})$ vibration disappeared in the spectra of complexes providing strong evidence for ligand coordination around the Ni(II) ion in its deprotonated form.

The IR spectra of the ligands H_2L^2 and H_2L^4 exhibit an intermolecular hydrogen bonded $\nu(\text{OH})$ vibrations at 3315 [20] and 3232 cm^{-1} respectively, which disappeared in the spectra of complexes having ONS donor ligands (except in **12**). It is further corroborated with the decrease in frequency of 60–80 cm^{-1} for $\nu(\text{CO})$ as well as an appearance of a band at 410–430 cm^{-1} region due to a $\nu(\text{Ni-O})$ stretch in the spectra of complexes [22]. It indicates coordination *via* phenolic oxygen. It means that in complex **12**, the phenolic group of the ligand is not coordinated to the metal. On coordination of azomethine nitrogen, $\nu(\text{C}=\text{N}_{\text{azo}})$ shifts to lower wavenumbers by 10–20 cm^{-1} , as the band shifts from $\sim 1613 \text{ cm}^{-1}$ in the uncomplexed thiosemicarbazone to $\sim 1596 \text{ cm}^{-1}$ in the spectra of complexes. Coordination of azomethine nitrogen is confirmed with the presence of new band in the range 450–490 cm^{-1} , assignable to $\nu(\text{Ni-N})$ for these complexes [23, 24]. The $\nu(\text{N-N})$ of the thiosemicarbazone is found in the 1035–1066 cm^{-1} range. The increase in the frequency of this band in the spectra of the complexes, due to the increase in the bond strength, again confirms the coordination *via* the azomethine nitrogen.

The bands in the ranges 1310–1340 and 820–865 cm^{-1} due to thioamide

stretching and bending vibrations, respectively, of the free ligands are shifted to lower values, indicating coordination of the thiolate sulfur to the Ni(II) ion. This decrease in frequency can be attributed to a change of bond order and strong electron delocalization upon chelation [25]. This negative shift of $\nu(\text{CS})$ in the complexes is already indicated by Campbell [26]. Coordination *via* thiolato sulfur is confirmed with the presence of new band in the range $320\text{--}350\text{ cm}^{-1}$, assignable to $\nu(\text{Ni-S})$ for these complexes [27, 28]. In all the Ni(II) complexes, another strong band is found in the range $1530\text{--}1550\text{ cm}^{-1}$, which may be due to the newly formed $\nu(\text{C}=\text{N})$ bond as a result of enolization. The IR spectra of the complexes **13**, **14**, **15**, **16**, **17**, **19** and **20** display bands characteristics of coordinated heterocyclic bases [29].

IR spectra of the complexes **12**, **13**, **14** and **17** are presented in Figures 4.9–4.12

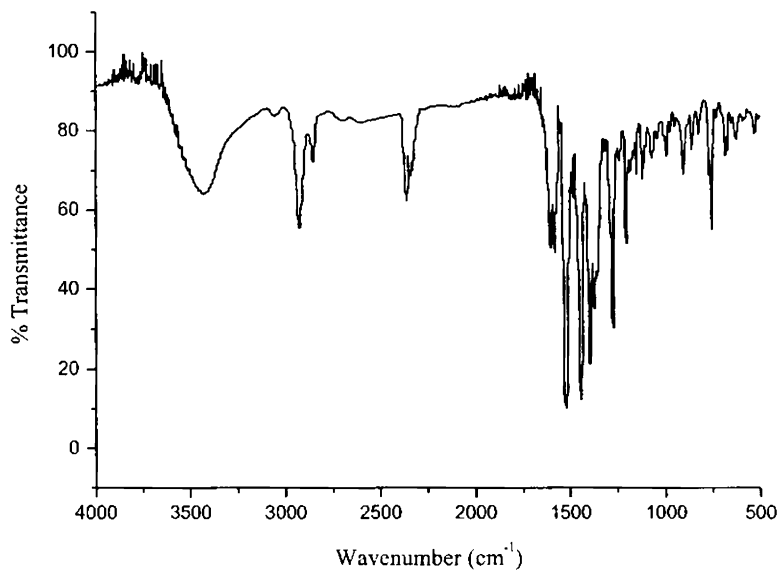


Figure 4.9. IR spectrum of the compound [Ni(HL²)₂] (12)

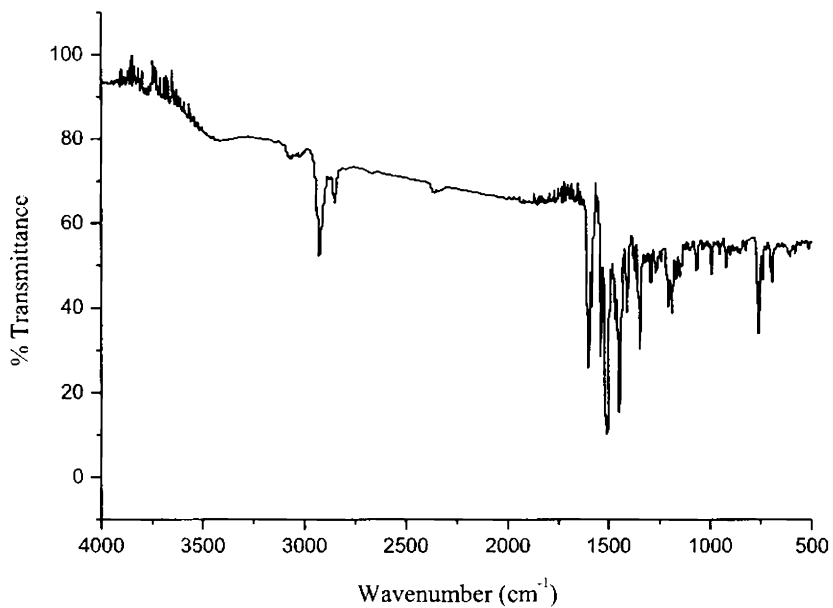


Figure 4.10. IR spectrum of the compound [NiL²py] (13)

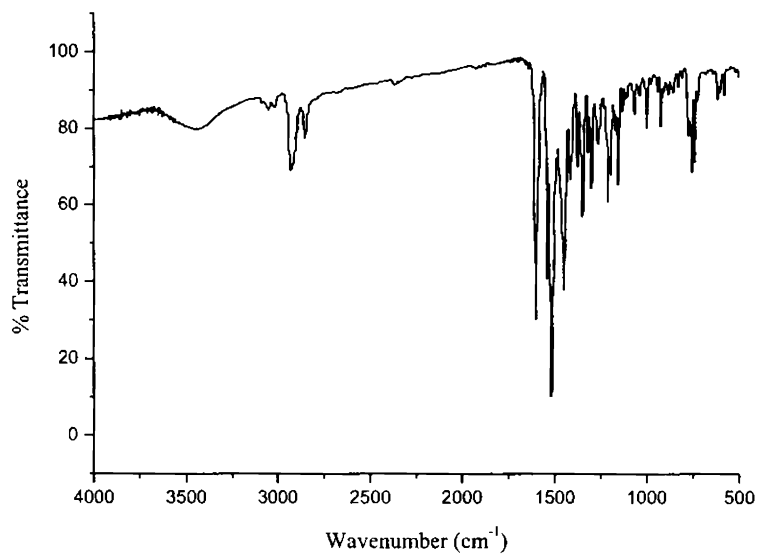


Figure 4.11. IR spectrum of the compound $[\text{NiL}^2\alpha\text{-pic}]$ (**14**)

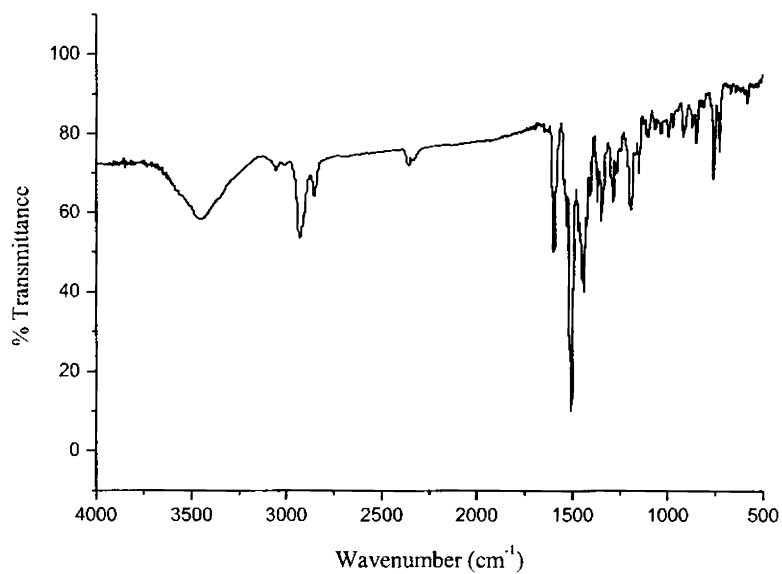


Figure 4.12. IR spectrum of the compound $[\text{Ni}_2\text{L}^2_2\text{phen}]$ (**17**)

Table 4.10. Selected IR bands (cm^{-1}) with tentative assignments of the ligands and its Ni(II) complexes

Compound	$\nu(\text{C}=\text{N}_{\text{azo}})$	$\nu(\text{C}=\text{N})$	$\nu(\text{N}-\text{N})$	$\nu/\delta[(\text{C}=\text{S})/(\text{C}-\text{S})]$	$\nu(\text{C}-\text{O})$	$\nu(\text{Ni}-\text{N})$	$\nu(\text{Ni}-\text{O})$	$\nu(\text{Ni}-\text{S})$	Bands due to heterocyclic bases
HL^1	1624	-----	1066	1334, 837	-----	-----	-----	-----	-----
$[\text{NiL}^1_2]$ (11)	1587	1549	1072	1282, 753	-----	463	-----	336	-----
H_2L^2	1612	-----	1037	1324, 861	1271	-----	-----	-----	-----
$[\text{Ni}(\text{HL}^2)_2]$ (12)	1581	1530	1071	1267, 753	1202	466	-----	350	-----
$[\text{NiL}^2\text{py}]$ (13)	1597	1536	1070	1288, 757	1207	463	430	345	1447, 691
$[\text{NiL}^2\alpha\text{-pic}]$ (14)	1601	1531	1063	1278, 752	1209	494	446	347	1448, 614
$[\text{NiL}^2\beta\text{-pic}]$ (15)	1597	1537	1066	1277, 755	1199	487	438	330	1450, 614
$[\text{NiL}^2\gamma\text{-pic}] \cdot \text{H}_2\text{O}$ (16)	1597	1537	1068	1270, 753	1208	460	420	332	1449, 714
$[\text{Ni}_2\text{L}^2\text{phen}]$ (17)	1597	1530	1065	1286, 757	1202	470	425	340	1441, 665
HL^3	1607	-----	1064	1312, 821	1255	-----	-----	-----	-----
$[\text{NiL}^3_2]$ (18)	1595	1549	1076	1275, 730	-----	463	-----	335	-----
H_2L^4	1622	-----	1034	1338, 839	1288	-----	-----	-----	-----
$[\text{NiL}^4\text{py}]$ (19)	1600	1538	1061	1290, 758	1210	490	422	334	1478, 693
$[\text{NiL}^4\gamma\text{-pic}]$ (20)	1600	1538	1055	1275, 757	1205	476	425	325	1480, 607

4.3.4. ^1H NMR Spectra

^1H NMR spectra of the thiosemicarbazones are already discussed in Chapter 2. ^1H NMR spectral assignments of H_2L^2 and its Ni(II) complexes **12**, **15** and **16** are given in Table 4.11. The signals for ^2NH are absent from the spectra of these complexes as expected and the phenolic OH is absent in the spectra of complexes **15** and **16**, because of their loss on complex formation, which is an evidence for the coordination of the ligand as doubly deprotonated anion. The spectra of the complexes **12**, **15** and **16** show sharp singlets which integrates as one hydrogen at $\delta=7.44$, 7.84 and 7.83 ppm respectively, corresponds to $^7\text{CH}=\text{}$ present in the thiosemicarbazone moiety. Complex **12** shows a peak at $\delta=12.51$ ppm due to the presence of the uncoordinated hydroxyl group. The more downfield shift of OH protons compared to the uncomplexed thiosemicarbazone may be due to the overall loss of electron density and hydrogen bonding interactions. A small downfield shift occurs to aliphatic protons in complexes due to the overall loss of electron density. ^1H NMR spectrum of **12** shows a multiplet, which integrates as two hydrogens at $\delta \sim 6.82$ ppm is assigned to the protons attached to the ^3C and ^5C of the phenyl ring. ^4CH and ^6CH protons of the phenyl ring appear at $\delta=7.13$ and 7.31 ppm respectively.

In complex **15**, the aromatic protons ^6CH and ^3CH resonate as doublets at $\delta=7.53$ and 6.81 ppm and ^5CH proton appears as triplet at $\delta=6.58$ ppm respectively. The spectrum shows a multiplet, which integrates as three hydrogens at $\delta \sim 7.16$ ppm corresponds to ^4CH and the base protons $\text{H}^{2'}$ and $\text{H}^{3'}$. The base protons $\text{H}^{1'}$ and $\text{H}^{4'}$ integrates as two hydrogens at $\delta \sim 8.68$ ppm. The downfield shift of these protons is the result of the withdrawal of electron density from the thiosemicarbazone moiety and the heterocyclic base, due to coordination with the metal atom [30]. Methyl protons resonate as a singlet at $\delta=2.37$ ppm

In complex **16**, the protons of the aromatic ring ³CH and ⁵CH appear at 6.81 and 6.58 ppm respectively. The spectrum shows a multiplet which integrates as four hydrogens at $\delta \sim 7.15$ ppm corresponds to ⁴CH, ⁶CH and the base protons H^{2'} and H^{2''}. The upfield shift of these base protons may be due to the presence of electron releasing methyl group present in the pyridine ring. The heterocyclic base protons (H^{1'} and H^{1''}) resonate as doublet, which integrates as two hydrogens, at $\delta=8.66$ ppm. Methyl protons appears as a singlet at $\delta=2.38$ ppm.

¹H NMR spectra of the compounds **12**, **15** and **16** are given in Figures 4.13-4.15.

Table 4.11. ¹H NMR (CDCl₃) assignments of ligand H₂L² and its Ni(II) complexes (δ in ppm)

Compound	Aromatic Protons								
	OH	H ⁶ Ph	H ⁴ Ph	H ³ Ph	H ⁵ Ph	⁷ CH=	^a CH ₂	^b CH ₂	^c CH ₂
H ₂ L ²	11.3	7.09	6.97	6.80	6.67	7.99	3.63	1.66	1.42
[Ni(HL ²) ₂] (12)	12.51	7.31	7.13	6.82	6.82	7.45	3.67	1.79	1.56
[NiL ² β -pic] (15)	----	7.53	7.16	6.81	6.58	7.84	3.64	1.75	1.56
[NiL ² γ -pic]·H ₂ O (16)	----	7.15	7.15	6.81	6.58	7.83	3.61	1.74	1.55

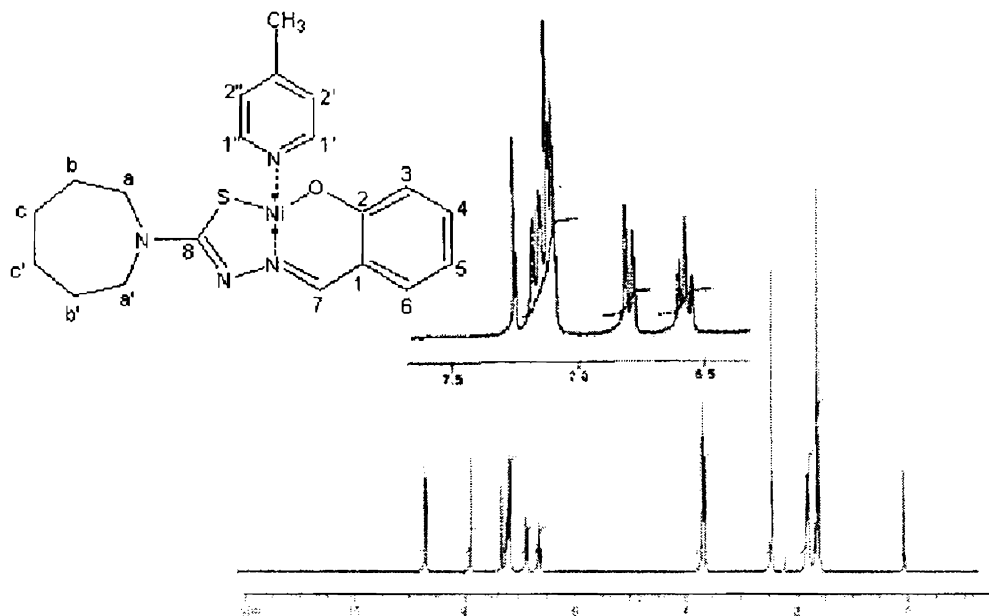


Figure 4.15. ^1H NMR spectrum of $[\text{NiL}^2\text{-}\gamma\text{-pic}]$ (16)

4.3.5. Electronic spectra

The electronic spectral assignments of the ligands and their complexes are given in Table 4.12. Each thiosemicarbazone and its nickel(II) complex shows a ring $\pi \rightarrow \pi^*$ band in the range $35000\text{--}37000\text{ cm}^{-1}$ and an $n \rightarrow \pi^*$ band in the range $28000\text{--}32000\text{ cm}^{-1}$, involving transitions within the thiosemicarbazone moiety [mainly, $\text{C}(7)=\text{N}(1)$ and $\text{C}(8)\text{--S}$ groups] [31]. These bands are slightly shifted upon complexation. The shift of the $\pi \rightarrow \pi^*$ bands to longer wavelength region in complexes is the result of the $\text{C}=\text{S}$ bond being weakened and the conjugation system enhanced on complexation [32, 33]. The $n \rightarrow \pi^*$ bands in the complex have shown a blue shift due to donation of lone pair of electrons to the metal and hence the coordination of azomethine with a reduction of intensity [32].

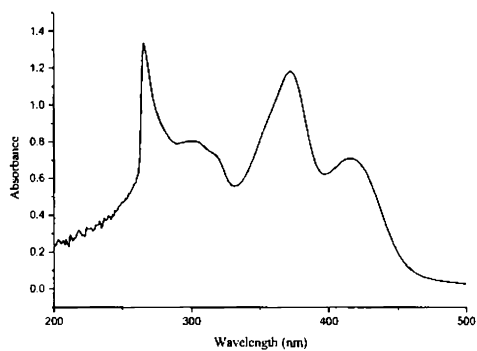
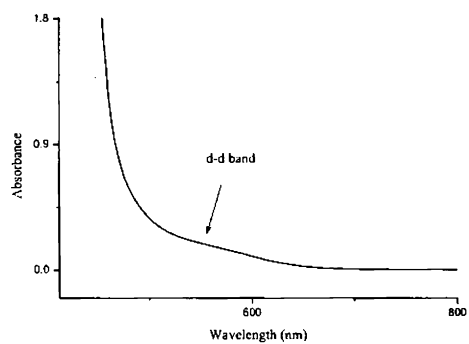
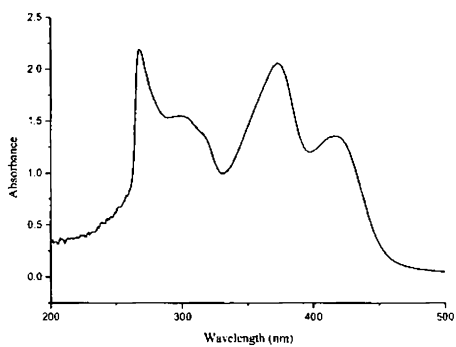
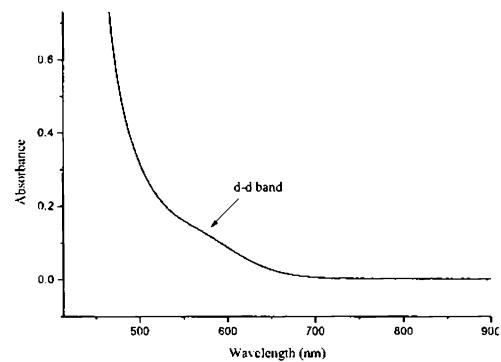
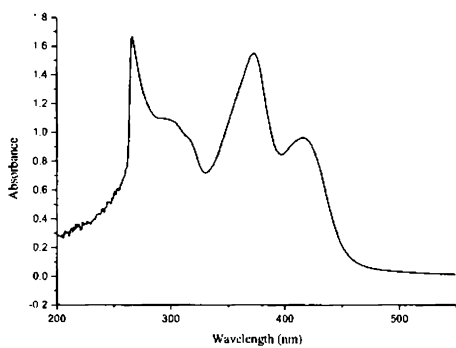
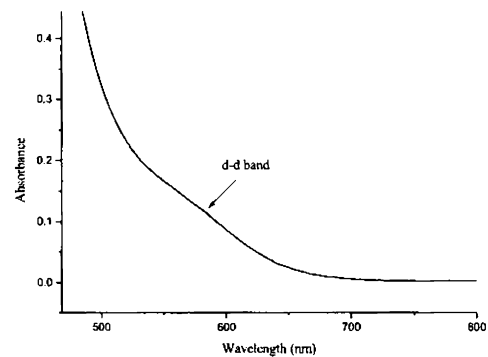
In the case of complexes having ONS donor ligands, the shift of two ligand to metal charge transfer bands are observed in the $25000\text{--}28000\text{ cm}^{-1}$ and

23000–24500 cm^{-1} ranges. In most of the dianionic complexes, LMCT maxima of the phenolate complexes show line broadening with a tail running into the visible part of the spectrum. This may result from a phenolate to Ni(II) LMCT band being superimposed on the low energy side of $\text{S} \rightarrow \text{Ni(II)}$ LMCT. Each complex has a broad $d-d$ combination band that appears as a shoulder on the intraligand and charge-transfer bands. For a square planar complex, these transitions can be assigned to ${}^1\text{E}_g \leftarrow {}^1\text{A}_{1g}$, ${}^1\text{A}_{2g} \leftarrow {}^1\text{A}_{1g}$ and ${}^1\text{B}_{1g} \leftarrow {}^1\text{A}_g$ in the order of decreasing energy [34]. These nickel complexes show a trend of increasing size of the N(4)-substituent and lower energy of the $d-d$ band maximum, presumably due to weakening of the coordinate bonding with increased bulkiness of the ligands. The absence of bands below 10000 cm^{-1} confirms the square planar nature of the complexes.

Representative spectra of the complexes **16**, **19** and **20** are presented in Figure 4.16.

Table 4.12. Electronic spectral assignments (cm^{-1}) of the ligands and its Ni(II) complexes

Compound	$\pi - \pi^*$	$n - \pi^*$	LMCT	d - d
HL ¹	36900	28250	----	----
[NiL ₂ ¹] (11)	36500	29940	26740	17610
H ₂ L ²	36110	29500	----	----
[Ni(HL ²) ₂] 12	35340	30210	26190	17240
[NiL ² py] 13	34840	30400	26450	16980
[NiL ² α -pic] 14	35420	30920, 33000	23640, 26700	17060
[NiL ² β -pic] 15	35570	30940, 32690	23810, 26880	17270
[NiL ² γ -pic]·H ₂ O 16	35580	30960, 33330	23980, 26740	17070
[Ni ₂ L ² ₂ phen] 17	35580	31250	23010, 26810	16530
HL ³	35340	31150	----	----
[NiL ₂ ³] 18	35210	30120	27470	17730
H ₂ L ⁴	36490	30210	-----	-----
[NiL ⁴ py] 19	36020	32680	23790, 26040	18480
[NiL ⁴ γ -pic] 20	36230	30210, 33780	23980, 26380	18520

 $[\text{NiL}^2\gamma\text{-pic}]\cdot\text{H}_2\text{O}$ (16) $[\text{NiL}^2\gamma\text{-pic}]\cdot\text{H}_2\text{O}$ (16) $[\text{NiL}^4\text{py}]$ (19) $[\text{NiL}^4\text{py}]$ (19) $[\text{NiL}^4\gamma\text{-pic}]$ (20) $[\text{NiL}^4\gamma\text{-pic}]$ (20)**Figure 4.16.** Electronic spectra of the compounds 16, 19 and 20

References

1. J.K. Swearingen, D.X. West, *Trans. Met. Chem.* 26 (2001) 252.
2. J.M. Wood, in: H. Sigel (Ed.), *Microbial Strategies in Resistance to Metal Ion Toxicity, Metal Ions in Biology*, Marcel Dekker, New York, 1984.
3. A. Castineiras, R. Carballo, T. Perez, *Polyhedron* 20 (2001) 441.
4. A.D. Naik, S.M. Annigeri, U.B. Gangadharmath, V.K. Revankar, V.B. Mahale, *J. Mol. Struct.* 616 (2002) 119.
5. G.M. Sheldrick, *SHELXL-97 and SHELXS-97 Program for the solution of Crystal Structures*, University of Göttingen, Germany, 1997.
6. K. Brandenburg, *DIAMOND version 3.1d*, Crystal Impact GbR, Bonn, Germany, 2006.
7. C.F. Macrac, P.R. Edgington, P. McCabe, E. Pidcock, G.P. Shields, R. Taylor, M. Towler, J. Van de Streek, *J. Appl. Cryst.* 39 (2006) 453.
8. H. Beraldo, L. P. Boyd, D. X West, *Trans. Met. Chem.* 23 (1998) 67.
9. H. Beraldo, S. B Kaisner, J. D. Turner, I. S. Billeh, J. S. Ives and D. X West, *Trans. Met. Chem.* 22 (1997) 459.
10. H.B. Gray, C.J. Ballhausen, *J. Am. Chem. Soc.* 85 (1963) 260.
11. E. Labisbal, K.D. Haslow, A. Sousa-Pedrares, J. Valdes- Martinez, A.H. Ortega, D.X. West, *Polyhedron* 22 (2003) 2831.
12. M.B. Ferrari, S. Capacchi, F. Bisceglie, G. Pelosi, P. Tarasconi, *Inorg. Chim. Acta* 312 (2001) 81.
13. Z. Afrasiabi, E. Sinn, W. Lin, Y. Ma, C. Campana, S. Padhye, *J. Inorg. Biochem.* 99 (2005) 1526.
14. H. Masui, *Coord. Chem. Rev.* 957 (2001) 219.
15. S. Brooker, P.D. Croucher, *J. Chem. Soc., Chem. Commun.* (1997) 459.
16. S. Brooker, P.D. Croucher, *J. Chem. Soc., Chem. Commun.* (1995) 1493.

17. A. Berkessel, G. Hermann, O.T. Rauch, M. Buchner, A. Jacobi, G. Huttner, *J. Chem. Ber.* 129 (1996) 1423.
18. D.E. Barber, Z. Lu, T. Richardson, R.H. Crabtree, *Inorg. Chem.* 31 (1992) 4709.
19. Z. Lu, C. White, A.L. Rheingold, R.H. Crabtree, *Inorg. Chem.* 32 (1993) 3991.
20. L. Latheef, E. Manoj, M.R.P. Kurup. *Acta Crystallogr. C* 62 (2006) 16.
21. D.X. West, Y. Yang, T.L. Klein, K.I. Goldberg, A.E. Liberta, *Polyhedron* 14 (1995) 3051.
22. M. Mikuriya, H. Okawa, S. Kida, *Bull. Chem. Soc. Japan* 53 (1980) 3717.
23. P. Sousa, J.A. Garcia-Vasquez, J.R. Masaguer, *Trans. Met. Chem.* 9 (1984) 318.
24. D.X. West, A.A. Nassar, F.A. El-Saied, M.I. Ayad, *Trans. Met. Chem.* 23 (1998) 423.
25. P. Bera, R.J. Butcher, S. Chaudhuri, N. Saha, *Polyhedron* 21 (2005) 1.
26. M.J.M. Campbell *Coord. Chem. Rev.* 15 (1975) 279.
27. S.K. Nag, D.S. Joarder, *Can. J. Chem.* 54 (1976) 2827.
28. R. Roy, M. Chaudhury, S.K. Mondal, K. Nag, *J. Chem. Soc., Dalton Trans.* (1984) 1681.
29. P.B. Sreeja, M.R.P. Kurup, *Spectrochim. Acta* 61A (2005) 331.
30. D.X. West, Y. Yang, T.L. Klein, K.I. Goldberg, A.E. Liberta, J. Valdes Martinez, R.A. Toscano, *Polyhedron* 14 (1995) 1681.
31. D.X. West, M.M. Salberg, G.A. Bain, A.E. Liberta, *Trans. Met. Chem.* 22 (1997) 180.
32. V. Philip, V. Suni, M.R.P. Kurup, *Polyhedron* 25 (2006) 1931.
33. I.-X. Li, H.A. Tang, Yi-Zhi Li, M. Wang, L.-F. Wang, C.-G. Xia, *J. Inorg. Biochem.* 78 (2000) 167.

34. D. Dave, P. Francis, Indian J. Chem. 22A (1983) 422.

Synthesis and spectral studies of Co(III) complexes of salicylaldehyde N(4)-ring incorporated thiosemicarbazones: crystal structure of a sulfenato complex

5.1. Introduction

Cobalt compounds have been used for centuries to impart a rich blue color to glass, glazes, and ceramics. It is a hard, lustrous, silver-gray metal and is ferromagnetic. Cobalt-60, an artificial isotope, is an important γ ray source, and is extensively used as a tracer and a radiotherapeutic agent. Single compact sources of ^{60}Co are readily available. Cobalt salts in small amounts are essential to many life forms, including humans. It is at the core of a vitamin called vitamin-B₁₂. Cobalt was announced to be an element by Georg Brandt about 1739 (or possibly 1735). He had been trying to demonstrate that the blue color of glass was because of a new element, cobalt, rather than bismuth, an element often found in the same locations as cobalt.

Cobalt(III) complexes derived from symmetrical and unsymmetrical schiff bases have also attracted considerable attention in the past for their relevance as biologically active compounds [1, 2]. Many model complexes of cobalt in both +2 and +3 oxidation states have been prepared and investigated, which emphasis on the reactivity of the metal ions in the trans methylation reaction and reversible absorption of molecular oxygen [3, 4].

Controlled oxidation of thiols which are coordinated to cobalt(III) leads to coordinated, S-bonded sulfenic acids. Since the resultant sulfenato complexes are

considerably more stable than the corresponding free sulfenic acid ligands, these complexes provide a means of investigating the chemistry of sulfenic acids. The nucleophilicity of coordinated sulfur seems to be very important in governing the chemistry and reactivity of sulfur-containing complexes [5, 6, 7, 8], just as the nucleophilicity of noncoordinated sulfur molecules is crucial to the chemistry and reactivity of these species.

This chapter deals with the synthesis, structural and spectral characterization of Co(III) complexes with different N(4)-ring incorporated thiosemicarbazone ligands. The structure of one of the compounds has been solved by single crystal X-ray crystallography.

5.2. Experimental

5.2.1. Materials

The syntheses of ligands are discussed in Chapter 2. The Co(II) acetate tetrahydrate (BDH), sodium azide (Merck), potassium thiocyanate and heterocyclic bases, viz, 2,2'-bipyridine (Central drug house) and 1,10-phenanthroline (Ranbaxy fine chemicals) were of reagent grade and were used as such. The reagents used were of Analar grade and used without further purification.

5.2.2. Synthesis of the complexes

[CoL²phenNCS]·0.5H₂O (21): The H₂L² (0.5 mmol, 0.138 g) was dissolved in methanol, to which was added 1,10-phenanthroline (0.5 mmol, 0.099 g) in the solid form. The mixture was slightly warmed to ensure complete dissolution of the ligands. To the above mixture was added methanolic solution of Co(OAc)₂·4H₂O (0.5 mmol, 0.124 g) with stirring. When a deep brown solution resulted, solid potassium thiocyanate (0.75 mmol, 0.728 g) was added. Stirring was continued for

about an hour. The product formed was filtered, washed with ethanol and ether and dried *in vacuo* over P_4O_{10} .

[CoL⁴bipyN₃]·CH₃OH (22): Co(OAc)₂·4H₂O (0.5 mmol, 0.124 g) dissolved in methanol was added to hot methanolic solution of H₂L⁴ (0.5 mmol, 0.124 g) and 2,2'-bipyridine (0.5 mmol, 0.078 g) and stirred for 15 minutes. Solid sodium azide (0.75 mmol, 0.048 g) was then added to the resulting solution followed by a further stirring of 2-3 h. The brown colored complex formed was filtered, washed with ethanol and ether and dried *in vacuo* over P_4O_{10} .

[CoL⁴bipyNCS]·H₂O (23): To a solution of H₂L⁴ (0.5 mmol, 0.124 g) in methanol, 2,2'-bipyridine (0.5 mmol, 0.078 g) in the solid form was added. The mixture was slightly warmed to ensure complete dissolution of the ligands. Methanolic solution of Co(OAc)₂·4H₂O (0.5 mmol, 0.124 g) was then added to the above mixture with stirring. To the resulting solution, solid potassium thiocyanate (0.75 mmol, 0.728 g) was added and stirring was continued for about an hour. A brown colored product formed was filtered, washed with ethanol and ether and dried *in vacuo* over P_4O_{10} .

[Co(L⁴O)phenN₃] (24): To a solution of H₂L⁴ (0.5 mmol, 0.124 g) and 1,10-phenanthroline (0.5 mmol, 0.099 g) in methanol, Co(OAc)₂·4H₂O (0.5 mmol, 0.124 g) dissolved in methanol was added with stirring. To the resulting brown colored solution, solid sodium azide was added and further stirred for 3-4 h. The product was then concentrated on a water bath and cooled at room temperature, filtered and kept overnight. Brown shining crystals separated out, which was filtered, washed with ethanol and ether and dried *in vacuo* over P_4O_{10} .

[CoL⁴phenNCS]·1.5H₂O (25): Solutions of H₂L⁴ (0.5 mmol, 0.124 g) and 1,10-phenanthroline (0.5 mmol, 0.099 g) in methanol were mixed and to this was added methanolic solution of Co(OAc)₂·4H₂O (0.5 mmol, 0.124 g) with stirring. The

stirring was continued for about 20 minutes. When a deep brown solution resulted, solid potassium thiocyanate (0.75 mmol, 0.728 g) was added. Stirring was continued for about an hour. A brown colored complex formed was filtered, washed with ethanol and ether and dried *in vacuo* over P₄O₁₀.

5.2.3. Physical measurements

Details regarding physical measurements are presented in Chapter 3.

5.2.4. X-ray crystallography

X-ray quality single crystals of the complex **24** were obtained from its solution in methanol by slow evaporation over a period of 10 days. Brown crystal of the compound **24** having approximate dimensions of 0.33 x 0.28 x 0.21 mm³ was selected. The compound was diffracted by CrysAlis CCD, Oxford Diffraction Ltd, with graphite-monochromated Mo K α ($\lambda=0.71073$ Å) radiation. The trial structure was solved using SHELXS-97 [9] and refinement was carried out by full-matrix least squares on F^2 (SHELXL) [9]. The graphical tool used was DIAMOND (version 3.1d) [10], PLATON [11] and MERCURY. All non-hydrogen atoms were refined anisotropically and hydrogen atoms were geometrically fixed at calculated positions. The crystallographic data and structure refinement parameters for the complex **24** are given in Table 5.1.

Table 5.1. Crystal data and experimental parameters of compound **24**

Empirical formula	C ₂₄ H ₂₂ Co N ₈ O ₂ S
Formula weight	528.47
Temperature	100(2) K
Wavelength	0.71073 Å
Crystal system	Monoclinic
Space group	<i>P</i> 2 ₁ / <i>n</i>
Unit cell dimensions	a = 10.4512(12) Å b = 18.877(4) Å c = 11.9526(12) Å α = 90° β = 90.858(9)° γ = 90°
Volume	2357.8(6) Å ³
Z	4
Density (calculated)	1.537 g/cm ³
Absorption coefficient	0.857 mm ⁻¹
F(000)	1124
Crystal size	0.33 x 0.28 x 0.21 mm ³
θ range for data collection	3.36 to 25.00°
Index ranges	-12 ≤ h ≤ 12, -22 ≤ k ≤ 22, -14 ≤ l ≤ 14
Reflections collected	20583
Independent reflections	4100 [R(int) = 0.0555]
Refinement method	Full-matrix on F ²
Data / restraints/parameters	4100 / 0 / 325
Goodness-of-fit on F ²	1.070
Final R indices [I > 2σ(I)]	R1 = 0.0392, wR2 = 0.1110
R indices (all data)	R1 = 0.0483, wR2 = 0.1162
Largest diff. peak and hole	0.440 and -0.391 e Å ⁻³

5.3. Results and discussion

The analytical data of the complexes are presented in Table 5.2. The Co(II) ion undergoes oxidation in the presence of methanol or chloroform unlike in ethanol [12]. All the complexes are brown in color. H₂L² was found to give the products more easily, while compounds of H₂L⁴ gave crystalline products on keeping. The elemental analyses data are consistent with the general empirical formula [MLBX] for all the complexes except **24**, where X are coligands like N₃

and NCS groups, and M is the cobalt metal atom, L is the doubly deprotonated thiosemicarbazone ligand and B are the heterocyclic bases *viz*, bipy and phen. Compounds **21–25** were prepared by a mathematical displacement of the acetate anion of the cobalt acetate by the addition of 0.75 mmol of the KSCN or NaN₃ to the reaction mixture of the principal ligand, cobalt acetate and heterocyclic base. In complex **24**, during the course of the synthetic reaction, the thiosemicarbazone may undergoes oxidation at the sulfur center whereby it is converted into sulfenate, and the transformed thiosemicarbazone is coordinated to cobalt as a dianionic tridentate ONS donor. The rate of oxidation of a coordinated thiol is relatively insensitive to the nature of the thiolate complex (thiolate chelate ring size or steric requirements, ancillary ligands, etc.). However, the rate of oxidation of a coordinated sulfur atom is very sensitive to the steric requirements of the sulfur atom, two coordinate sulfur being oxidized more than 10³ times faster than three coordinate sulfur. Thus the sulfenato complex formed is stable. The oxidation at sulfur depends on the nucleophilicity of the sulfur atom and it is assumed that there is at least some π -back bonding character in the M–S bond. Since cobalt(III) has six t_{2g} electrons, metal to sulfur π -bonding places more electron density on the sulfur atom coordinated to cobalt(III) and consequently causes this species to be the more effective nucleophile [13]. One molecule of 1,10-phenanthroline and one molecule of azide are also coordinated to cobalt(III). It is notable that azido coordination is unidentate and non-bridging where in most of the reported cases it is bridging [14].

Caution! Azide complexes of metals with organic ligands are potentially explosive and should be handled with care.

Table 5.2. Analytical data

Compound	Anal: Found (Calcd.) %		
	C	H	N
[CoL ² phenNCS]·0.5H ₂ O (21)	55.99(55.76)	4.37(4.51)	14.58(14.45)
[CoL ⁴ bipyN ₃]·CH ₃ OH (22)	51.67(51.49)	4.94(4.70)	20.91(20.89)
[CoL ⁴ bipyNCS]·H ₂ O (23)	51.17(51.30)	4.25(4.30)	15.81(15.61)
[Co(L ⁴ O)phenN ₃] (24)	53.50(52.94)	4.13(3.89)	20.85(20.58)
[CoL ⁴ phenNCS]·1.5H ₂ O (25)	52.24(52.53)	4.05(4.23)	15.57(14.98)

Magnetic susceptibility measurements at 293 K suggest that the compounds are diamagnetic indicating the oxidation of cobalt(II) to cobalt(III) and hence corresponds to d^6 ion in a strong field.

5.3.1. Crystal structure of the compound [Co(L⁴O)phenN₃]

The molecular structure of [Co(L⁴O)phenN₃] (**24**) along with atom labeling scheme is shown in Figure 5.1 and selected bond lengths and bond angles are summarized in Table 5.3. Dark brown X-ray quality single crystals of the compound **24** were grown by slow evaporation of its solution in methanol. Earlier reports have shown that controlled oxidation of thiols which are coordinated to cobalt(III) gave sulfenato complexes [6, 15-17]. The salient structural characteristic of the compound is that the coordinated sulfur atom is bonded to one and only one, oxygen atom. This conclusively establishes that the isolated complex does indeed contain a coordinated sulfenic acid, and thus oxidation of the [CoL⁴phenN₃] occurs without disruption of the primary coordination sphere of the cobalt center. The oxidized tridentate ligand provides one azomethine nitrogen, a sulfur from the sulfenato group and phenolic oxygen, while two nitrogens from the phenanthroline and terminal azide group complete the coordination geometry.

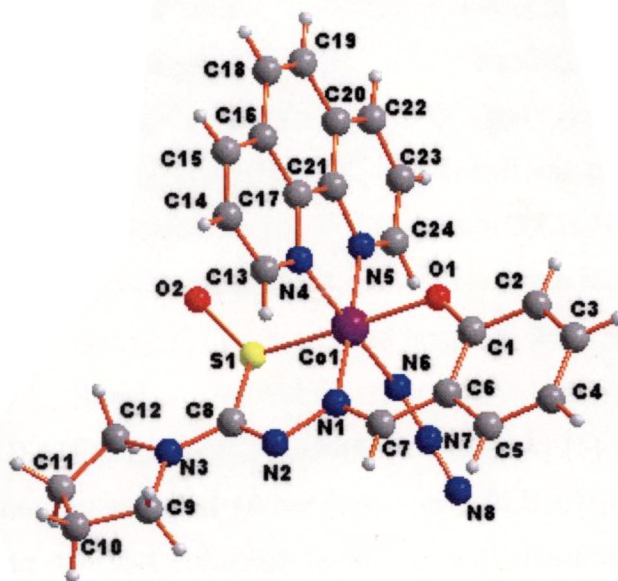


Figure 5.1. Structure and labeling diagram of the compound 24

The molecular structure of the compound was found to be distorted octahedral, fully expected from the known structures of the analogous thiolate [18], sulfenato [5] and sulfinato [14] complexes. The bond angles N6-Co1-N4 [$173.41(10)^\circ$] and N5-Co1-N4 [$83.56(10)^\circ$] define largest distortion of the geometry. Figure 5.1 shows that the L^4O ligand is functioning as an ONS donor ligand like the parent H_2L^4 and it is coordinated in a meridional arrangement along with phen and terminal azido group. This coordination results in two five membered and one six membered rings in this complex. The bond angles indicate a distorted octahedral geometry in this complex. The azido group is coordinated to metal as a terminal ligand with a bond distance of $1.942(3)$ Å (Co1-N6). This value is comparable with that of bipyridine analog of thiosemicarbazone and phenanthroline analog of semicarbazone reported elsewhere [18, 19]. The sulfenato sulfur atom is three coordinated (the cobalt atom, the carbon atom of the chelate ring and the oxygen atom) in an approximately tetrahedral (counting the sulfur lone pair of electrons as occupying the fourth site) configuration.

The Co–S bond length in the compound [2.1952(8) Å] is significantly shorter than the analogous thiolate {[CoL⁴bipyN₃]; 2.2126(7) Å [18] and [(en)₂CoSCH₂CH₂NH₂]²⁺; 2.226(2) Å [5]} and greater than the sulfinato [(en)₂CoS(O)₂CH₂NH₂]²⁺; 2.191(2) Å [5] cobalt complexes. The Co–S bond length is shorter compared to that for [(en)₂CoS(O)CH₂NH₂]²⁺; 2.253(1) Å [5]. This means that the π -bonding in the cobalt(III) system increases the bond order of the cobalt-sulfur linkage. The S–O bond length in **24** [1.491(3) Å] is longer than the S–O bond lengths observed in sulfinato complex [(en)₂CoS(O)₂CH₂CH₂NH₂]²⁺; 1.456(4)–1.476(4) Å [5] but shorter compared to sulfenato complex reported earlier [(en)₂CoS(O)CH₂CH₂NH₂]²⁺ 1.552(3) Å [5]. The oxidation state three of cobalt is shown by its coordination bond lengths Co–S, Co–N_(azomethine) and Co–O_{phenolic} (Table 5.3) which are in the expected ranges of 2.201–2.230, 1.882–1.901, 1.866–1.9373 Å respectively. The coordination lengthens the oxidized thiosemicarbazone moiety's C8–S1 bond (1.811(3)°) and shortens C8–N2 bond (1.298(3) Å) compared to salicylaldehyde with a seven membered ring rather than five in the present case [salicylaldehyde 3-hexamethyleiminyl thiosemicarbazone C8–S1= 1.684(3) Å, C8–N2= 1.362(3) Å] [20]. Strong coordination of azomethine nitrogen is indicated by much shorter Co1–N1 (1.882(2) Å) bond length.

In the cobalt-thiol system discussed here, two oxidation reactions occur in the presence of air. The cobaltous ion is oxidized to the +3 state; the thiol is oxidized to sulfenate.

The azide anions which are nearly linear [N6–N7–N8=175.2(3)°] is coordinated with a N7–N6–Co1 angle of 122.2(2)°. The N–N bond lengths in the azide group are not equal. The longer N–N bonds involve the N atoms coordinated to the metal centre [N6–N7 = 1.204(3) Å, N7–N8 = 1.143(4) Å] and these values are comparable {1.199(7) and 1.163(7) Å respectively for

[CoLN₃{o-(CH₃C=O)C₆H₄O}] [21]; 1.196(3) and 1.151(3) Å respectively for [CoL⁴bipyN₃] [18] and 1.214(6) and 1.147(7) Å for [CoLphenN₃] [19]} to the corresponding values in other Co(III) azido complexes.

Table 5.3. Selected bond lengths (Å) and bond angles (°) for **24**

Bond lengths (Å)			
Co1–N1	1.882(2)	S1–C8	1.811(3)
Co1–O1	1.9373(19)	O1–C1	1.298(3)
Co1–N6	1.942(3)	N1–C7	1.292(3)
Co1–N5	1.947(2)	N1–N2	1.397(3)
Co1–N4	1.948(2)	N2–C8	1.298(3)
Co1–S1	2.1952(8)	N3–C8	1.331(3)
S1–O2	1.491(3)	N6–N7	1.204(3)
N7–N8	1.143(4)		
Bond angles (°)			
N1–Co1–N6	91.30(10)	N5–Co1–S1	90.62(7)
O1–Co1–N6	92.05(11)	N4–Co1–S1	89.14(8)
N1–Co1–N5	177.51(9)	C8–S1–Co1	93.54(9)
O1–Co–N5	86.02(9)	C1–O1–Co1	125.64(17)
N6–Co1–N5	90.81(10)	C7–N1–N2	113.9(2)
N1–Co1–N4	94.25(9)	C7–N1–Co1	124.55(18)
O1–Co1–N4	90.98(10)	N2–N1–Co1	121.51(16)
N6–Co1–N4	173.41(10)	C8–N2–N1	113.6(2)
N5–Co1–N4	83.56(10)	N7–N6–Co1	122.2(2)
N1–Co1–S1	88.15(7)	N8–N7–N6	175.2(3)
O1–Co1–S1	176.60(6)	N2–N1–Co1	121.51(16)
Co1–S1–O2	113.19(12)	C8–S1–O2	106.39(15)

The molecules of **24** are packed in an ‘offset’ manner within the unit cell (Figure 5.2). The assemblage of molecules in the respective manner within the unit cell is resulted by the diverse π – π stacking, CH and hydrogen bonding (Figure 5.3) interactions depicted in Table 5.4.

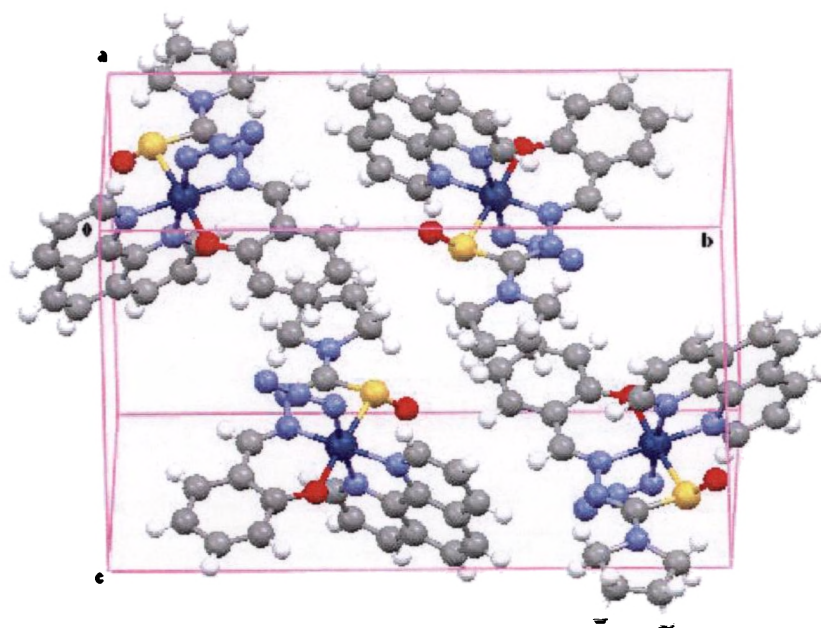


Figure 5.2. Unit cell packing diagram of the compound 24

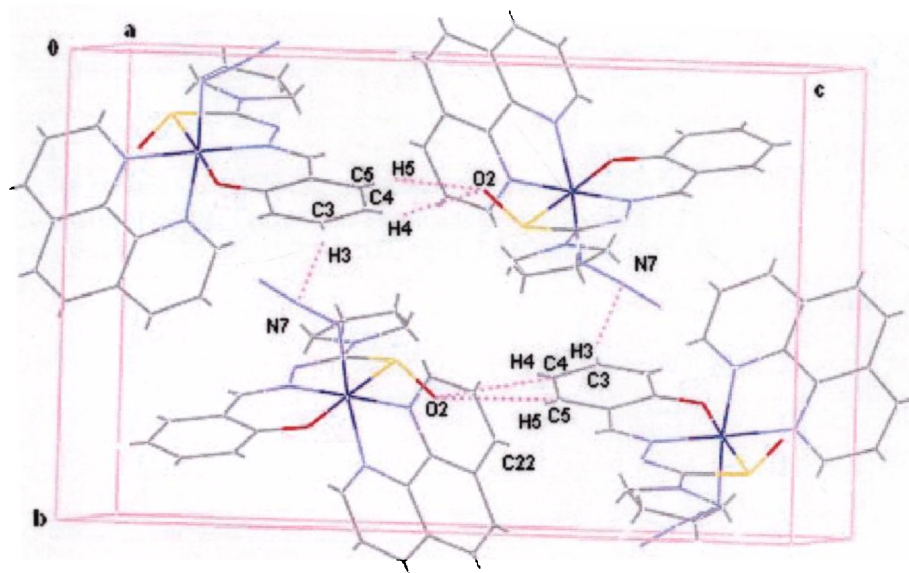


Figure 5.3. Hydrogen bonding interactions for the compound 24

Table 5.4. Interaction parameters of the compound 24 **π - π interactions**

Cg(I)-Res(1)···Cg(J)	Cg-Cg (Å)	α°	β°
Cg(1) [1] -> Cg(5) ^a	3.8169	84.04	28.65
Cg(3) [1] -> Cg(7) ^b	3.9326	13.16	16.04
Cg(7) [1] -> Cg(3) ^c	3.9326	13.16	18.45

Equivalent position code: a= x, y, z; b= 1/2+x, 1/2-y, -1/2+z; c= -1/2+x, 1/2-y, -1/2+z
 Cg(1)= Co1, S1, C8, N1, N2; Cg(3)= N3, C9, C10, C11, C12; Cg(5)= N4, C13, C14, C15, C16, C17; Cg(7)= C1, C2, C3, C4, C5, C6

CH- π interactions

X-H(I)···Cg(J)	H...Cg (Å)	X-H...Cg (°)	X...Cg (Å)
Y-X (I)···Cg(J)			
C13-H13 [1] -> Cg(1) ^a	2.69	144	3.4857
N7-N8 [1] -> Cg(4) ^a	2.69	139	3.4420

Equivalent position code: a= x, y, -z
 Cg(4)= Co1, O1, N1, C1, C6, C7

H-bonding

D-H...A	D...H (Å)	H...A (Å)	D...A (Å)	D-H...A (°)
C3-H3...N7 ^a	0.930	2.620(2)	3.476(4)	153.21(21)
C5-H5...O2 ^b	0.930	2.498(3)	3.148(4)	127.15(18)
C4-H4...O2 ^b	0.930	2.640(3)	3.208(4)	120.02(21)

D= donor, A= acceptor, α = Dihedral angle between planes I and J (°)

β = Angle Cg(I)->Cg(J) or Cg(I)->Me vector and normal to plane I (°)

Equivalent position code: a= x-1/2, -y+1/2, +z+1/2; b= -x+1/2+1, y+1/2, -z+1/2

5.3.2. IR spectra

Assignments of selected characteristic IR bands ($4000\text{--}200\text{ cm}^{-1}$) for the free ligands (H_2L^2 and H_2L^4) and its cobalt(III) complexes, compiled in Table 5.5, indicate the bonding sites of the primary ligand molecule when complexed with the cobalt(III) ion. A medium band at 3050 cm^{-1} (H_2L^2) and 3072 cm^{-1} (H_2L^4) in the free ligands due to the $\nu(^2\text{NH})$ vibration disappeared in the spectra of complexes providing strong evidence for ligand coordination around the Co(III) ion in its deprotonated form.

IR spectra of H_2L^2 and H_2L^4 show broad bands at 3315 and 3232 cm^{-1} , respectively, due to intermolecular hydrogen bonded phenolic --OH groups. These bands disappeared in the spectra of the complexes. It is further corroborated with the downward shift of $60\text{--}80\text{ cm}^{-1}$ for $\nu(\text{CO})$ as well as an appearance of a band at $510\text{--}565\text{ cm}^{-1}$ region due to a $\nu(\text{Co--O})$ band in the spectra of complexes resulting from coordination of phenolic oxygen [18]. Absence of any bands in the $2800\text{--}2550\text{ cm}^{-1}$ region points towards the lack of --SH stretching frequencies in the molecule. It reveals the presence of only the thione tautomer in the solid state. Compounds **21**, **22**, **23** and **25** show broad IR bands at $\sim 3400\text{ cm}^{-1}$, which are due to the O--H stretching modes of uncoordinated water molecules.

The infrared spectrum of compound **24** exhibits an intense band which is not present in the spectra of corresponding thiolate complexes. This band is therefore assigned as arising from the expected sulfur–oxygen stretch of the S–bonded sulfenato moiety. The frequency observed for this band is 997 cm^{-1} is in agreement with the frequencies reported earlier

$\{[(\text{en})_2\text{Co}(\text{S}(\text{O})\text{CH}_2\text{CH}_2\text{NH}_2)](\text{SCN})_2,$			986 cm^{-1} [18];
$[(\text{en})_2\text{Co}(\text{S}(\text{O})\text{CH}_2\text{CH}_2\text{NH}_2)](\text{NO}_3)_2,$	993	cm^{-1}	[18];
$[(\text{en})_2\text{Co}(\text{S}(\text{O})\text{CH}_2\text{CH}_2\text{NH}_2)](\text{NO}_3)(\text{ClO}_4),$	998	cm^{-1}	[18];

$[(en)_2Co(S(O)CH_2CH(COOH)NH_2)]I_2$, 953 cm^{-1} [16]} for the S-bonded sulfenato moiety.

Negative shift of bands assigned to $\nu(C=N_{azo})$ of the free ligands at $\sim 1615\text{ cm}^{-1}$ to $1592\text{--}1597\text{ cm}^{-1}$ in its complexes, is consistent with coordination of azomethine nitrogen to the central cobalt(III) ion; the bands at $460\text{--}473\text{ cm}^{-1}$ in the complexes are then assigned to $\nu(Co-N)$ [18, 22-26]. The $\nu(N-N)$ of the thiosemicarbazone is found at $\sim 1035\text{ cm}^{-1}$ region. The increase in frequency of this band in the spectra of complexes is due to the increase in bond strength, again confirmed the coordination *via* the azomethine nitrogen.

The presence of the azide group in the coordination sphere is evidenced from the very strong and sharp absorption peak at $\sim 2020\text{ cm}^{-1}$. The azido group is bound to cobalt as a terminal one is indicated by a strong absorption at 2030 cm^{-1} characteristic of a terminal azido group [21, 26]. The slight lowering in values is assumed to the result of its coordination to the metal [27]. In the thiocyanato complexes, the very strong band observed at $\sim 2090\text{ cm}^{-1}$ corresponds to $\nu(C=N)$ of NCS [21]. Bands at $\sim 714\text{ cm}^{-1}$ is assigned to $\delta(NCS)$. These facts indicate that thiocyanate group is N-coordinated to Co(III) [18], since the characteristic bands formed due to sulfur coordination are observed at $\sim 2150\text{ cm}^{-1}$ [27].

In the uncomplexed thiosemicarbazones, strong bands at $1324, 861\text{ cm}^{-1}$ (H_2L^2) and $1338, 839\text{ cm}^{-1}$ (H_2L^4) due to thioamide stretching and bending vibrations, respectively, are shifted to lower frequencies in the ranges $1270\text{--}1290$ and $750\text{--}800\text{ cm}^{-1}$. This negative shift of the $\nu(C=S)$ band in the complexes are indicated by the coordination *via* the thiolato sulfur atom. In all the Co(III) complexes, another strong band is found in the range $1530\text{--}1550\text{ cm}^{-1}$, which may be due to the newly formed $\nu(C=^2N)$ bond as a result of enolization. Strong bands observed in the $340\text{--}353\text{ cm}^{-1}$ region have been assigned to the

$\nu(\text{Co-S})$ band [23]. The IR spectra of the complexes display bands characteristics of coordinated heterocyclic bases [18].

IR spectra of the complexes **21–24** are presented in Figures 5.4-5.7.

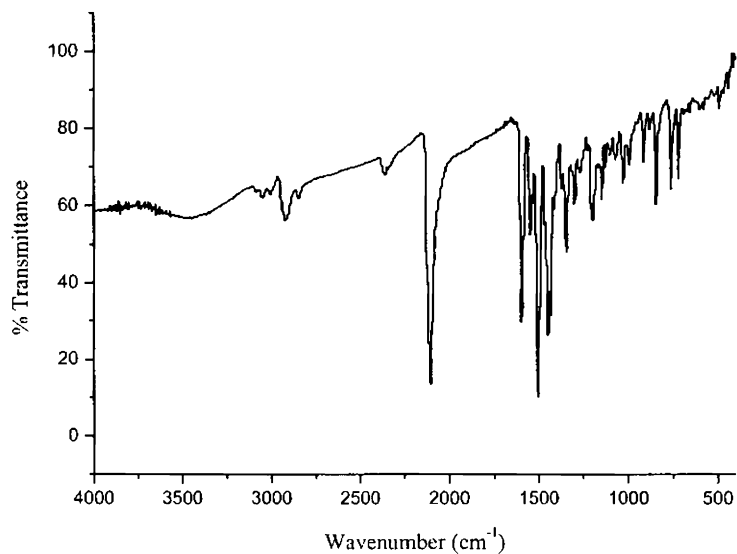


Figure 5.4. IR spectrum of the compound $[\text{CoL}^2\text{phenNCS}] \cdot 0.5\text{H}_2\text{O}$ (**21**)

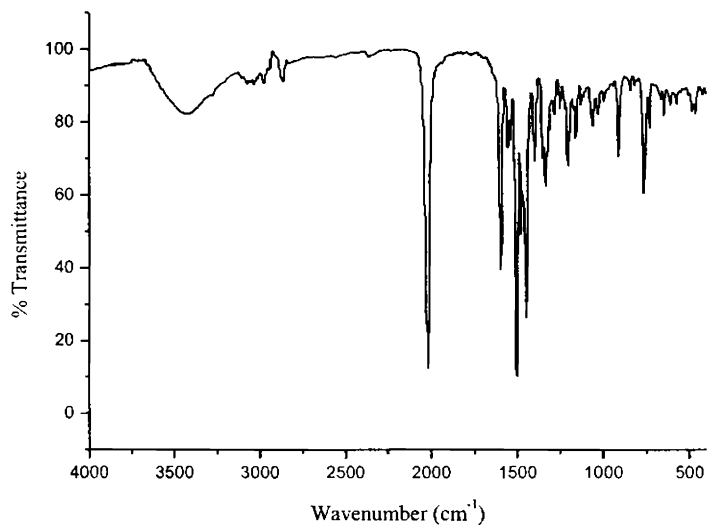


Figure 5.5. IR spectrum of the compound $[\text{CoL}^4\text{bipyN}_3] \cdot \text{CH}_3\text{OH}$ (**22**)

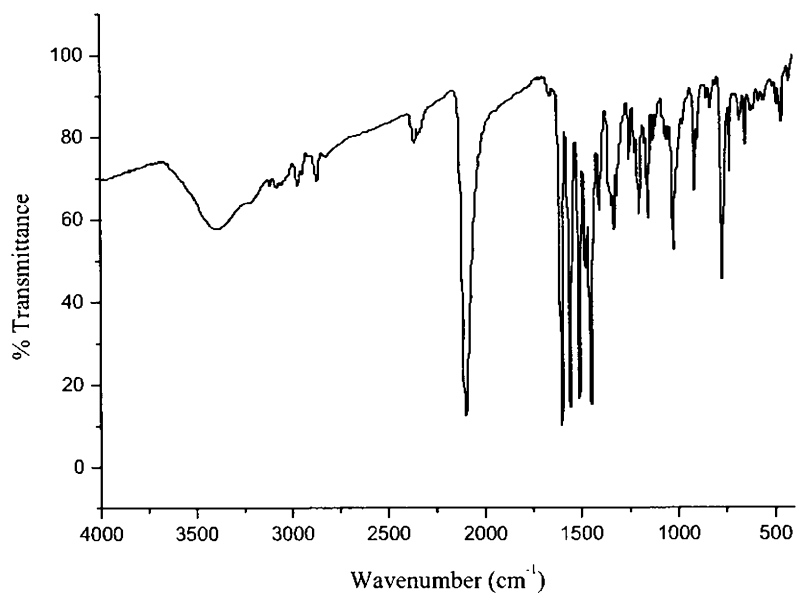


Figure 5.6. IR spectrum of the compound $[\text{CoL}^4\text{bipyNCS}] \cdot \text{H}_2\text{O}$ (23)

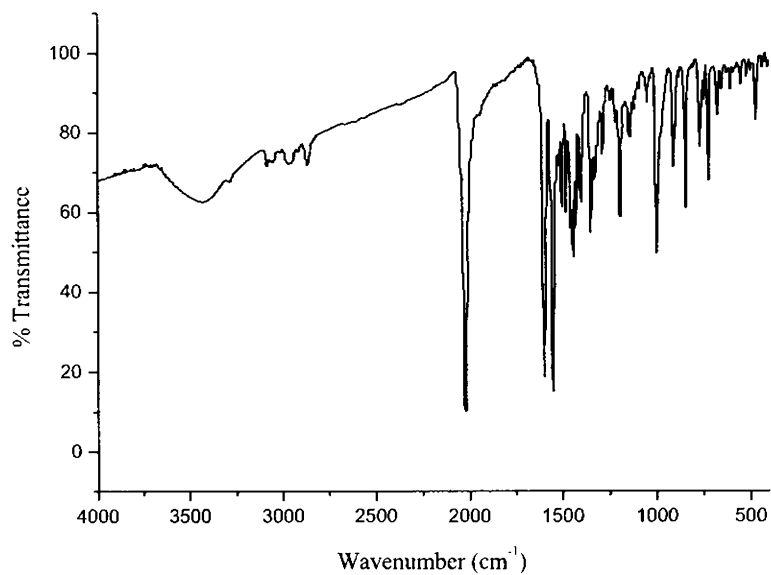


Figure 5.7. IR spectrum of the compound $[\text{Co}(\text{L}^4\text{O})\text{phenN}_3]$ (24)

Table 5.5. Selected IR bands (cm^{-1}) with tentative assignments of the ligands and its Co(III) complexes

Compound	$\nu(\text{C}=\text{N}_{\text{azo}})$	$\nu(\text{C}=\text{N})$	$\nu(\text{N}-\text{N})$	$\nu^{\delta}[(\text{C}=\text{S})/(\text{C}-\text{S})]$	$\nu(\text{C}-\text{O})$	$\nu(\text{Co}-\text{N})$	$\nu(\text{Co}-\text{O})$	$\nu(\text{N}_3)/\text{NCS}$	Bands due to heterocyclic bases
H_2L^2	1612	----	1037	1324, 861	1271	----	----	----	----
$[\text{CoL}^2\text{-phenNCS}] \cdot 0.5\text{H}_2\text{O}$ (21)	1592	1548	1068	1278, 798	1189	479	566	2104, 710	1432, 831
H_2L^4	1622	----	1034	1338, 839	1288	----	----	----	----
$[\text{CoL}^4\text{-bipyN}_3]\text{-CH}_3\text{OH}$ (22)	1592	1548	1057	1283, 754	1200	462	567	2010	1443, 892
$[\text{CoL}^4\text{-bipyNCS}] \cdot \text{H}_2\text{O}$ (23)	1598	1549	1048	1270, 768	1199	454	543	2094, 723	1446, 892
$[\text{Co}(\text{L}^4\text{O})\text{phenN}_3]$ (24)	1597	1553	1053	1277, 760	1206	468	539	2022	1437, 831
$[\text{CoL}^4\text{-phenNCS}] \cdot 1.5\text{H}_2\text{O}$ (25)	1597	1542	1052	1287, 754	1206	473	572	2098, 714	1443, 842

5.3.3. Electronic spectra

The electronic spectral assignments of the ligands and their complexes are given in Table 5.6. Both the thiosemicarbazones and their cobalt(III) complexes show a ring $\pi \rightarrow \pi^*$ band in the range 35500–36500 cm^{-1} and an $n \rightarrow \pi^*$ band in the range 29500–34000 cm^{-1} (involving transitions within the thiosemicarbazone moiety mainly, C(7)=N(1), C(8)–S groups), is of reduced intensity in the spectra of the complexes [28]. In the case of complexes having ONS donor ligands, the shift of two ligand to metal charge transfer bands are found in the 24500–28000 and 23000–24000 cm^{-1} ranges. The higher energy band is assigned to S→Cu(II) transitions.

The electronic spectra of spin paired trivalent cobalt complexes of approximate O_h symmetry have the following assignments of $d-d$ bands: two spin allowed transitions at relatively low energy, ${}^1T_{1g} \leftarrow {}^1A_{1g}$, ${}^1T_{2g} \leftarrow {}^1A_{1g}$. There are additional spin-forbidden transitions ${}^3T_{1g} \leftarrow {}^1A_{1g}$ and ${}^3T_{2g} \leftarrow {}^1A_{1g}$ at higher energies and these are usually complicated by the overlap of intraligand and charge transfer transitions [18]. In all the complexes, only one broad band is observed for the $d-d$ band.

Representative spectra of the complexes **23**, **24** and **25** are presented in Figure 5.8.

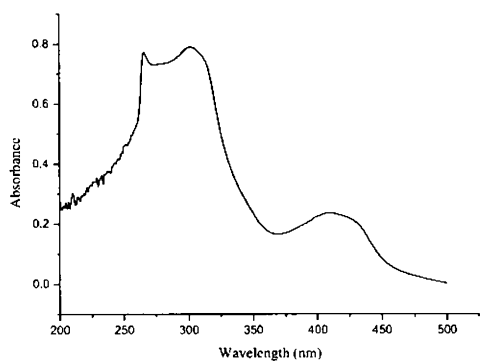
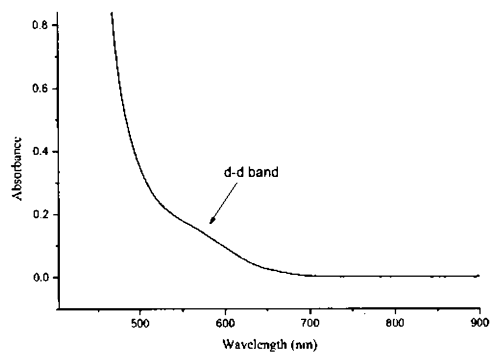
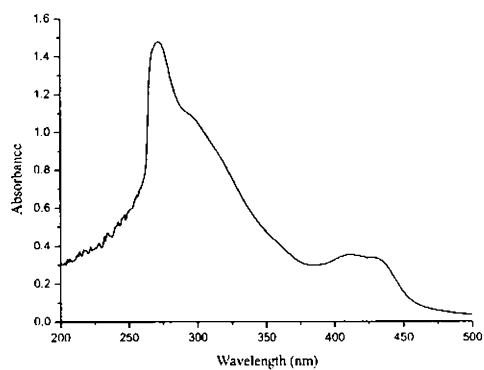
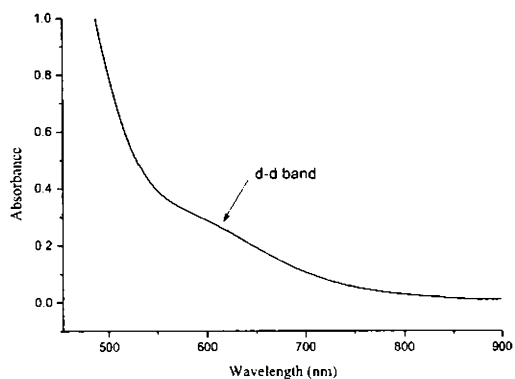
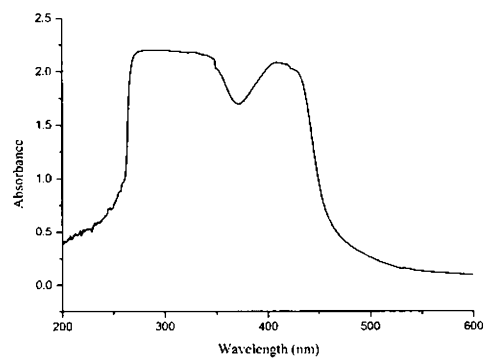
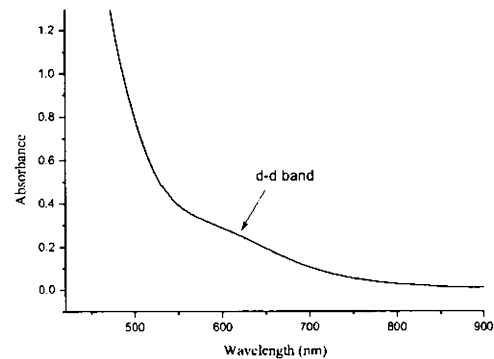
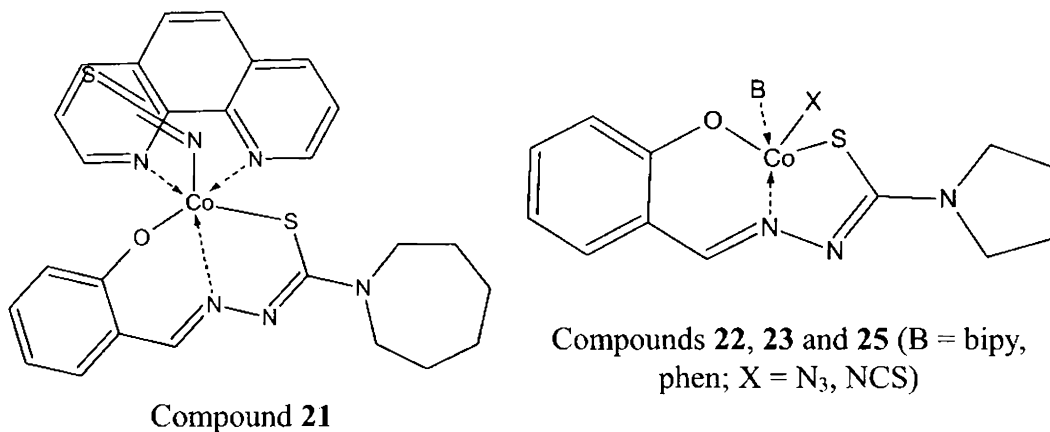
 $[\text{CoL}^4\text{bipyNCS}]\cdot\text{H}_2\text{O}$ (23) $[\text{CoL}^4\text{bipyNCS}]\cdot\text{H}_2\text{O}$ (23) $[\text{Co}(\text{L}^4\text{O})\text{phenN}_3]$ (24) $[\text{Co}(\text{L}^4\text{O})\text{phenN}_3]$ (24) $[\text{CoL}^4\text{phenNCS}]\cdot 1.5\text{H}_2\text{O}$ (25) $[\text{CoL}^4\text{phenNCS}]\cdot 1.5\text{H}_2\text{O}$ (25)**Figure 5.8.** Electronic spectra of complexes 23, 24 and 25

Table 5.6. Electronic spectral assignments (cm^{-1}) of the ligands and its Co(III) complexes

Compound	$\pi - \pi^*$	$n - \pi^*$	LMCT	d - d
H_2L^2	36110	29500	----	----
$[\text{CoL}^2\text{phenNCS}] \cdot 0.5\text{H}_2\text{O}$ (21)	36010	30250	26190	17360
H_2L^4	36490	30210	----	----
$[\text{CoL}^4\text{bipyN}_3] \cdot \text{CH}_3\text{OH}$ (22)	35620	30940	23510, 25880	16390
$[\text{CoL}^4\text{bipyNCS}] \cdot \text{H}_2\text{O}$ (23)	36310	33220	23360, 24510	17250
$[\text{Co}(\text{L}^4\text{O})\text{phenN}_3]$ (24)	36110	33780	23040, 24880	17510
$[\text{CoL}^4\text{phenNCS}] \cdot 1.5\text{H}_2\text{O}$ (25)	36100	30480	23250, 24690	16180

Based on the elemental analyses and spectral studies following tentative structures were assigned for the complexes (Figure 5.9).

**Figure 5.9.** Tentative structures of the complexes

References

1. R.K. Parashar, R.C. Sharma, A. Kumar, G. Mohan, *Inorg. Chim. Acta* 151 (1988) 201.
2. H. Chen, D. Han, H. Yan, W. Tang, Y. Yang, H. Wang, *Polyhedron* 12 (1993) 1097.
3. J.P. Costes, G. Cros, M.H. Darbieu, J.P. Laurent, *Inorg. Chim. Acta* 60 (1982) 111.
4. A. Bottcher, T. Takeuchi, K.I. Hardcastle, T.J. Meade, H.B. Gray, D.C. Wickel, M. Kapon, Z. Dori, *Inorg. Chem.* 36 (1997) 2498.
5. I.K. Adzamli, K. Libson, J.D. Lydon, R.C. Eldeer, E. Deutsch, *Inorg. Chem.* 18 (1979) 303.
6. D.L. Herting, C.P. Solan, A.W. Cabral, J.H. Krueger, *Inorg. Chem.* 17 (1978) 1649.
7. M.J. Heeg, R.C. Elder, E. Duetsch, *Inorg. Chem.* 18 (1979) 2036.
8. G.J. Kennard, E. Duetsch, *Inorg. Chem.* 17 (1978) 2225.
9. G.M. Sheldrick, SHELXL-97 and SHELXS-97 Program for the solution of Crystal Structures, University of Göttingen, Germany, 1997.
10. K. Brandenburg, DIAMOND version 3.1 d, Crystal Impact GbR, Bonn, Germany, 2006.
11. A.L. Spek, *J. Appl. Cryst.* 36 (2003) 7.
12. M.B. Ferrari, G.G. Fava, M. Lanfranchi, C. Pelizzi, A. Tarasconi, *J. Chem. Soc., Dalton Trans.* (1991) 1951.
13. J. Ribas, A. Escuer, M. Monfort, R. Vincente, R. Corte, L. Lezama, T. Rojo, *Coord. Chem. Rev.* 1027 (1999) 193.
14. J.P. Barton, J.E. Packer, R.J. Sims, *J. Chem. Soc., Perkin Trans. 2* (1973) 1547.

15. B.A. Lange, K. Libson, E. Deutsch, R.C. Elder, *Inorg. Chem.* 15 (1976) 2985.
16. C.P. Solan, J.H. Kruenger, *Inorg. Chem.* 14 (1975) 1481.
17. W.G. Jackson, A.M. Sargeson, P.O. Whimp, *J. Chem. Soc., Chem. Commun.* (1976) 934.
18. R.P. John, A. Sreekanth, M.R.P. Kurup, S.M. Mobin, *Polyhedron* 21 (2002) 2515.
19. A. Sreekanth, U.L. Kala, C.R. Nayar, M.R.P. Kurup, *Polyhedron* 23 (2004) 41.
20. N. Mondal, D.K. Dey, S. Mitra, K.M. Abdul Malik, *Polyhedron* 19 (2000) 2707.
21. L. Latheef, E. Manoj, M.R.P. Kurup, *Acta. Crystallogr. C* 62 (2006) 16.
22. N.C. Saha, A. Seal, R.J. Butcher, N. Saha, *J. Indian Chem. Soc.* 78 (2001) 601.
23. D.K. Sau, N. Saha, R.J. Butcher, S. Chaudhuri, *Trans. Met. Chem.* 28 (2003) 229.
24. P. Bera, R.J. Butcher, S. Chaudhuri, N. Saha, *Polyhedron* 21 (2002) 1.
25. A. Mitra, T. Banerjee, P. Roychowdhuri, S. Chaudhuri, P. Bera, N. Saha, *Polyhedron* 16 (1997) 3735.
26. A.L. Balch, L.A. Fosset, R.R. Guimerans, M.M. Olmstead, P.E. Reed, F.E. Wood, *Inorg. Chem.* 25 (1986) 1248.
27. K. Nakamoto, *Infrared and Raman Spectra of Inorganic and Coordination Compounds*, 5th ed., Wiley, New York, 1978, 124.
28. D.X. West, M.M. Salberg, G.A. Bain, A.E. Liberta, *Trans. Met. Chem.* 22 (1997) 180.

Synthesis, spectral and structural studies of Zn(II) complexes of salicylaldehyde N(4)-ring incorporated thiosemicarbazones

6.1. Introduction

Zinc occurs in the earth's crust to the extent of 132 ppm by weight. It is the twenty-fourth most abundant element. Zinc atom has an important role in several enzymes, both as metallo-enzyme and enzyme-activator, as well as filling a structural role [1]. Zinc(II)- sulfur interactions are of great interest in biochemical systems, due to the presence of sulfur at the active sites of several enzymes, vitamins and proteins [2]. Biologically it is the second most important transition metal. Its most vital function may be concerned with the synthesis of DNA and RNA. Zinc deficiency leads to impaired DNA synthesis, delayed wound healing and decrease in collagen synthesis [3]. Zinc is a critical component of more than 300 proteins including farnesyltransferase, matrix metalloproteinases and endostatin that are involved in the front-line cancer research, and a host of proteins termed zinc fingers that mediate protein-protein and protein-nucleic acid interactions. Thiosemicarbazones usually react as ligands with metal cations by bonding through the sulfur and the azomethine nitrogen atoms, although in some cases they behave as terdentate ligands bonded through the sulfur and azomethine nitrogen and another donor atom (O or N) [4-9].

Zinc element has a $d^{10}s^2$ electronic arrangement and they typically form M^{2+} ion. However, many of their compounds are appreciably covalent. The most stable oxidation state of Zn is +2. The Zn(II) complex of thiosemicarbazones can exist

both in a monomeric solvated 4-coordinate form and as a phenolic oxygen bridged dimer. They have tetrahedral, square pyramidal, trigonal bipyramidal and octahedral geometries.

This chapter describes the synthesis and characterization of ten Zn(II) complexes of salicylaldehyde N(4)-ring incorporated thiosemicarbazones using infrared, electronic and ^1H NMR studies. The structure of one of the compound has been solved by single crystal X-ray crystallography and was found to be distorted tetrahedral in geometry.

6.2. Experimental

6.2.1. Materials

The syntheses of ligands are already discussed in Chapter 2. $\text{Zn}(\text{OAc})_2 \cdot 2\text{H}_2\text{O}$ (S.D.Fine chemicals), pyridine, α/γ picoline, 2,2'-bipyridine (bipy) (Central drug house) and 1,10-phenanthroline (phen) (Ranbaxy fine chemicals) were used. The reagents used were of Analar grade and used without further purification.

6.2.2. Synthesis of the complexes

[Zn(HL²)₂] (26): This complex was synthesized by refluxing an ethanolic solution of H_2L^2 (2 mmol, 0.554 g) with an ethanolic solution of $\text{Zn}(\text{OAc})_2 \cdot 2\text{H}_2\text{O}$ (1 mmol, 0.219 g) for 2 h. The yellow shining crystals formed was filtered, washed with ethanol and finally with ether and dried over P_4O_{10} *in vacuo*.

[ZnL²py] (27): To a solution of H_2L^2 (1 mmol, 0.277 g) in hot ethanol was added slight excess of heterocyclic base pyridine (3 mmol, 0.237 g) with constant stirring. To this was added a hot ethanolic solution of $\text{Zn}(\text{OAc})_2 \cdot 2\text{H}_2\text{O}$ (1 mmol, 0.219 g). The solution was then refluxed for an hour. The yellow complex formed was filtered, washed with ethanol and finally with ether and dried over P_4O_{10} *in vacuo*.

[ZnL²α-pic]·4H₂O (28): Zn(OAc)₂·2H₂O (1 mmol, 0.219 g) dissolved in ethanol was added to a solution of H₂L² (1 mmol, 0.277 g) in hot ethanol and slight excess of heterocyclic base α-picoline (3 mmol, 0.279 g) with constant stirring. The solution is then refluxed for 2 h. The yellow complex formed was filtered, washed with ethanol and finally with ether and dried over P₄O₁₀ *in vacuo*.

[ZnL²γ-pic] (29): Solutions of H₂L² (1 mmol, 0.277 g) and slight excess of heterocyclic base γ-picoline (3 mmol, 0.279 g) in ethanol were mixed and to this was added a hot ethanolic solution of Zn(OAc)₂·2H₂O (1 mmol, 0.219 g) and refluxed for 30 minutes. The yellow colored product formed was filtered, washed with ethanol and finally with ether and dried over P₄O₁₀ *in vacuo*.

[ZnL²bipy] (30): The H₂L² (1 mmol, 0.277 g) was dissolved in ethanol, to which was added an ethanolic solution of Zn(OAc)₂·2H₂O (1 mmol, 0.219 g) with constant stirring. This was followed by the addition of the base 2,2'-bipyridine (1 mmol, 0.156 g) in the solid form. The stirring was continued for about an hour when yellow compound began to separate. This was filtered, washed with ethanol and ether and dried *in vacuo* over P₄O₁₀.

[ZnL²phen]·H₂O (31): An ethanolic solution of Zn(OAc)₂·2H₂O (1 mmol, 0.219 g) was added to a solution of H₂L² (1 mmol, 0.277 g) in hot ethanol with stirring. To this was added 1,10-phenanthroline (1 mmol, 0.198 g) in the solid form. The stirring was continued for about 2 h, when yellow compound began to separate. This was filtered, washed with ethanol and ether and dried *in vacuo* over P₄O₁₀.

[Zn(HL⁴)₂] (32): Ethanolic solutions of the ligand H₂L⁴ (2 mmol, 0.498 g) and Zn(OAc)₂·2H₂O (1 mmol, 0.219 g) in 2:1 ratio was refluxed for 2 h. The yellow complex formed was filtered, washed with ethanol and finally with ether and dried over P₄O₁₀ *in vacuo*.

[ZnL⁴py]·3H₂O (33): Zn(OAc)₂·2H₂O (1 mmol, 0.219 g) dissolved in ethanol was added to a hot ethanolic solution of H₂L⁴ (1 mmol, 0.249 g) and slight excess of heterocyclic base pyridine (3 mmol, 0.237 g) with constant stirring. The stirring was then continued for 2-3 h. The product formed was filtered, washed with ethanol and finally with ether and dried over P₄O₁₀ *in vacuo*.

[ZnL⁴γ-pic] (34): Solutions of H₂L⁴ (1 mmol, 0.249 g) and heterocyclic base γ-picoline (3 mmol, 0.279 g) in ethanol were mixed and to this was added a hot ethanolic solution of Zn(OAc)₂·2H₂O (1 mmol, 0.219 g). The solution was then refluxed for 2 h. The yellow complex formed was filtered, washed with ethanol and finally with ether and dried over P₄O₁₀ *in vacuo*.

[ZnL⁴bipy]·5H₂O (35): An ethanolic solution of H₂L⁴ (1 mmol, 0.249 g) was mixed with an ethanolic solution of Zn(OAc)₂·2H₂O (1 mmol, 0.219 g) and this was followed by the addition of the base 2,2'-bipyridine (1 mmol, 0.156 g) in the solid form. The stirring was continued for about an hour when yellow compound began to separate. This was filtered, washed with ethanol and ether and dried *in vacuo* over P₄O₁₀.

6.2.3. Physical measurements

Details regarding physical measurements are presented in Chapter 3. ¹H NMR spectra were recorded on a Bruker AMX 300 in CDCl₃ with TMS as internal standard.

6.2.4. X-ray crystallography

The molecular structure of compound [Zn(HL²)₂] (**26**) was determined by single crystal X-ray diffraction method. Intensity data and cell refinement parameters were recorded at room temperature (293 K) on a Nonius, MACH3 diffractometer equipped with graphite monochromated Mo Kα (λ=0.71073 Å) radiation. Crystallographic and experimental details for the structure are

summarized in Table 6.1. The Maxus (Nonius software) were used for data reduction [10]. Two atoms C11 and C12 in the ring containing N3 are disordered as two carbons split over two sets of positions. Restraints were applied to assist the geometry of the disordered atoms. The ratio of major to minor disorder component is 56.8:43.2. The trial structure was solved using SHELXS-97 [11] and refinement was carried out by full-matrix least squares on F^2 (SHELXL-97) [12]. The non-hydrogen atoms were refined by anisotropic thermal parameters. All hydrogen atoms were geometrically fixed and refined using riding model. The intensity data were collected by the ω -scan mode within $1.59^\circ < \theta < 24.99^\circ$ for hkl ($-12 \leq h \leq 12$, $-13 \leq k \leq 13$, $-15 \leq l \leq 0$) on a triclinic system. Molecular graphics employed were DIAMOND version 3.1d [13] and PLATON [14].

Table 6.1. Crystal data and structure refinement parameters for **26**

Empirical formula	$C_{28} H_{36} N_6 O_2 S_2 Zn$
Formula weight	618.12
Temperature	293(2) K
Wavelength	0.71073 Å
Crystal system, space group	Triclinic, $P\bar{1}$
Unit cell dimensions	$a = 10.3390(8)$ Å $\alpha = 82.641(8)^\circ$ $b = 11.0940(10)$ Å $\beta = 82.662(7)^\circ$ $c = 13.0270(14)$ Å $\gamma = 79.174(7)^\circ$
Volume	$1447.3(2)$ Å ³
Z, Calculated density	2, 1.418 g/cm ³
Absorption coefficient	1.030 mm ⁻¹
F(000)	648
Crystal size	$0.30 \times 0.15 \times 0.15$ mm ³
Theta range for data collection	1.59 to 24.99° .
Index ranges	$-12 \leq h \leq 12$, $-13 \leq k \leq 13$, $-15 \leq l \leq 0$
Reflections collected / unique	5298/5053 [R(int) = 0.0260]
Completeness to 2θ	24.99 to 99.2%
Absorption correction	Ψ -scan
Max. and min. transmission	0.8609 and 0.7476
Refinement method	Full-matrix least-squares on F^2
Data / restraints / parameters	5053 / 0 / 371
Goodness-of-fit on F^2	1.012
Final R indices [$I > 2\sigma(I)$]	$R_1 = 0.0417$, $wR_2 = 0.0891$
R indices (all data)	$R_1 = 0.1122$, $wR_2 = 0.1049$

6.3. Results and discussion

The analytical data of all the complexes are listed in Table 6.2. All the complexes except **26** and **32** were assigned the general formula MLB , where B are heterocyclic bases, pyridine, α/γ -picoline, 2,2'-bipyridine and 1,10-phenanthroline. The analytical data indicate that the ligands behave as monoprotic (in complexes **26** and **32**) as well as biprotic molecules (all complexes except **26** and **32**) and forms both bisligated $[M(HL)_2]$ and base adducts $[MLB]$ with bivalent metal ions. As expected, all the complexes are diamagnetic. The complexes **28**, **30**, **31**, **33** and **35** contain uncoordinated water molecules also. Mononuclear $Zn(II)$ complexes are formed in all the complexes. All the complexes are found to be diamagnetic as expected due to the d^{10} configuration of the metal ion.

Table 6.2. Analytical data

Compound	color	Anal: Found (Calcd.) %		
		C	H	N
$[Zn(HL^2)_2]$ (26)	yellow	54.27(54.4)	5.98(5.87)	13.60(13.60)
$[ZnL^2py]$ (27)	yellow	54.23(54.35)	5.30(5.28)	13.26(13.34)
$[ZnL^2\alpha\text{-pic}] \cdot 4H_2O$ (28)	yellow	47.24(47.48)	6.39(6.37)	10.85(11.07)
$[ZnL^2\gamma\text{-pic}]$ (29)	yellow	54.86(55.36)	5.76(5.58)	12.81(12.91)
$[ZnL^2bipy] \cdot 3.5H_2O$ (30)	yellow	51.67(51.47)	5.77(5.76)	12.54(12.51)
$[ZnL^2phen] \cdot H_2O$ (31)	yellow	57.87(57.94)	5.27(5.05)	13.43(12.99)
$[Zn(HL^4)_2]$ (32)	yellow	51.25(51.29)	5.38(5.02)	14.93(14.95)
$[ZnL^4py] \cdot 3H_2O$ (33)	yellow	45.75(45.79)	5.08(5.43)	12.04(12.57)
$[ZnL^4\gamma\text{-pic}]$ (34)	yellow	52.95(53.27)	4.64(4.97)	13.67(13.81)
$[ZnL^4bipy] \cdot 5H_2O$ (35)	yellow	47.14(47.27)	5.14(5.59)	13.27(12.53)

6.3.1. Crystal structure of the compound $[Zn(HL^2)_2]$

The molecular structure of the compound $[Zn(HL^2)_2]$ (**26**) along with atom numbering scheme is given in Figure 6.1 and selected bond lengths and bond angles are summarized in Table 6.3. The ligands coordinate to the Zn(II) ion, through azomethine nitrogen and thiolate sulfur atoms of the deprotonated form after thiolation, to form a highly distorted tetrahedral geometry. The phenolic group of the ligand is retained as such and is placed away from the metal centre. This is because of the change of conformation of the ligand from *E* form to *Z* form about the azomethine bond. The free ligand H_2L^2 in its solid form is in a position to bond the metal in a tridentate ONS manner which we discussed in Chapter 2. The conformation change of a ligand from bidentate to tridentate manner on coordination is known, but this reverse case is seen for the first time for thiosemicarbazone ligands in Zn(II) complexes. However, a CSD search shows a similar conformation in Zn(II) hydrazones [15].

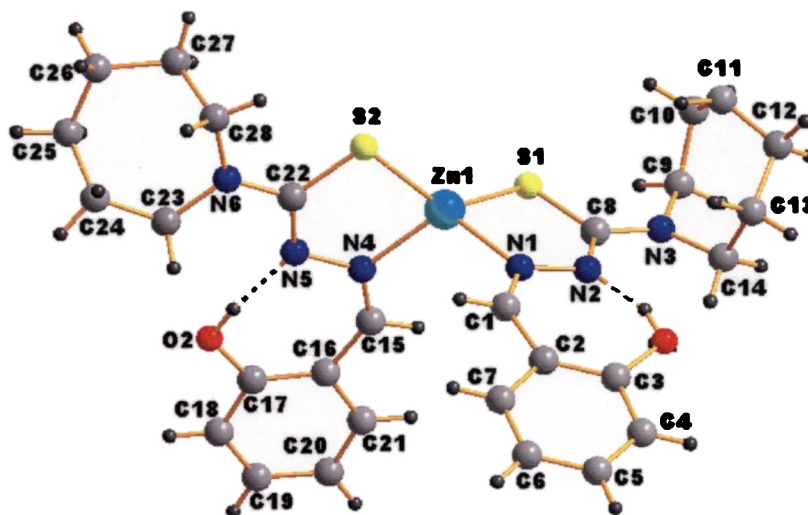


Figure 6.1. Molecular structure of $[Zn(HL^2)_2]$. Minor disorder components at C11/C12 removed for clarity. Intramolecular hydrogen bonding interactions are shown as dashed lines

The NS chelation results in two five membered planar rings Zn1, N1, N2, C8, S1 having a maximum deviation of $-0.053(4)$ Å for C8 and Zn1, S2, N4, N5, C22 with a maximum deviation of $0.002(3)$ Å for N4. The dihedral angle between these planar rings is $89.28(9)^\circ$. The smaller angles around Zn(II) are $86.29(9)^\circ$ for N4–Zn1–S2 and $86.57(10)^\circ$ for N1–Zn1–S1. These factors clearly point out the rigidity of core thiosemicarbazone moiety even after coordination and the highly distorted tetrahedral coordination. The other angles around zinc are in between $110.90(12)^\circ$ and $134.39(5)^\circ$.

The Zn–N distances in the complex are smaller compared to [Zn(Acehexim)₂], {Zn–N12 $2.044(9)$ and Zn–N22 $2.068(10)$ Å} [16]; [Zn(PzAm4M)₂]·2CH₃CN, {Zn1–N12 $2.072(2)$ and Zn1–N22 $2.071(2)$ Å} [17]; [ZnL¹₂MeOH], {Zn–N3 $2.114(2)$ Å and Zn–N13 $2.108(2)$ } [18], [Zn(Am4m)(OAc)₂]₂, {Zn1–N2 $2.050(2)$ Å and Zn1¹–N2¹ $2.227(2)$ } [19]; [Zn(HAm4E)I₂] {Zn–N12 $2.120(7)$ Å} [20] indicates stronger coordination of azomethine nitrogen in compound **26** and the Zn–S distances are comparable. The coordination results in the changes of bond lengths and angles of the thiosemicarbazone moiety, as expected. The C–S bond length increases from $1.684(3)$ Å to $1.744(4)$ and $1.749(4)$ Å. Similarly C8–N2 {and C22–N5} suffers significant decrease from $1.362(3)$ Å seen in the free ligand. These changes indicate the coordination of deprotonated sulfur after enolization. The other bond lengths and angles also suffer some changes, but not significantly. The chair conformation of hexamethyleneiminyl rings are retained in this complex.

Table 6.3. Selected bond lengths (Å) and bond angles (°) for [Zn(HL²)₂] (**26**)

Bond lengths (Å)		Bond angles (°)	
Zn1–N1	2.026(3)	N1–Zn1–N4	110.90(12)
Zn1–N4	2.040(3)	N1–Zn1–S2	123.53(10)
Zn1–S1	2.2597(13)	N4–Zn1–S2	86.29(9)
Zn1–S2	2.2462(12)	N1–Zn1–S1	86.57(10)
C1–N1	1.293(5)	N4–Zn1–S1	116.40(10)
C15–N4	1.296(5)	S2–Zn1–S1	134.39(5)
N1–N2	1.385(4)	C15–N4–N5	119.6(3)
N4–N5	1.383(4)	C15–N4–Zn1	121.9(3)
N2–C8	1.332(5)	N5–N4–Zn1	118.5(2)
N5–C22	1.329(4)	C1–N1–N2	119.5(3)
C8–S1	1.744(4)	C1–N1–Zn1	122.2(3)
C22–S2	1.749(4)	N2–N1–Zn1	118.1(2)
		N2–C8–N3	117.2(3)
		N2–C8–S1	125.8(3)
		N3–C8–S1	117.0(3)
		N5–C22–N6	115.9(3)
		N5–C22–S2	126.3(3)
		N6–C22–S2	117.8(3)

The intramolecular hydrogen bond O–H...N_{azomethine} seen in the free ligand is retained in the compound **26**, but the O–H...S bond disappears. Relevant hydrogen bonding interactions are given in Table 6.4. However no significant π - π or C–H... π interactions are found in the packing. In the unit cell, the molecules are packed in a ‘face to face’ manner and the weak intermolecular hydrogen bond C18–H18...O1 link the molecules into one-dimensional sheets along the *c* axis (Figure 6.2). Intra and intermolecular hydrogen bonding interactions are shown in Figure 6.3.

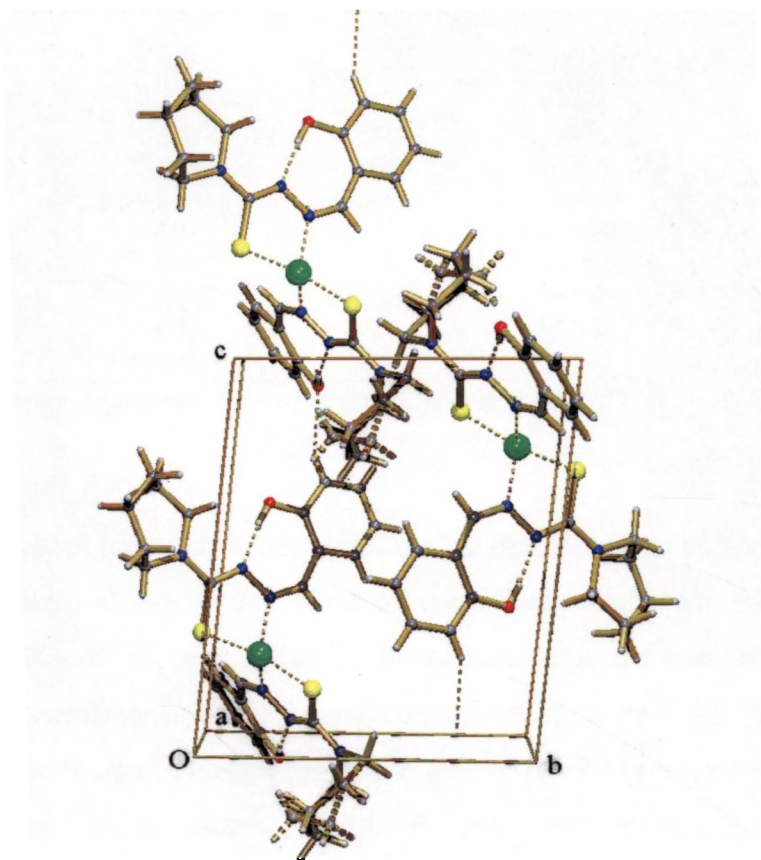


Figure 6.2. Unit cell packing diagram of the compound 26 viewed along the *c* axis

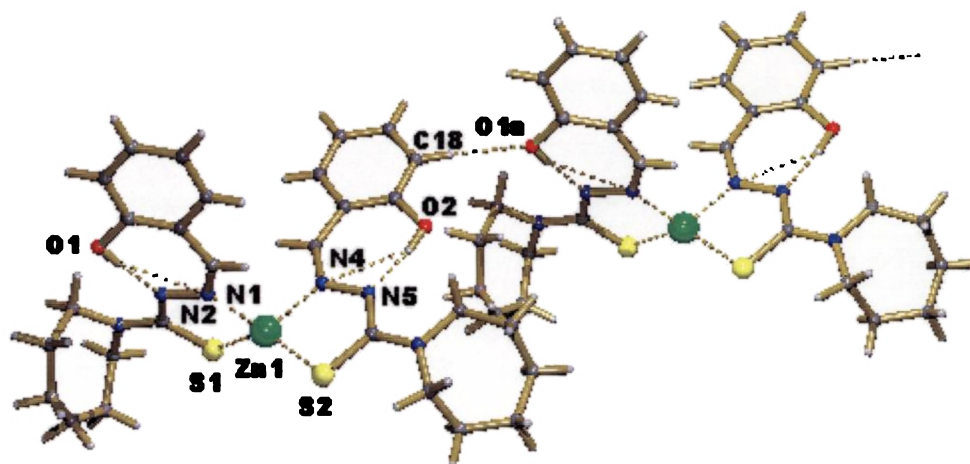


Figure 6.3. Intra and intermolecular hydrogen bonding interactions for 26

Table 6.4. H-bonding interactions in compound 26

D-H...A	D...H (Å)	H...A (Å)	D...A (Å)	D-H...A (°)
O1-H1O1...N1 ^a	0.79(5)	2.57(5)	3.232(5)	143(4)
O1-H1O1...N2 ^a	0.79(5)	1.77(5)	2.556(5)	174(5)
O2-H1O2...N4 ^a	0.85(6)	2.54(6)	3.249(5)	142(6)
O2-H1O2...N5 ^a	0.85(6)	1.73(6)	2.568(5)	172(6)
C14-H14B...O1 ^a	0.97	2.44	3.207(6)	136
C23-H23B...O2 ^a	0.97	2.57	3.081(6)	113
C9-H9A...S1 ^a	0.97	2.58	2.963(4)	104
C28-H28A...S2 ^a	0.97	2.42	2.977(4)	116
C18-H18...O1 ^b	0.93	2.51	3.365(6)	153

D=donor, A=acceptor, Equivalent position code: a= x, y, z, b= x, +y, +z+1

6.3.2. IR spectra

The IR spectral bands are most useful for the determination of the mode of coordination is given in Table 6.5. None of these compounds have any bands between 2500–2800 cm⁻¹ suggesting that the ligands are not in the thiol form either before or after coordination. The bands corresponding to $\nu(\text{N-H})$ appear at ~ 3100 cm⁻¹ for the ligands, disappeared in the spectra of all the complexes. The band at ~ 1620 cm⁻¹ due to $\nu(\text{C}=\text{N}_{\text{azo}})$ of the thiosemicarbazone moiety shifts to ~ 1590 cm⁻¹ upon coordination [21]. This confirms the coordination *via* azomethine nitrogen. Coordination of azomethine nitrogen is also consistent with the presence of a band at ~ 405–420 cm⁻¹, assignable to $\nu(\text{Zn-N})$ for these complexes [22, 23]. A small shift in the absorption bands due to the $\nu(\text{N-N})$ stretching vibrations from ~ 1030 cm⁻¹ to higher region is due to the increase in double bond character off-setting the loss of electron density *via* donation to the metal and is a confirmation of the coordination of the ligand through the azomethine nitrogen atom [24]. Coordination *via* thiolate sulfur is indicated by a decrease in the frequency of the thioamide band, which is partly $\nu(\text{C=S})$, and found at 1330 and 850 cm⁻¹ in the uncomplexed thiosemicarbazone by 20–100 cm⁻¹ in the complexes [25]. This decrease in stretching frequency of thiolate sulfur in the

complexes is indicated by Campbell [26]. Another strong band is found in the region of $1535\text{--}1545\text{ cm}^{-1}$ is due to the newly formed $\nu(\text{C}=\text{N})$ bond in the spectra for these complexes. The bands at $325\text{--}360\text{ cm}^{-1}$ assignable to $\nu(\text{Zn}\text{--}\text{S})$ in the complexes are consistent with sulfur coordination [22]. The new peaks observed in the range $520\text{--}540\text{ cm}^{-1}$ are due to the $\text{Zn}\text{--}\text{O}_{(\text{phenolic})}$ bond [27]. Except in complexes **26** and **32**, coordination *via* phenolic oxygen is indicated by a decrease in frequency of the $\nu(\text{CO})$, and found at 1271 cm^{-1} in the uncomplexed thiosemicarbazone by $60\text{--}80\text{ cm}^{-1}$ in the spectra of complexes. In complexes **26** and **32**, the $\nu(\text{CO})$ does not shift to much lower numbers indicating that the coordination not occur through phenolic oxygen. Representative spectra of **26**, **30** and **31** are given in Figures 6.4-6.6.

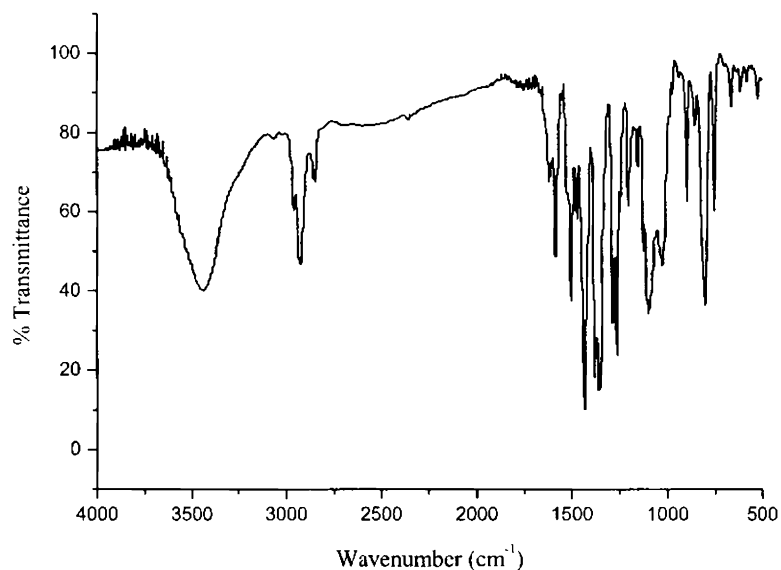


Figure 6.4. IR spectrum of $[\text{Zn}(\text{HL}^2)_2]$ (**26**)

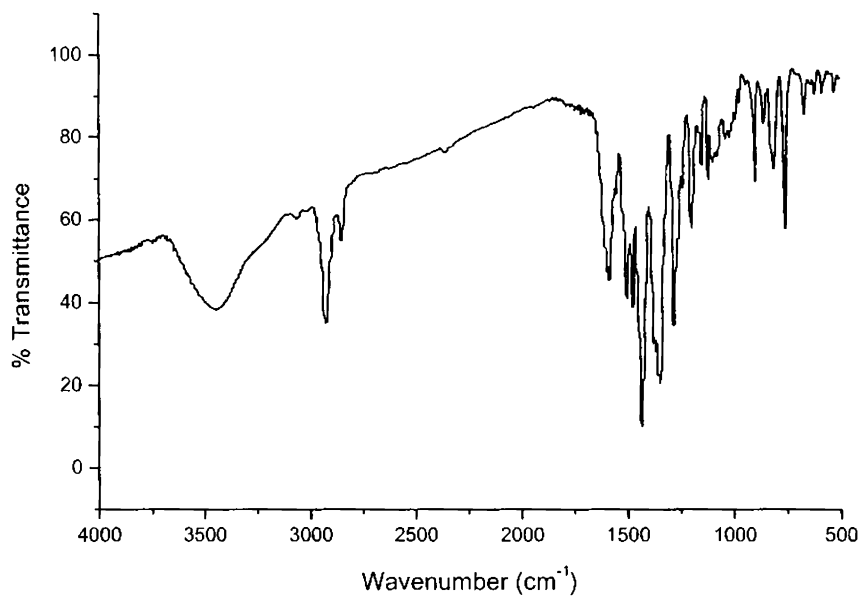


Figure 6.5. IR spectrum of $[\text{ZnL}^2\text{bipy}] \cdot 3.5\text{H}_2\text{O}$ (**30**)

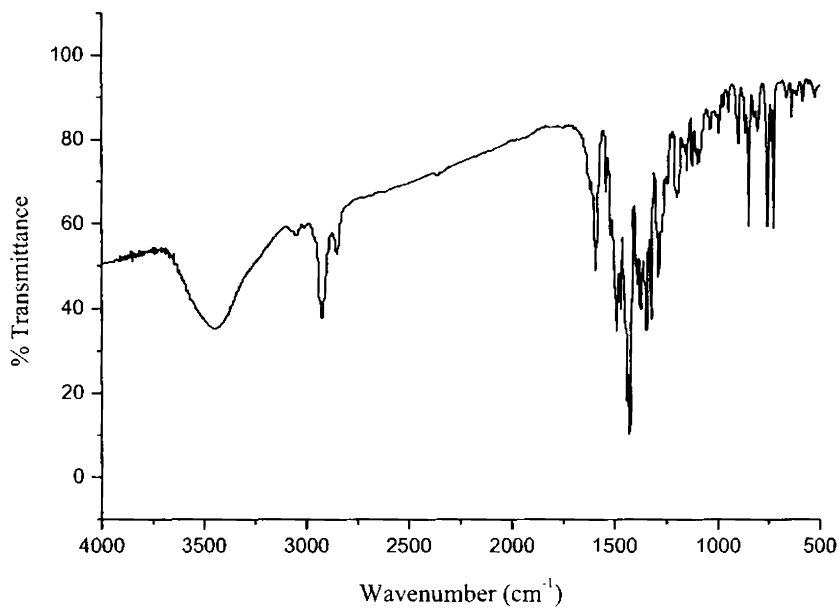


Figure 6.6. IR spectrum of $[\text{ZnL}^2\text{phen}] \cdot \text{H}_2\text{O}$ (**31**)

Table 6.5. Selected IR bands (cm^{-1}) with tentative assignments of the ligands and its Zn(II) complexes

Compound	$\nu(\text{C}=\text{N}_{\text{azo}})$	$\nu(\text{C}=\text{N})$	$\nu(\text{N}-\text{N})$	$\nu[\delta[(\text{C}=\text{S})/(\text{C}-\text{S})]]$	$\nu(\text{C}-\text{O})$	$\nu(\text{Zn}-\text{N})$	$\nu(\text{Zn}-\text{S})$	Bands due to heterocyclic bases
H_2L^2	1612	----	1037	1324, 861	1271	----	----	----
$[\text{Zn}(\text{HL}^2)_2]$ (26)	1583	1543	1097	1285, 754	1261	404	330	----
$[\text{ZnL}^2\text{py}]$ (27)	1592	1550	1091	1276, 753	1190	417	345	1421, 632
$[\text{ZnL}^2\text{-}\alpha\text{-pic}] \cdot 4\text{H}_2\text{O}$ (28)	1591	1545	1095	1295, 758	1191	418	342	1416, 668
$[\text{ZnL}^2\text{-}\gamma\text{-pic}]$ (29)	1589	1540	1099	1298, 755	1188	416	350	1420, 664
$[\text{ZnL}^2\text{-bipy}] \cdot 3.5\text{H}_2\text{O}$ (30)	1584	1544	1083	1285, 755	1202	415	347	1434, 664
$[\text{ZnL}^2\text{-phen}] \cdot \text{H}_2\text{O}$ (31)	1590	1537	1099	1287, 755	1200	420	352	1425, 640
H_2L^4	1622	----	1034	1338, 839	1288	----	----	----
$[\text{Zn}(\text{HL}^4)_2]$ (32)	1589	1530	1074	1278, 758	1278	425	355	----
$[\text{ZnL}^4\text{py}] \cdot 3\text{H}_2\text{O}$ (33)	1605	1557	1080	1277, 759	1197	420	358	1450, 646
$[\text{ZnL}^4\text{-}\gamma\text{-pic}]$ (34)	1585	1545	1088	1295, 760	1196	418	360	1422, 667
$[\text{ZnL}^4\text{-bipy}] \cdot 5\text{H}_2\text{O}$ (35)	1590	1555	1090	1288, 758	1190	417	348	1420, 663

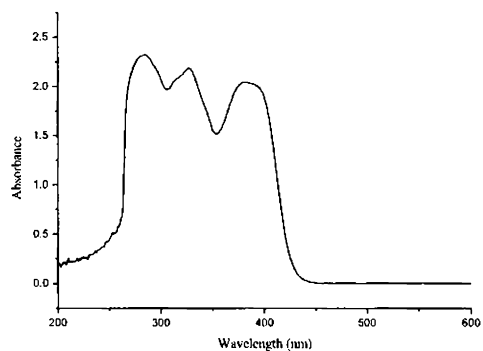
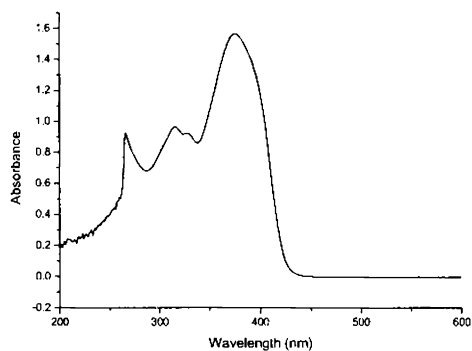
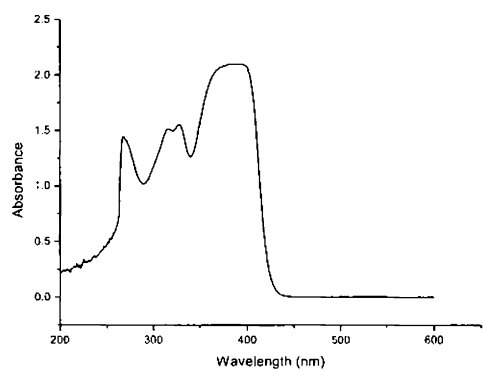
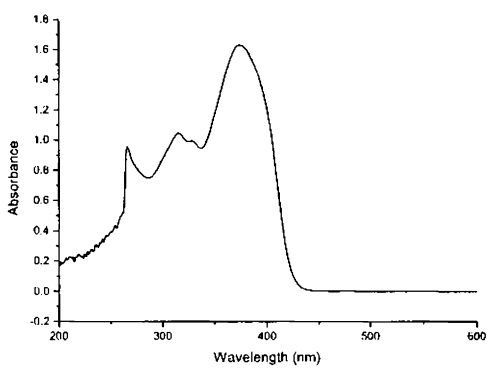
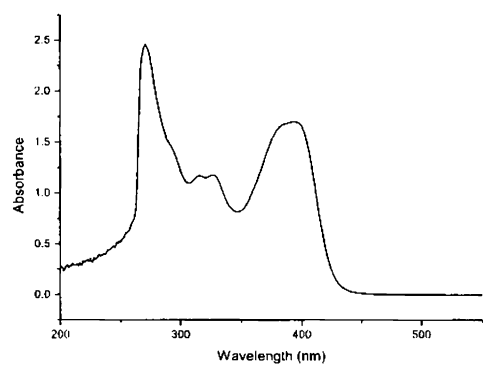
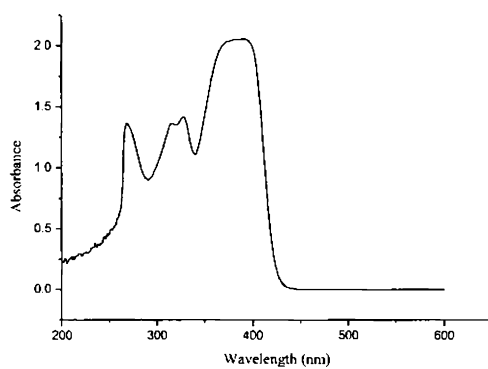
6.3.3. Electronic spectra

The electronic absorption bands of the Zn(II) complexes, recorded in DMF solution, are given in Table 6.6 and representative spectra are in Figure 6.7. The electronic spectra of the ligands recorded in DMF show bands at ~ 35000 and 31500 cm^{-1} assignable to $\pi \rightarrow \pi^*$ transitions of the phenyl ring [28-30] and $n \rightarrow \pi^*$ transitions of the azomethine and thioamide functions respectively [31, 32]. The energy of these bands slightly shifted upon complexation. The shift of the $\pi \rightarrow \pi^*$ bands to longer wavelength region in complexes is the result of the C=S bond being weakened and the conjugation system enhanced on complexation [33, 34]. The $n \rightarrow \pi^*$ bands in the complexes have shown a blue shift due to donation of lone pair of electrons to the metal and hence the coordination of azomethine with a reduction of intensity.

A moderately intense broad band for the complex in the region $25000\text{--}27000\text{ cm}^{-1}$ is assigned to Zn(II) \rightarrow S transitions. MLCT maxima of the phenolate complexes show line broadening with a tail running into the visible part of the spectrum. This may result from a Zn(II) to phenolate MLCT band being superimposed on the low energy side of Zn(II) \rightarrow S transitions [35]. Zn(II) to phenolate absorption is not obtained in compounds **26** and **32**. No appreciable absorptions occurred above 500 nm in DMF solution indicating the absence of $d\text{--}d$ bands which is in accordance with the d^{10} configuration of the Zn(II) ion.

Table 6.6. Electronic spectral assignments (cm^{-1}) of the ligands and its Zn(II) complexes

Compound	$\pi - \pi^*$	$n - \pi^*$	MLCT
H_2L^2	36110	29500	----
$[\text{Zn}(\text{HL}^2)_2]$ (26)	35340	30210	25980
$[\text{ZnL}^2\text{py}]$ (27)	35580	31750, 30300	26740
$[\text{ZnL}^2\alpha\text{-pic}] \cdot 4\text{H}_2\text{O}$ (28)	36010	31950, 30350	25770
$[\text{ZnL}^2\gamma\text{-pic}]$ (29)	35580	31850, 30210	26530
$[\text{ZnL}^2\text{bipy}] \cdot 3.5\text{H}_2\text{O}$ (30)	35330	32150, 30210	25780
$[\text{ZnL}^2\text{phen}] \cdot \text{H}_2\text{O}$ (31)	35560	31850, 30380	25380
H_2L^4	36490	30210	----
$[\text{Zn}(\text{HL}^4)_2]$ (32)	35460	31850, 30210	25380
$[\text{ZnL}^4\text{py}] \cdot 3\text{H}_2\text{O}$ (33)	36400	31850, 30490	25840
$[\text{ZnL}^4\gamma\text{-pic}]$ (34)	36100	31850, 30210	25780
$[\text{ZnL}^4\text{bipy}] \cdot 5\text{H}_2\text{O}$ (35)	36370	32680, 30030	25130

 $[Zn(HL^2)_2]$ (26) $[ZnL^2py]$ (27) $[ZnL^2\alpha\text{-pic}] \cdot 4H_2O$ (28) $[ZnL^2\gamma\text{-pic}]$ (29) $[ZnL^2phen] \cdot H_2O$ (31) $[ZnL^4py] \cdot 3H_2O$ (33)**Figure 6.7.** Electronic spectra of the compounds 26, 27, 28, 29, 31 and 33

6.3.4. ^1H NMR spectra

Proton Magnetic Resonance spectroscopy is a helpful tool for the identification of organic compounds in conjugation with other spectroscopic informations. ^1H NMR spectra of H_2L^2 and H_2L^4 show sharp singlets, which integrates as one hydrogen at $\delta \sim 10.8$ ppm (s, 1H) is assigned to the proton attached to the oxygen atom. Absence of any coupling interactions by ^2NH due to the unavailability of protons on neighbouring atoms render singlet peak for the imine proton at $\delta \sim 8.7$ ppm (s, 1H). A sharp singlet at $\delta \sim 8$ ppm (s, 1H) corresponds to $^7\text{CH}=\text{proton}$. Aromatic protons ^3CH , ^4CH , ^5CH and ^6CH appear in the range of 6.67–7.26 ppm. Aliphatic protons were observed as three signals at ~ 3.36 (s, 4H), 1.66 (s, 4H) and 1.42 ppm (s, 4H) assigned to positions a, b and c respectively. ^1H NMR assignments are in agreement with values already reported [24, 28, 29, 36].

^1H NMR assignments for the ligands and its Zn(II) complexes are included in Table 6.7. The signals for phenolic OH (except in **26** and **32**) and ^2NH are absent from the spectra of complexes as expected because of their loss on complex formation, which is an evidence for the coordination of the ligand as doubly deprotonated anion. This confirms the coordination through phenolic oxygen and also *via* thiolate sulfur atom in those complexes. The $^7\text{CH}=\text{proton}$ also shifted to downfield region. This may be due to the loss of electron density *via* coordination through azomethine nitrogen atom. Complexes **26** and **32** show peaks at $\delta \sim 13$ ppm due to the presence of uncoordinated hydroxyl group. The more downfield shift of OH protons compared to uncomplexed thiosemicarbazone is due to overall loss of electron density and intra and intermolecular hydrogen bonding interactions. In compound **26**, the downfield shift of OH proton is more compared to **32**, suggesting greater hydrogen bonding in compound **26**. This is confirmed from crystal structure of **26**. There is downfield shifting of the signals for the ring

protons in the spectra of complexes compared to the uncomplexed thiosemicarbazones. This is due to the loss of electron density *via* coordination of the ligand to the metal centre. More downfield shift for the ring protons for compounds **26** and **32** may be due to the intra and intermolecular hydrogen bonding interactions. Protons due to heterocyclic bases appear in the region of 7.15–8.50ppm. The downfield shift of proton peaks corresponding to heterocyclic bases are the result of the withdrawal of electron density from the thiosemicarbazone moiety and the heterocyclic bases, due to coordination with the metal atom [37]. Compounds **28**, **29** and **34** show sharp peaks at $\delta \sim 2.1$ ppm attributable for the $-\text{CH}_3$ protons present in the molecule. A small downfield shift occurs to aliphatic protons in complexes due to the overall loss of electron density. ^1H NMR spectra of compounds **26**, **27** and **31** are given in Figures 6.8-6.10.

Table 6.7. ^1H NMR (CDCl_3) assignments of the ligands and its Zn(II) complexes (δ in ppm)

Compound	OH	Aromatic protons	$^7\text{CH}=\text{}$	Heterocyclic base protons	$^a\text{CH}_2$	$^b\text{CH}_2$	$^c\text{CH}_2$
H_2L^2	11.3	6.67 - 7.12	7.99	----	3.63	1.66	1.42
$[\text{Zn}(\text{HL}^2)_2]$ (26)	13.36	6.82 - 7.34	8.20	----	3.89	1.88	1.59
$[\text{ZnL}^2\text{py}]$ (27)	----	6.68 - 7.27	8.41	7.31 - 8.62	3.83	1.78	1.54
$[\text{ZnL}^2\alpha\text{-pic}] \cdot 4\text{H}_2\text{O}$ (28)	----	6.74 - 7.17	8.42	7.20 - 8.20	3.82	1.80	1.55
$[\text{ZnL}^2\gamma\text{-pic}]$ (29)	----	6.81 - 7.15	8.52	7.17 - 8.50	3.75	1.75	1.53
$[\text{ZnL}^2\text{bipy}] \cdot 3.5\text{H}_2\text{O}$ (30)	----	6.82 - 7.25	8.44	7.35 - 8.12	3.85	1.88	1.62
$[\text{ZnL}^2\text{phen}] \cdot \text{H}_2\text{O}$ (31)	----	6.83 - 7.22	8.86	7.65 - 8.49	3.65	1.71	1.49
H_2L^4	10.3	6.87 - 7.26	8.00	----	3.65	1.71	1.49
$[\text{Zn}(\text{HL}^4)_2]$ (32)	12.85	6.92 - 7.46	8.45	----	3.62	1.75	1.53
$[\text{ZnL}^4\text{py}] \cdot 3\text{H}_2\text{O}$ (33)	----	6.96 - 7.36	8.49	7.62 - 8.38	3.55	1.76	1.48
$[\text{ZnL}^4\gamma\text{-pic}]$ (34)	----	6.91 - 7.27	8.48	7.28 - 8.41	3.66	1.87	1.59
$[\text{ZnL}^4\text{bipy}] \cdot 5\text{H}_2\text{O}$ (35)	----	6.89 - 7.38	8.45	7.40 - 8.16	3.67	1.86	1.53

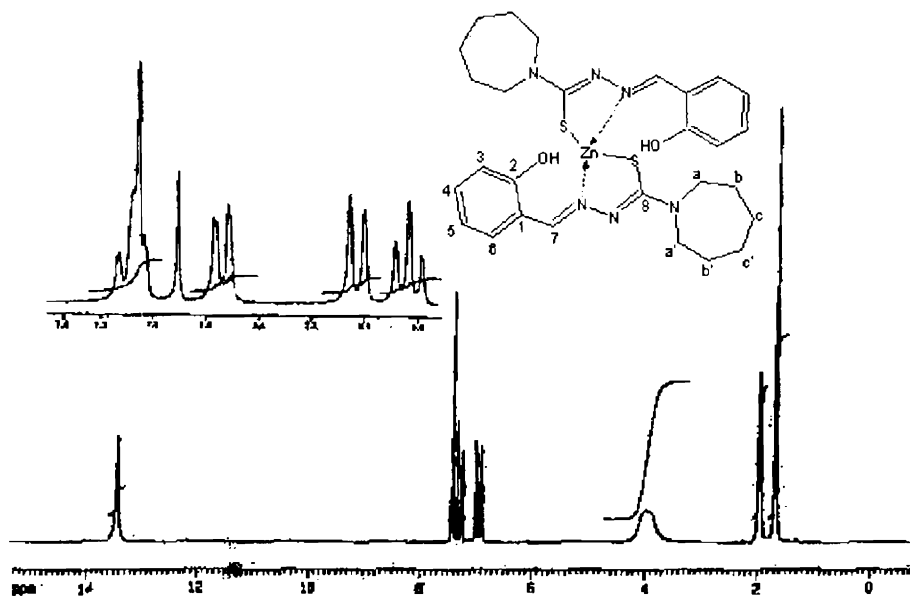


Figure 6.8. 1H NMR spectrum of $[Zn(HL^2)_2]$ (26)

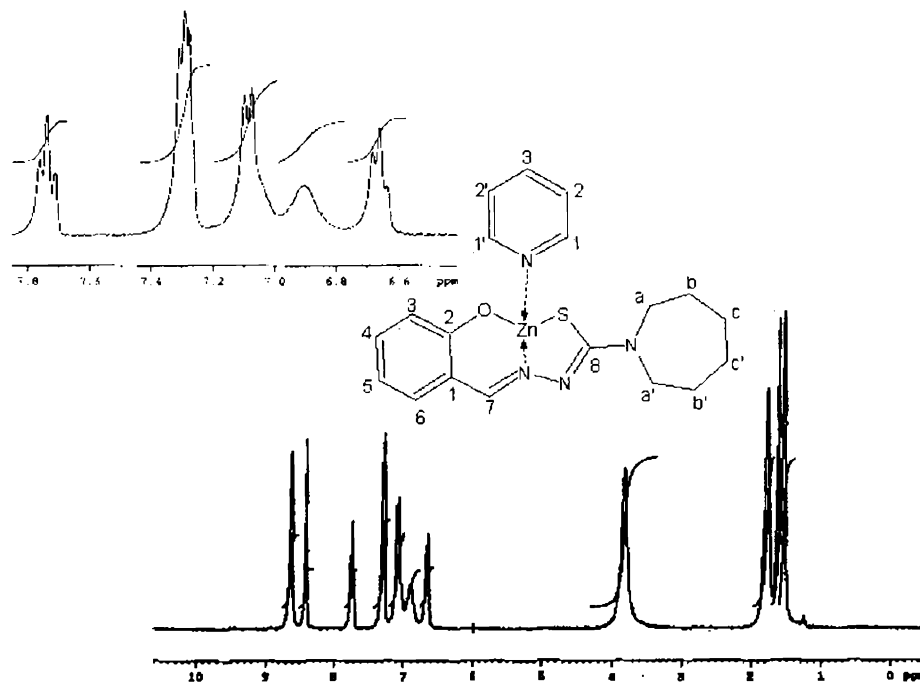


Figure 6.9. 1H NMR spectrum of $[ZnL^2py]$ (27)

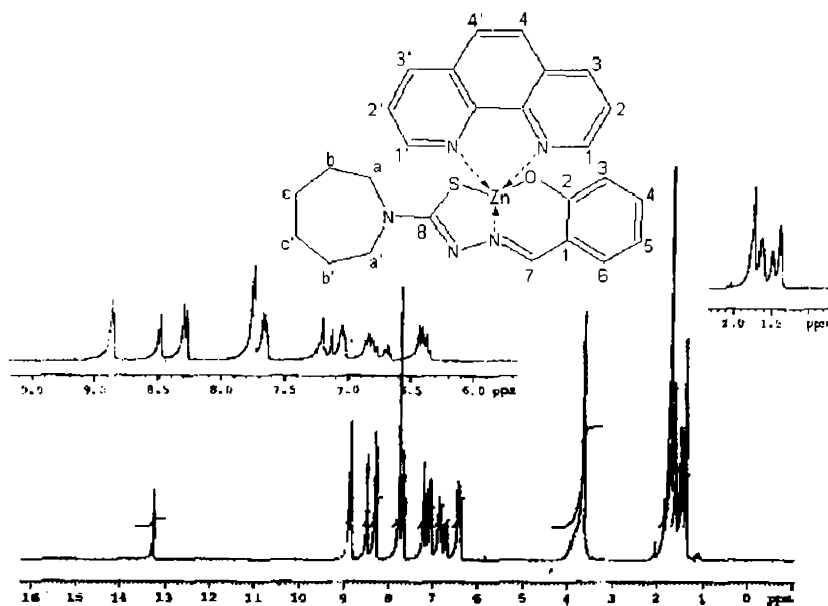


Figure 6.10. ^1H NMR spectrum of $[\text{ZnL}^2\text{phen}]\cdot\text{H}_2\text{O}$ (31)

Based on the elemental analyses and spectral studies following tentative structures were assigned for the complexes (Figure 6.11).

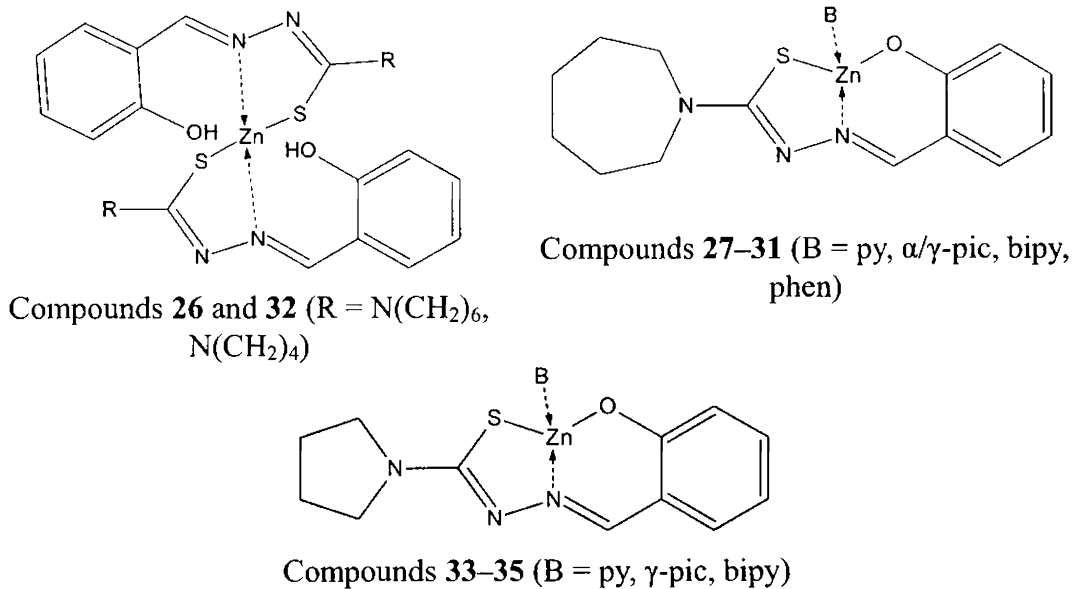


Figure 6.11. Tentative structures of the compounds

References

1. M.B. Ferrari, G.G. Fava, C. Pelizzi, P. Tarasconi, *J. Chem. Soc., Dalton Trans.* 2153 (1992).
2. R.H. Prince, *Adv. Inorg. Radiochem.* 22 (1979) 349.
3. L.S. Sarma, J.R. Kumar, K.J. Reddy, T. Thriveni, A.V. Reddy, *J. Braz. Chem. Soc.* 17 (2006) 463.
4. P. Souza, A.I. Matesanz, V. Fernandez, *J. Chem. Soc., Dalton Trans.* (1996) 3011.
5. A.G. Quoroga, J.M. Perez, I. Lopez-Solera, J.R. Masaguer, A. Luque, P. Roman, A. Edwards, C. Alonso, C. Navarro-Ranninger, *J. Med. Chem.* 41 (1998) 1399.
6. D.H. Petering, H.G. Petering, in: A.C. Sartorelli, D.G. Johns (Eds.), *Handbook of experimental Pharmacology*, Springer, Berlin (1975) 841.
7. D.H. Petering, W.E. Antholine, L.A. Saryan, in: R.M. Ottenbrite, G.B. Butler (Eds.), *Anticancer and Interferon Agents, Synthesis and Properties*, Marcel Dekker, New York, (1984) 203.
8. P. Souza, L. Sanz, V. Fernandez, A. Arquero, E. Gutierrez, A. Monge, Z. *Naturforsch., Teil B* 46 (1991) 767.
9. C. Dowling, G. Perkin, *Polyhedron* 15 (1996) 2463.
10. Nonius (1997) MACH3 software, B.V. Nonius, Delft, The Netherlands.
11. G.M. Sheldrick, *Acta Crystallogr.* 46A (1990) 467.
12. G.M. Sheldrick, *SHELXL-97 and SHELXS-97 Program for the solution of Crystal Structures*, University of Göttingen, Germany, 1997.
13. K. Brandenburg, *DIAMOND version 3.1d*, 2006, Crystal Impact GbR, Bonn, Germany.
14. A.L. Spek, *J. Appl. Cryst.* 36 (2003) 7.

15. A. Lyubchova, N. Jouini, A. Massat, J.P. Doucet, K. Boubekeur, A. Cosse-Barbi, Z. Kristallogr. 216 (2001) 556; H. Ali, N.A. Khamis, W.J. Basirun, B.M. Yamin, Acta Crystallogr. E60 (2004) m873; H. Ali, N.A. Khamis, B.M. Yamin, Acta Crystallogr. E60 (2004) m1311.
16. A. Castineiras, D.X. West, J. Mol. Struct. 604 (2002) 113.
17. E. Labisbal, A. Sousa-Pedrares, A. Castineiras, J.K. Swearingen, D.X. West, Polyhedron 21 (2002) 1553.
18. J.S. Casas, M.V. Castano, M.S. Garcia-Tasende, A. Sanchez, J. Sordo, A. Touceda, Polyhedron 24 (2005) 3057.
19. I. Garcia, E. Bermejo, A.K. El Sawaf, A. Castineiras, D.X. West, Polyhedron 21 (2002) 729.
20. E. Bermejo, A. Castineiras, L.M Fostiak, I.G. Santos, J.K. Swearingen, D.X. West, Polyhedron 23 (2004) 2303.
21. R.P. John, A. Sreekanth, V. Rajakannan, T.A. Ajith, M.R.P. Kurup, Polyhedron 23 (2004) 2549.
22. E. Bermejo, A. Castineiras, I. Garcia-Santos, D.X. West, Z. Anorg. Allg. Chem. 630 (2004) 1097.
23. K. Nakamoto, Infrared and Raman Spectra of Inorganic and Coordination compounds, 5th ed., Wiley, New York, 1997.
24. P. Bindu, M.R.P. Kurup, T.R. Satyakeerthy, Polyhedron 18 (1999) 321.
25. D.X. West, A.C. Whyte, F.D. Sharif, H. Gabremedhin, A.E. Liberta, Trans. Met. Chem. 18 (1993) 238.
26. M.J.M. Campbell, Coord. Chem. Rev. 15 (1975) 279.
27. G.C. Percy, D.A. Thornton, J. Inorg. Nuclear. Chem. 34 (1972) 3351.
28. R.P. John, A. Sreekanth, M.R.P. Kurup, A. Usman, I.A. Razak, H.- K. Fun, Spectrochim. Acta A 59 (2003) 1349.
29. M. Nazimuddin, M.A. Ali, F.E. Smith, Polyhedron 10 (1991) 327.

30. E. Bermejo, R. Carballo, A. Castineiras, R. Dominguez, A. E. Liberta, C. Maichle-Mossmer, D. X. West, *Z. Naturforsch., B: Chem. Sci.* 54 (1999) 777.
31. A. Castineiras, E. Bermejo, D. X. West, L.J. Ackerman, J. V. Martinez, S. H. Ortega, *Polyhedron* 18 (1999) 1469.
32. A.D. Naik, V.K. Revankar, *Proc. Indian Acad. Sci (Chem. Sci.)* 113 (2001) 285.
33. V. Philip, V. Suni, M.R.P. Kurup, *Polyhedron* 25 (2006) 1931.
34. I.-X. Li, H.A. Tang, Yi-Zhi Li, M. Wang, L.-F. Wang, C.-G. Xia, *J. Inorg. Biochem.* 78 (2000) 167.
35. A. Sreekanth, S. Sivakumar, M.R.P. Kurup, *J. Mol. Struct.* 655 (2003) 47.
36. D.X. West, Y. Yang, T.L. Klein, K.I. Goldberg, A.E. Liberta, J.V. Martinez, R.A. Toscano, *Polyhedron* 14 (1995) 1681.
37. S. Jayasree, K.K. Aravindakshan, *Trans. Met. Chem.* 18 (1993) 85.

Synthesis and spectral studies of Cd(II) complexes of N(4)-ring incorporated thiosemicarbazones

7.1. Introduction

Cadmium (Latin *cadmia*, Greek *kadmeia* meaning "calamine") was discovered in Germany in 1817 by Friedrich Strohmeyer. Cadmium-containing ores are rare and when found they occur in small quantities. Greenockite (CdS), the only cadmium mineral of importance, is nearly always associated with sphalerite (ZnS).

Cadmium element has a $d^{10} s^2$ electronic arrangement and they typically form M^{2+} ions. However, many of their compounds are appreciably covalent. The most stable oxidation state of Cd is +2. They have tetrahedral, square pyramidal, trigonal bipyramidal and octahedral geometries.

In a tridentate ONS donor ligands, the coordination takes place through the azomethine nitrogen, thione/thiol sulphur and phenolic oxygen. The ability to coordinate *via* sulphur is enhanced for cadmium (compared to zinc), whose toxic properties could be related to strong cadmium(II)-sulfur bond [1]. Moreover, chelating sulphur donors are actually under study as antidotes in cadmium(II) poisoning [2, 3]. The enhancement of antitumor activity in presence of Cd(II) [4] ions has been reported.

IIB group metal complexes of thiosemicarbazones are pale in color and quite thermally stable [5]. It has also been reported that some cadmium complexes of thiosemicarbazides and thiosemicarbazones can show quite large SHG efficiency

[6]. It could be possible that the design and synthesis of IIB metal complexes derived from thiosemicarbazones might be possible way to obtain the potential non linear optical materials.

This chapter describes the synthesis and characterization of six Cd(II) complexes of N(4)-ring incorporated thiosemicarbazones using infrared, electronic and ^1H NMR studies.

7.2. Experimental

7.2.1. Materials

The syntheses of ligands are discussed in Chapter 2. $\text{Cd}(\text{OAc})_2 \cdot 2\text{H}_2\text{O}$ (S.D. Fine chemicals), pyridine, α -picoline, 2,2'-bipyridine (bipy) (Central drug house) were used. The reagents used were of Analar grade and used without further purification.

7.2.2. Synthesis of the complexes

[CdL¹]₂ (36): This complex was synthesized by refluxing an ethanolic solution of HL¹ (2 mmol, 0.522 g) with an ethanolic solution of $\text{Cd}(\text{OAc})_2 \cdot 2\text{H}_2\text{O}$ (1 mmol, 0.266 g) for 2-3 h. The yellow colored complex formed was filtered, washed with ethanol and finally with ether and dried over P_4O_{10} *in vacuo*.

[CdL²py]·3H₂O (37): To a hot ethanolic solution of the ligand H₂L² (1 mmol, 0.277 g), added a hot ethanolic solution of $\text{Cd}(\text{OAc})_2 \cdot 2\text{H}_2\text{O}$ (1 mmol, 0.266 g) with constant stirring. This was followed by the addition of slight excess of the base pyridine (2 mmol, 0.158 g). The above yellow solution was refluxed for about 2-3 h. The complex formed was filtered, washed with ethanol and ether and dried *in vacuo* over P_4O_{10} .

[CdL² α -pic]·4H₂O (38): $\text{Cd}(\text{OAc})_2 \cdot 2\text{H}_2\text{O}$ (1 mmol, 0.266 g) dissolved in ethanol was added to a solution of H₂L² (1 mmol, 0.277 g) in hot ethanol and slight excess

of heterocyclic base α -picoline (3 mmol, 0.279 g) with constant stirring. The solution was then refluxed for 2 h. The yellow complex formed was filtered, washed with ethanol and finally with ether and dried over P_4O_{10} *in vacuo*.

[CdL²bipy]-2H₂O (39): The H₂L² (1 mmol, 0.277 g) was dissolved in ethanol, to which was added an ethanolic solution of Cd(OAc)₂·2H₂O (1 mmol, 0.266 g) with constant stirring. This was followed by the addition of the base 2,2'-bipyridine (1 mmol, 0.156 g) in the solid form. The stirring was continued for about an hour when yellow compound began to separate. This was filtered, washed with ethanol and ether and dried *in vacuo* over P_4O_{10} .

[CdL³]₂ (40): Ethanolic solutions of the ligand HL³ (2 mmol, 0.582 g) and Cd(OAc)₂·2H₂O (1 mmol, 0.266 g) in 2:1 ratio was refluxed for 2 h. The yellow complex formed was filtered, washed with ethanol and finally with ether and dried over P_4O_{10} *in vacuo*.

7.2.3. Physical measurements

Details regarding physical measurements are presented in Chapter 3.

7.3. Results and discussion

The analytical data of all the complexes are listed in Table 7.1. The complexes **36** and **40** have the general formula ML₂. The complexes **37**, **38** and **39** were assigned the general formula MLB, where B are heterocyclic bases, pyridine, α -picoline and 2,2'-bipyridine. The complexes **37**, **38** and **39** contain uncoordinated water molecules also. All the six complexes are found to be diamagnetic as expected.

Table 7.1. Analytical data

Compound	color	Anal: Found (Calcd.) %		
		C	H	N
[CdL ₂] ¹ (36)	yellow	53.10(53.11)	5.97(5.73)	13.24(13.27)
[CdL ₂ py]·3H ₂ O (37)	yellow	43.21(43.81)	5.61(5.42)	10.80(10.76)
[CdL ² α -pic]·4H ₂ O (38)	yellow	43.22(43.44)	5.24(5.83)	10.78(10.13)
[CdL ² bipy]·2H ₂ O (39)	yellow	49.74(49.70)	4.72(5.04)	12.34(12.07)
[CdL ₂] ³ (40)	yellow	51.79(51.98)	5.66(5.82)	12.03(12.12)

7.3.1. IR spectra

The IR spectral bands most useful for the determination of the mode of coordination are given in Table 7.2. None of these compounds have any bands between 2500–2800 cm⁻¹ suggesting that the ligands are not in the thiol form either before or after coordination. The bands corresponding to $\nu(\text{N-H})$ appear at ~ 3100 cm⁻¹ for the ligands, disappeared in the spectra of all the complexes suggesting the deprotonation of the thiosemicarbazone ligand during complexation. The strong bands observed at ~ 1610 cm⁻¹ due to $\nu(\text{C}=\text{N}_{\text{azo}})$ of the thiosemicarbazone moiety shifts to ~ 1590 cm⁻¹ upon complexation [7]. This lowering of frequencies confirms the coordination *via* azomethine nitrogen. Coordination of azomethine nitrogen is also consistent with the presence of a new band in the range 420–440 cm⁻¹, assignable to $\nu(\text{Cd-N})$ for these complexes [8]. A small shift in the absorption bands due to the $\nu(\text{N-N})$ stretching vibrations from ~ 1055 cm⁻¹ to higher region is due to the increase in double bond character offsetting the loss of electron density *via* donation to the metal and is a confirmation of the coordination of the ligand through the azomethine nitrogen atom [9]. Coordination *via* thiolate sulfur is indicated by a decrease in the frequency of the thioamide band, which is partly $\nu(\text{C}=\text{S})$, and found at ~ 1300 and 840 cm⁻¹ in the

uncomplexed thiosemicarbazone by 30–110 cm^{-1} in the spectra of complexes [10, 11]. This confirms the change of the carbon–sulphur bond order from two in the ligands to one in the complexes. This decrease in stretching frequency of thiolate sulfur in the complexes is indicated by Campbell [12]. Another strong band found in the region of 1530–1555 cm^{-1} is due to the newly formed $\nu(\text{C}=\text{N})$ band in the spectra for these complexes. The bands at 320–350 cm^{-1} assignable to $\nu(\text{Cd-S})$ in the complexes are consistent with sulfur coordination [8, 13]. The new peaks observed in the range 480–490 cm^{-1} are due to the $\nu(\text{Cd-O})$ band [14–17]. In all the complexes, coordination *via* phenolic oxygen is indicated by a decrease in frequency of the $\nu(\text{CO})$, and found at 1271 cm^{-1} in the uncomplexed thiosemicarbazone by 60–85 cm^{-1} in the spectra of complexes. The complexes **37**, **38** and **39** contain broad peak at $\sim 3400 \text{ cm}^{-1}$ corresponding to uncoordinated water molecules. Representative spectra of **36**, **37** and **38** are given in Figures 7.1-7.3

Table 7.2. Selected IR bands (cm^{-1}) with tentative assignments of the ligands and its Cd(II) complexes

Compound	$\nu(\text{C}=\text{N}_{\text{azo}})$	$\nu(\text{C}=\text{N})$	$\nu(\text{C}=\text{N})$	$\nu(\text{N}-\text{N})$	$\nu\delta[(\text{C}=\text{S})/(\text{C}-\text{S})]$	$\nu(\text{C}-\text{O})$	$\nu(\text{Cd}-\text{N})$	$\nu(\text{Cd}-\text{S})$	Bands due to heterocyclic bases
HL^1	1624	----	1066	1334, 837	----	----	----	----	
$[\text{CdL}^1_2]$ (36)	1594	1530	1096	1290, 763	----	432	332	----	
H_2L^2	1612	----	1037	1324, 861	1271	----	----	----	
$[\text{CdL}^2\text{-py}] \cdot 3\text{H}_2\text{O}$ (37)	1592	1542	1068	1277, 755	1196	435	325	1427, 616	
$[\text{CdL}^2\text{-}\alpha\text{-pic}] \cdot 4\text{H}_2\text{O}$ (38)	1597	1553	1069	1272, 760	1190	440	345	1432, 611	
$[\text{CdL}^2\text{-bipy}] \cdot 2\text{H}_2\text{O}$ (39)	1592	1546	1072	1279, 766	1192	436	336	1430, 663	
$[\text{HL}^3]$	1607	----	1064	1312, 821	----	----	----	----	
$[\text{CdL}^3_2]$ (40)	1580	1555	1078	1280, 765	----	426	348	----	

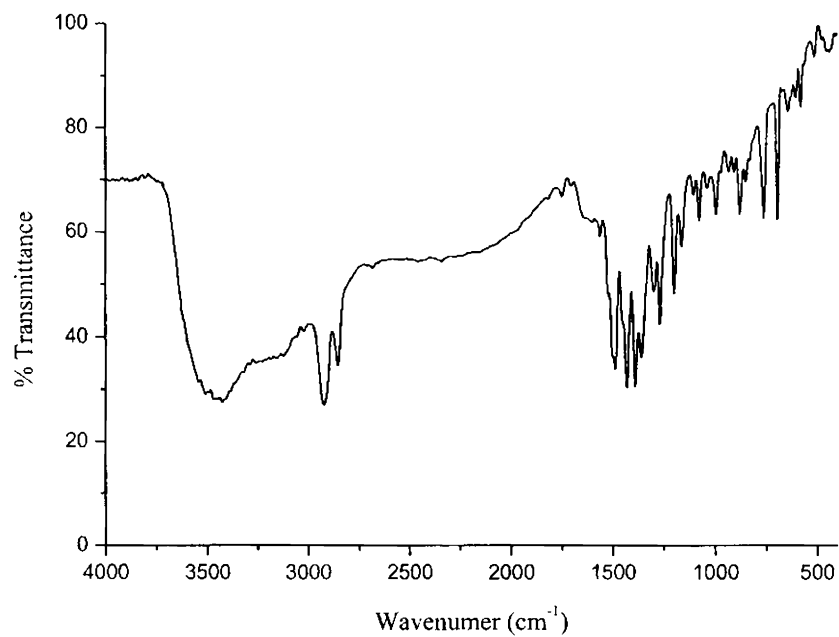


Figure 7.1. IR spectrum of compound [CdL²] (36)

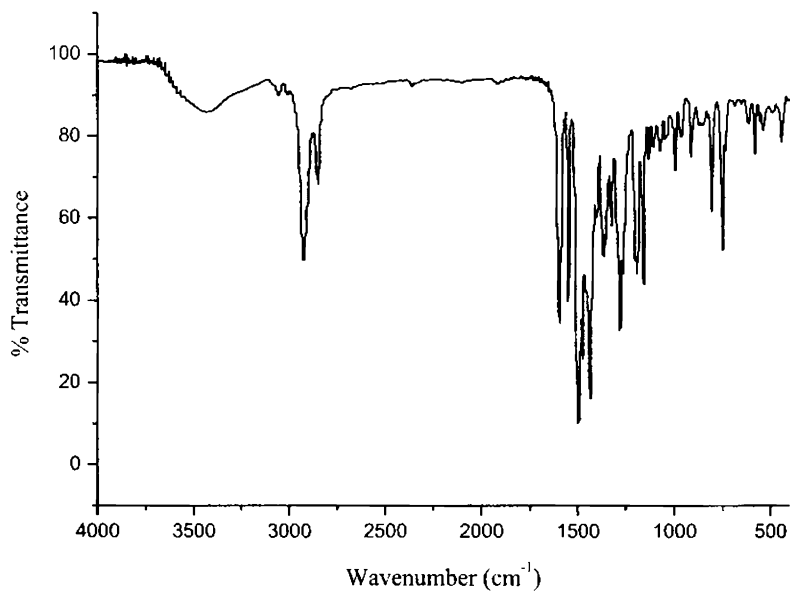


Figure 7.2. IR spectrum of compound [CdL²py]·3H₂O (37)

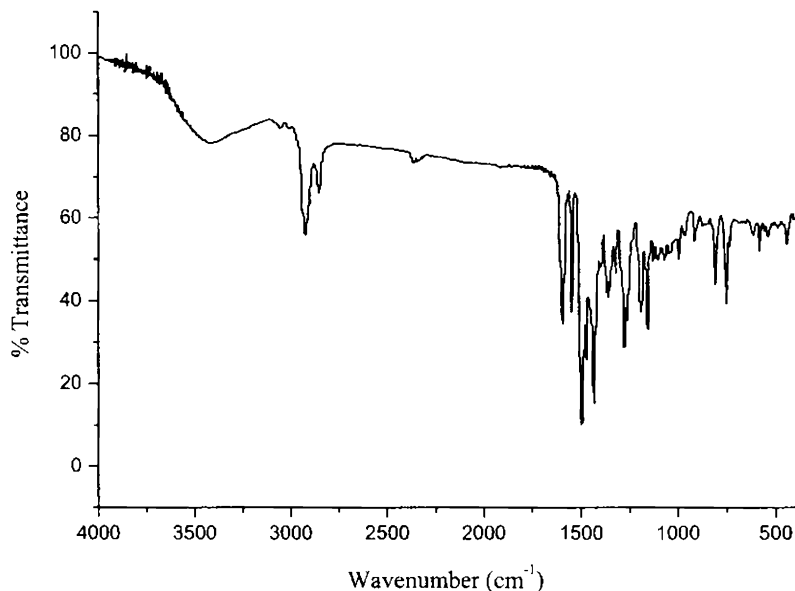


Figure 7.3. IR spectrum of compound $[\text{CdL}^2\alpha\text{-pic}]\cdot 4\text{H}_2\text{O}$ (38)

7.3.2. Electronic spectra

The electronic absorption bands of the Cd(II) complexes, recorded in DMF solution, are given in Table 7.3 and representative spectra are in Figure 7.4. The electronic spectra of the ligands recorded in DMF show bands at ~ 35000 and 29600 cm^{-1} assignable to $\pi\rightarrow\pi^*$ transitions of the phenyl ring [18-20] and $n\rightarrow\pi^*$ transitions of the azomethine and thioamide functions respectively [21, 22]. The energy of these bands is slightly shifted upon complexation. The shift of the $\pi\rightarrow\pi^*$ bands to longer wavelength region in complexes is the result of the C=S bond being weakened and the conjugation system enhanced on complexation [23, 24]. The $n\rightarrow\pi^*$ bands in the complexes have shown a blue shift due to donation of lone pair of electrons to the metal and hence the coordination of azomethine with a reduction of intensity.

A moderately intense broad band for the complexes in the region 25000–27000 cm^{-1} is assigned to Cd(II)→S transitions. MLCT maxima of the phenolate complexes show line broadening with a tail running into the visible part of the spectrum. This may result from Cd(II) to a phenolate MLCT band being superimposed on the low energy side of Cd(II)→S transitions. No appreciable absorptions occurred above 500 nm in DMF solution indicating the absence of $d-d$ bands which is in accordance with the d^{10} configuration of the Cd(II) ion.

Table 7.3. Electronic spectral assignments (cm^{-1}) of the ligands and its Cd(II) complexes

Compound	$\pi - \pi^*$	$n - \pi^*$	MLCT
HL ¹	36900	28250	----
[CdL ¹ ₂] (36)	36100	30960	25580
H ₂ L ²	36110	29500	----
[CdL ² py]·3H ₂ O (37)	35970	30400, 32150	27100, 24870
[CdL ² α -pic]·4H ₂ O (38)	35840	29940, 31760	25780
[CdL ² bipy]·2H ₂ O (39)	35340	29500, 30960	25190
[HL ³]	35340	31150	----
[CdL ³ ₂] (40)	35270	30120	26110

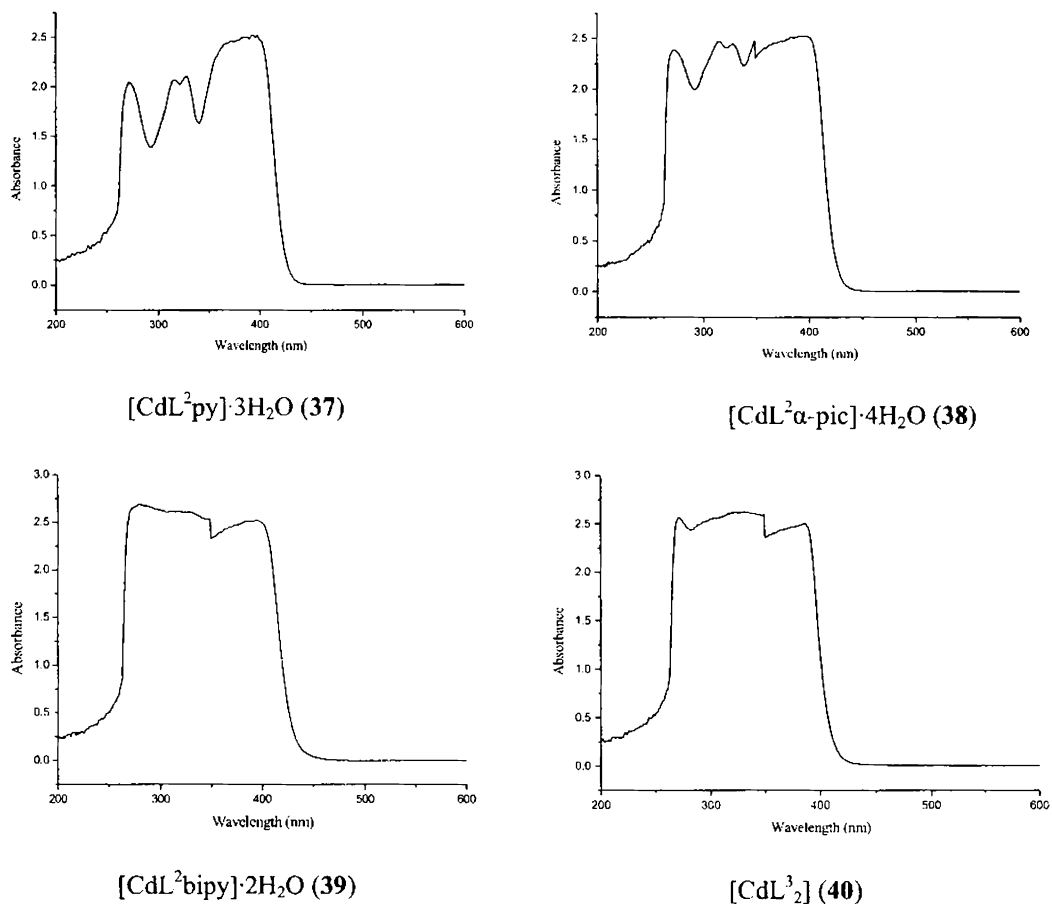


Figure 7.4. Electronic spectra of the compounds 37, 38, 39 and 40

7.3.3. ^1H NMR spectra

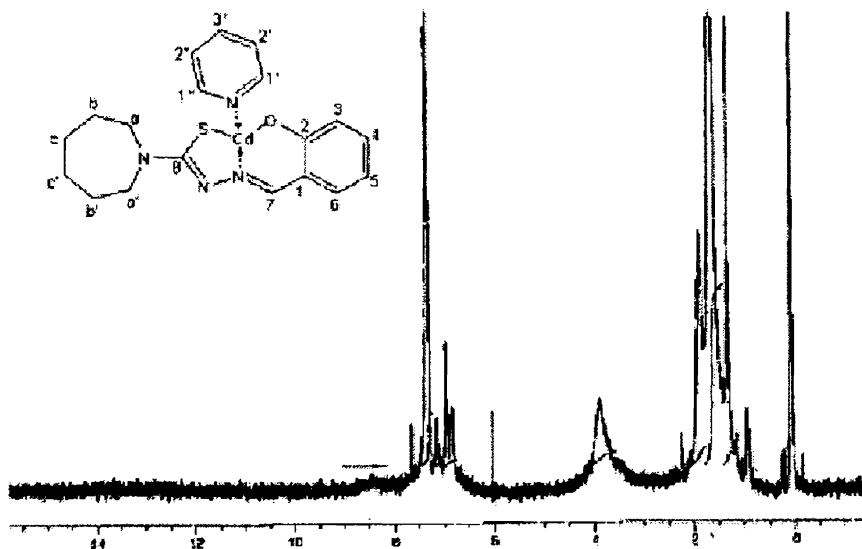
^1H NMR spectrum of H_2L^2 shows a sharp singlet, which integrates as one hydrogen at $\delta = 11.3$ ppm (s, 1H) is assigned to the proton attached to the oxygen atom. Absence of any coupling interactions by ^2NH due to the unavailability of protons on neighboring atoms render singlet peak for the imine proton at $\delta \sim 8.8$ ppm (s, 1H). A sharp singlet at $\delta \sim 8$ ppm (s, 1H) corresponds to $^7\text{CH}=\text{C}$ proton. Aromatic protons appear in the range of 6.67–7.85 ppm. Aliphatic protons were

observed as three signals at ~ 3.80 (s, 4H), 1.70 (s, 4H) and 1.50 ppm (s, 4H) assigned to positions a, b and c respectively.

^1H NMR assignments for the Cd(II) complexes are included in Table 7.4. The signals for phenolic OH (except in **36** and **40**) and ^2NH are absent from the spectra of complexes as expected because of their loss on complex formation show that the anionic form of the ligands are present. This confirms the coordination through phenolic oxygen and also *via* thiolate sulfur atom in these complexes. The downfield shift of $^7\text{CH}=\text{}$ protons in the complexes may be due to the loss of electron density *via* coordination of azomethine nitrogen to the metal atom. There is downfield shifting of the signals for the ring protons in the spectra of complexes compared to the uncomplexed thiosemicarbazone. This may be due to the loss of electron density *via* coordination of the ligand to metal centre. The compound **38** shows a sharp peak at $\delta=2.2$ ppm attributable for the $-\text{CH}_3$ protons present in the molecule. The compound **40** shows a sharp peak at $\delta=4$ ppm attributable for the $-\text{OCH}_3$ protons present in the molecule. A small downfield shift occurs to aliphatic protons in complexes due to the overall loss of electron density. ^1H NMR spectra of compounds **38** and **40** are given in Figures 7.5 and 7.6.

Table 7.4. ^1H NMR (CDCl_3) assignments of the ligands and its Cd(II) complexes (δ in ppm)

Compound	OH	Aromatic protons	Heterocyclic base protons	$^7\text{CH}=\text{}$	$^a\text{CH}_2$	$^b\text{CH}_2$	$^c\text{CH}_2$
HL^1	----	7.26 - 7.65	----	7.96	4.02	1.94	1.64
$[\text{CdL}^1_2] \text{ (36)}$	----	7.28 - 7.85	----	8.25	4.06	1.98	1.78
H_2L^2	11.3	6.67 - 7.12	----	7.99	3.63	1.66	1.42
$[\text{CdL}^2\text{py}] \cdot 3\text{H}_2\text{O} \text{ (37)}$	----	6.69 - 7.20	7.60 - 7.74	8.38	3.84	1.82	1.57
$[\text{CdL}^2\alpha\text{-pic}] \cdot 4\text{H}_2\text{O} \text{ (38)}$	----	6.68 - 7.17	7.27 - 7.54	8.32	3.76	1.74	1.52
$[\text{CdL}^2\text{bipy}] \cdot 2\text{H}_2\text{O} \text{ (39)}$	----	6.80 - 7.25	7.33 - 7.60	8.44	3.86	1.74	1.61
$[\text{HL}^3]$	----	6.89 - 7.60	----	8.12	3.83	1.93	1.62
$[\text{CdL}^3_2] \text{ (40)}$	----	6.92 - 7.72	----	8.25	3.86	1.98	1.66

**Figure 7.5.** ^1H NMR spectrum of compound $[\text{CdL}^2\text{py}] \cdot 3\text{H}_2\text{O} \text{ (37)}$

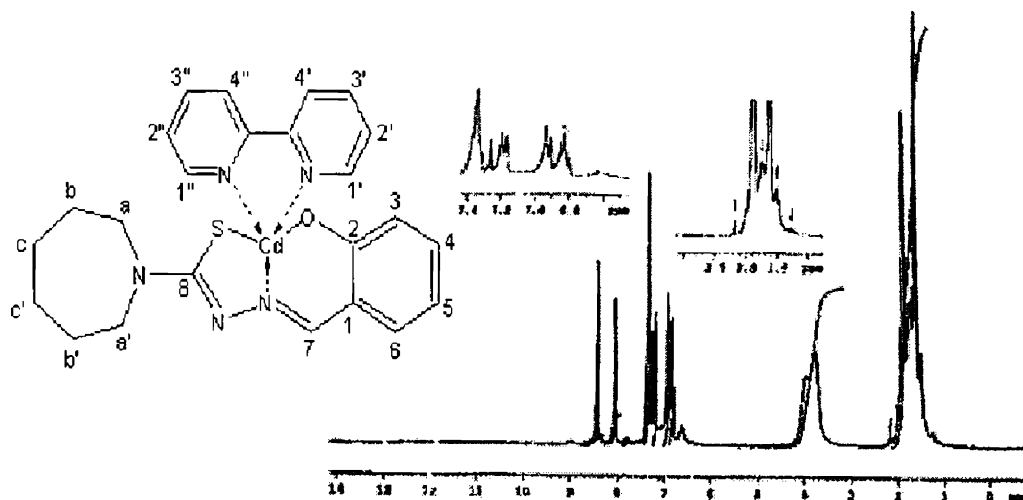


Figure 7.6. ^1H NMR spectrum of compound $[\text{CdL}^2\text{bipy}]\cdot 2\text{H}_2\text{O}$ (39)

Based on the elemental analyses and spectral investigations, following tentative structures were assigned for the complexes (Figure 7.7).

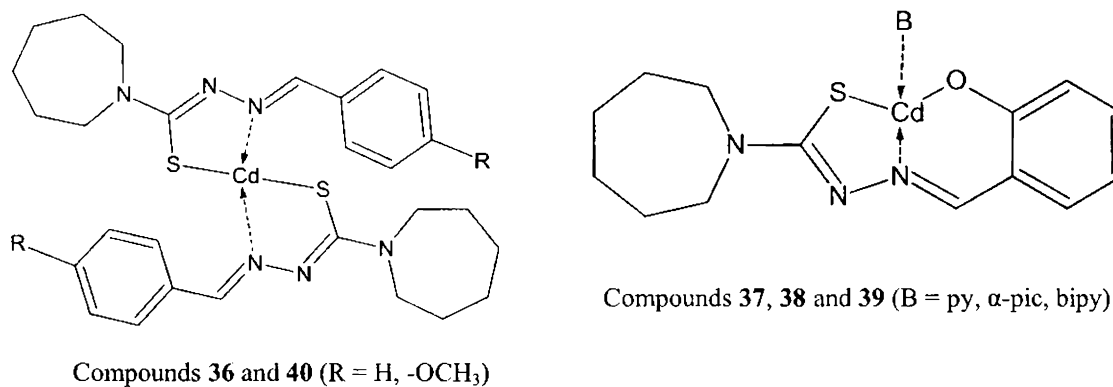


Figure 7.7. Tentative structures of the compounds 36-40

References

1. G. Fraglia, R. Graziani, Z. Guo, U. Casellato, S. Sitran, *Inorg. Chim. Acta* 192 (1992) 17.
2. J.S. Casas, A. Sanchez, J. Bravo, S. Garcia-Fontan, E.E Castellano, M.M. Jones, *Inorg. Chim. Acta* 158 (1989) 119.
3. M.A. Romero-Molina, M.D. Gutierrez-Valere, R. Lopez-Garzon, J.M. Salas-Peregrin, M.I. Arriortua, F.J. Zuniga, *Inorg. Chim. Acta* 136 (1987) 87.
4. G. Atassi, P. Dumont, J.C. Harteel, *Eur. J. Cancer* 15 (1979) 451.
5. A.E. Liberta, D.X. West, *Biometals* 5 (1992) 121.
6. C.Y. Duan, Y.P. Tian, C.Y. Zhao, X.Z. You, Thomas C.W. Mak, *Polyhedron* 16 (1997) 2857.
7. R.P. John, A. Sreekanth, V. Rajakannan, T.A. Ajith, M.R.P. Kurup, *Polyhedron* 23 (2004) 2549.
8. E. Bermejo, A. Castineiras, I. Garcia-Santos, D.X. West, *Z. Anorg. Allg. Chem.* 630 (2004) 1096..
9. P. Bindu, M.R.P. Kurup, T.R. Satyakeerthy, *Polyhedron* 18 (1999) 321.
10. K. Nakamoto, *Infrared and Raman Spectra of Inorganic and Coordination compounds*, 5th ed., Wiley, New York, 1997.
11. K. Balakrishnan, K.K. Aravindakshan, *J. Ind. Chem. Soc.* 68 (1991) 187.
12. M.J.M. Campbell, *Coord. Chem. Rev.* 15 (1975) 279.
13. N.T. Akinchan, P.M. Drozdowski, R. Akinchan, *Polish J. Chem.* 76 (2002) 1381.
14. I. Ghassan, M.A. Khan, E. Chebli, G.M. Bouet, *Trans. Met. Chem.* 24 (1999) 294.

15. G. Ibrahim, M.A. Khan, P. Richomme, O. Benali-Baitich, G. Bouet, *Polyhedron* 16 (1997) 3455.
16. M.P. Swami, D. Gupta, M. Mohan, A.K. Srivastava, *Prog. Nat. Acad. Sci. India A* 50 (III) (1980) 176.
17. E.M. Jouad, M. Allain, M.A. Khan, G.M. Bouet, *Polyhedron* 24 (2005) 327.
18. R.P. John, A. Sreekanth, M.R.P. Kurup, A. Usman, I.A. Razak, H.-K. Fun, *Spectrochim. Acta A* 59 (2003) 1349.
19. M. Nazimuddin, M.A. Ali, F.E. Smith, *Polyhedron* 10 (1991) 327.
20. E. Bermejo, R. Carballo, A. Castineiras, R. Dominguez, A. E. Liberta, C. Maichle-Mossmer, D. X. West, *Z. Naturforsch., B: Chem. Sci.* 54 (1999) 777.
21. A. Castineiras, E. Bermejo, D. X. West, L.J. Ackerman, J. V. Martinez, S. H. Ortega, *Polyhedron* 18 (1999) 1469.
22. A.D. Naik, V.K. Revankar, *Proc. Indian Acad. Sci (Chem. Sci.)* 113 (2001) 285.
23. V. Philip, V. Suni, M.R.P. Kurup, *Polyhedron* 25 (2006) 1931.
24. I.-X. Li, H.A. Tang, Yi-Zhi Li, M. Wang, L.-F. Wang, C.-G. Xia, *J. Inorg. Biochem.* 78 (2000) 167.

Summary and conclusion

This thesis describes the synthesis, structural and spectral characterization of four *N*(4)-ring incorporated thiosemicarbazones of benzaldehyde, 2-hydroxybenzaldehyde and 4-methoxybenzaldehyde and their metal complexes.

Chapter 1 gives a prologue of the bonding and stereochemistry of the thiosemicarbazones. The different analytical and spectroscopic techniques used for the analysis of the ligands and metal complexes are discussed.

Chapter 2 deals with the synthesis of four thiosemicarbazone ligands. The ligands synthesized are:

- benzaldehyde 3-hexamethyleneiminylthiosemicarbazone [HL¹]
- 2-hydroxybenzaldehyde 3-hexamethyleneiminylthiosemicarbazone [H₂L²]
- 4-methoxybenzaldehyde 3-hexamethyleneiminylthiosemicarbazone [HL³]
- 2-hydroxybenzaldehyde 3-tetramethyleneiminylthiosemicarbazone [H₂L⁴]

Crystal and molecular structure of the ligand H₂L² was described in detail. Thiosemicarbazones are synthesized by adapting a three step procedure reported elsewhere. The ligands are characterized by elemental analyses, IR, UV and ¹H NMR techniques. H₂L² crystallizes with one molecule per asymmetric unit into triclinic crystal system with a space group of *P2₁/n*. The molecule adopts *E* configuration about azomethine bond. The crystal structure data indicated that the ligand exists in the thione form.

Chapter 3 describes the synthesis of ten copper(II) complexes (**1-10**) using the four types of ligands. These are characterized by partial elemental analyses, IR, UV-vis and EPR spectra. Single crystal X-ray diffraction studies of one of the

complexes [CuL⁴bipy] (**10**) were carried out. The copper in the mononuclear complex is five coordinated and is having an approximate square pyramidal (SPY) geometry. The copper centre is coordinated by the phenolato oxygen, O1, azomethine nitrogen, N1, and the thiolato sulphur, S1, of the thiosemicarbazone and the pyridine nitrogens, N5 and N4, of bipyridine. Magnetic moments of the complexes were calculated from magnetic susceptibility measurements. Mononuclear Cu(II) complexes exhibit magnetic moments in the range 1.5–2.05 B.M, which are close to their spin-only value. Magnetic moment of binuclear Cu(II) complex [(CuL²)₂] (**2**) is 1.25 BM which is in the range of 1.15–1.40 BM, found for binuclear complexes. The EPR spectra of all the Cu(II) complexes were recorded both in polycrystalline state at 298 K and in DMF at 77 K. The g values and the various EPR spectral parameters were calculated. The g values calculated indicate that in all the complexes the unpaired electron is present in the d_{x²-y²} orbital. In the electronic spectral studies, the *d-d* transitions are found to be broad. So the three *d-d* transitions could not be resolved. IR spectral data indicates that the complexes with ONS donor ligands are tridentate coordinated through phenolic oxygen, azomethine nitrogen and thione/thiolate sulfur atoms and with NS donor ligands through azomethine nitrogen and thiolate sulfur atoms.

Chapter 4 includes the synthesis of ten nickel(II) complexes (**11-20**) using the four types of ligands. It also describes the X-ray diffraction studies of [NiL²py] (**13**), [NiL²α-pic] (**14**), [NiL²β-pic] (**15**) and [Ni₂L²₂phen] (**17**) of the complexes. The complexes **13**, **14** and **15** have distorted square planar structure and compound **17** is a typical binuclear complex having two types of coordination centers and also having different spin states. It is discussed in detail in this chapter. All the complexes except **17** are diamagnetic due to square planar nature of the complexes. The reason for paramagnetism in the compound **17** may be due to the presence of phenanthroline coligand present in the molecule. But the magnetic moment is

lower compared to the octahedral Ni(II) complexes. Some of the magnetic moments may be cancelled due to square planar coordination. IR, NMR and electronic spectral studies are also done.

Chapter 5 represents the synthesis, structural and spectral characterization of five Co(III) complexes (**21-25**). The thiosemicarbazones, heterocyclic bases viz., phenanthroline/bipyridine and azide/potassium thiocyanate ion act as ligands. Magnetic susceptibility measurements at 293 K suggest that the compounds are diamagnetic indicating the oxidation of cobalt(II) to cobalt(III) and hence corresponds to d^6 ion in strong field. Attempts to prepare the single crystals of the Co(III) compounds resulted in a sulfenato complex due to oxidation of thiol in the thiosemicarbazone moiety. In complex $[\text{Co}(\text{L}^4\text{O})\text{phenN}_3]$ (**24**), during the course of the synthetic reaction, the thiosemicarbazone may undergo oxidation at the sulfur center whereby it is converted into sulfenate, and the transformed thiosemicarbazone is coordinated to cobalt as a dianionic tridentate ONS donor. The oxidation at sulfur depends on the nucleophilicity of the sulfur atom and it is assumed that there is at least some π - back bonding character in the M-S bond. The coordination around the cobalt metal centre is found to be distorted octahedral. IR and electronic spectral studies are also done.

Chapters 6 and 7 portray the synthesis and characterization of ten zinc (**26-35**) and five cadmium metal complexes (**36-40**) of thiosemicarbazones. All the zinc complexes are prepared from ONS donor thiosemicarbazones and cadmium complexes are prepared from ONS/NS donor thiosemicarbazones. It was possible to isolate single crystals of $[\text{Zn}(\text{HL}^2)_2]$ (**26**) and it is studied in detail. The ligands coordinate to the Zn(II) ion, through azomethine nitrogen and thiolate sulfur atoms of the deprotonated form after thiolation, to form a highly distorted tetrahedral geometry. The phenolic group of the ligand is retained as such and is placed away

from the metal centre. All the complexes are diamagnetic as expected. These are characterized by elemental analysis, IR, electronic and ^1H NMR spectra.

Curriculum Vitae

PERSONAL PROFILE

Date of Birth 31st May 1981
Permanent address Ahammed Manzil
Ponjassery P.O
Perumbavoor 683 547, Kerala
Ph.No. 0484 - 2525406

EDUCATION

1996 SSLC
St. Francis GHS, Aluva
(85 %)

1996-1998 Pre-Degree
St. Paul's College, Kalamassery
(71.4%)

1998-2001 B. Sc. Petrochemicals
Al-Ameen College, Edathala, Aluva
(85.5%)

2001-2003 M. Sc. Chemistry
Nirmala College, Muvattupuzha
(77%)

2003 CSIR-JRF

2004 GATE 90.4 percentile

RESEARCH PUBLICATIONS/COMMUNICATED

1. Salicylaldehyde 4,4'-(hexane-1,6-diyl)-thiosemicarbazone, L. Latheef,
M.R.P. Kurup, E. Manoj, Acta Crystallogr. C 62 (2006) 16.

2. Synthesis and spectral characterization of zinc(II) complexes of N(4)-substituted thiosemicarbazone derived from salicylaldehyde: Structural study of a novel –OH free Zn(II) complex, L. Latheef, M.R.P. Kurup, E. Manoj, *Polyhedron* 26 (2007) 4107.
3. Spectral and structural studies of copper(II) complexes of thiosemicarbazones derived from salicylaldehyde and containing ring incorporated at N(4)-position, L. Latheef, M.R.P. Kurup, *Spectrochim. Acta*, in press doi:10.1016/j.saa.2007.07.015
4. Spectral and structural studies of nickel(II) complexes of salicylaldehyde 3-azacyclothiosemicarbazones, Leji Latheef, M.R.P. Kurup, *Polyhedron*, in press.
5. Spectral studies of cobalt(III) salicylaldehyde N(4)-ring incorporated thiosemicarbazone complexes: crystal structure of a sulfenato complex, Leji Latheef, M.R.P. Kurup, Communicated.
6. Synthesis, spectral and structural studies of Ni(II) complexes of ONS donor thiosemicarbazone ligands, Leji Latheef, E.B. Seena, M.R.P. Kurup, Communicated